Development of a Separation-Based Sensor using Microdialysis Coupled to Microchip Electrophoresis with Electrochemical Detection for Monitoring Catecholamines

Rachel A. Saylor

Submitted to the graduate degree program in Chemistry and the Graduate Faculty of the University of Kansas in partial fulfillment of the requirements for the degree of Doctor of Philosophy.

_____
Chairperson: Dr. Susan M. Lunte

_____
Dr. Robert C. Dunn

_____
Dr. David D. Weis

_____
Dr. Timothy A. Jackson

_____
Dr. Brian D. Ackley

Dissertation Defense: October 13, 2015

The Dissertation Committee for Rachel A. Saylor
certifies that this is the approved version of the following dissertation:

Development of a Separation-Based Sensor using Microdialysis Coupled to Microchip Electrophoresis with Electrochemical Detection for Monitoring Catecholamines

_____

Dr. Susan M. Lunte

Date approved: October 13, 2015

Abstract

Microdialysis is a powerful separation technique capable of simultaneously monitoring multiple analytes in the extracellular fluid of the brain. This technique generates small sample volumes in a continuous flow stream. Traditional methods used for sample analysis forfeit temporal information regarding dynamic neurochemical processes due to the larger volumes necessary for analysis. Additionally, sample acquisition methods traditionally involve some form of tethering or anesthetizing the animal under study, greatly reducing the available behavioral information. In order to preserve both temporal resolution and behavioral information, the ideal analysis system is one that can be employed on-line, has fast analysis times of small sample volumes, and can be placed on a freely-roaming animal. Microdialysis sampling coupled on-line to microchip electrophoresis with electrochemical detection creates a separation-based sensor that fulfills these constraints. The ability to place the device directly on-animal, without tethering, allows for the neurochemical information to be correlated with the animal's behavior, allowing for further understanding of the neurochemical basis behind each behavior. Additionally, neuroactive drug metabolism can be monitored alongside behavior when employing an on-animal separation-based sensor, potentially aiding in drug development.

The goal of this thesis is therefore to develop a separation-based sensor that is capable of monitoring neurochemicals *in vivo*. Towards this aim, the separation and detection of analytes in the dopamine metabolic pathway was accomplished using microchip electrophoresis with electrochemical detection at a carbon electrode. The substrate material in this separation was also optimized. In order to integrate this separation and detection with microdialysis sampling, a novel fabrication procedure was developed. This procedure creates a PDMS/glass hybrid device capable of integrating hydrodynamic microdialysis flow with electrophoretic flow and detection

at a carbon electrode using a flow-gated interface. Lastly, the developed method was used to monitor the dopamine metabolic pathway *in vivo* in rat after the administration of L-DOPA. In the future, the complete device and associated instrumentation can be used remotely and on-animal, for near-real time *in vivo* monitoring.

Acknowledgements

Every individual is shaped by their experiences and the people that surround them; I have been extraordinarily lucky in both of these regards. There are so many people who have shaped who I am as a scientist and person and without whom none of this would have been possible.

First and foremost, I would like to thank my advisor and mentor, Susan Lunte. I consider joining the group one of the luckiest and best decisions I have ever made, and I know that I would not be who I am today without her mentorship. Throughout the peaks and valleys of grad school, Sue gave constant reminders that even when a peak (literally) has not been seen in weeks or months, with hard work something would eventually succeed. Sue has provided many amazing opportunities for me to grow and learn as a scientist, including helping with grant writing, mentoring new grad students and undergraduates, editing papers, lab management, presenting at conferences all over the globe (including being an invited speaker), and organizing conference symposia. Additionally, when experiments weren't cooperating or things got stressful, I know that Sue believed in me more than I believed in myself. Anything that I have managed to accomplish here or will do in the future is a direct result of her mentoring and confidence in me. It is my goal to live up to her expectations. In addition to being a science mentor, both Sue and Craig served as constant examples that you can be a world renowned research scientist while still being a kind, generous, and caring person. Thank you, Sue.

I would also like to thank all of the Sue Lunte research group members, both past and present, for their impact on both my research and development as a scientist. This group of people has become my research family, and I am truly grateful to have been able to work beside all of them. There are, however, group members who I would like to thank individually.

The first person I need to thank here is Dr. Tom (TDawg) Linz, whom I irritated and badgered into helping me my first few years here. Tom taught me so much about working in the Sue Lunte Lab, from how to properly place a carbon fiber electrode into a PDMS trench, to device trouble shooting (did you turn on the high voltage power supply?), to demanding the best from yourself, regardless of what else was going on. Tom, when you left the lab felt so empty; emails just aren't as good as Walktimes(?!). Thank you so much for your help, guidance, and friendship, both while you were here at KU and after you graduated. I really appreciate all the time you spent mentoring me, and I know you will be an amazing professor someday. I would also like to thank Dr. Dulan Gunasekara, who taught me how to run my first ME-EC device, was always there with ideas and trouble-shooting assistance, and who became a good friend. Dulan was an amazing coworker; always there with help or a kind word and so excited about science and research. His outlook definitely made assisting with grants much more enjoyable!

I also need to thank Nate Oborny, Richard Piffer Soares de Campos, and Dr. Jessica Creamer. Each of these talented scientists has influenced my science and life in countless ways, and I consider them all good friends. Lastly, I have mentored two outstanding scientists, Erin Reid and Shamal Gunawardhana. I am extremely proud to know both of these people, and only hope that I taught them as much as they have taught me.

I would also like to thank all the Craig Lunte group members, past and present, for their friendship and help. It is a unique situation to have an extended lab-family just down the hall, and one for which I am grateful. Special thanks go to Dr. Sara Thomas, Amanda Furness, and Ryan Johnson; I consider all of you good friends. Sara and Amanda have taught most of what I currently know about animal research and microdialysis sampling. Sara, thank you so much for your help and friendship in these last few months.

The professors in the Department of Chemistry at Wittenberg University are a large reason that I am a chemist today, specifically Dr. Kristin Cline, Dr. Dave Finster, and Dr. Ray Dudek. Dr. Cline in particular mentored me both as a student of analytical chemistry and as a researcher doing electrochemistry, both of which are now instrumental in my career. I would also like to thank Dr. Cathy Pederson for helping to expand my knowledge and love of neuroscience and pharmacology while I was at Wittenberg. All of these professors influenced me greatly, and many of the decisions I made in grad school reflect their impact on my life.

I would also like to thank my both my defense committee and the professors I have had here at KU. Dr. David Weis, in addition to serving on my committee, has mentored me in teaching undergraduates. I learned a great deal and gained invaluable experience as a T.A. under his guidance. Lastly, I was fortunate enough to learn separations from Dr. Craig Lunte.

The Craig Lunte lab for use of their animal care facilities, the Laurence lab for the use of their cell culture hood, and the Ralph N. Adams Institute COBRE Core Microfabrication Facility are all gratefully acknowledged. Additionally, I would like to thank Cady Bush for the many miscellaneous things that she does, including making everyone's day a bit brighter.

Outside of the lab (but often just down the hall, downstairs, or in the next desk over) the friends that I have made in grad school have made my time here enjoyable. Dr. Sarah (Wildgen) Borland has been an amazing friend. It has been an honor to go through grad school with you; I do not think I could have survived without your support, calm demeanor, and lunch dates. Thank you so much for being the best friend I could ask for while navigating the struggles and joys of grad school. Another good friend, Christa Snyder, has managed to be an integral part of my life in Kansas despite the unfortunate fact that she turned coat and decided to pursue her Ph.D. at Indiana University. She is always just a phone call or email away, and is wise enough

to recognize that sometimes a shiny bottle of new nail polish is all you need to deal with a day of failed experiments. Christa, your care packages and emails constantly brighten my day, and you are one of my closest friends. Dr. Lydia (Homefri) Kisley and Molly (P!) Tingley have also offered their support and friendship from afar, and for that I am thankful. Lastly, Nate Oborny and Rachel Hattaway have made my time here in Lawrence much more enjoyable. Their friendship has meant a great deal to me.

Family is an important part of any success, and all of my family has been very supportive of me. Without my parents, I would have never even made it to grad school. Their selfless sacrifices and constant support has meant so much to me. My mom, especially, has always wanted the best for both me and my brother, and she has worked tirelessly (and often thanklessly) to help give us opportunities. She has always been just a phone call away to share in my triumphs or failures, offering love and advice. Mom, thank you so much. Additionally, I am fortunate to have a wonderful brother, Zachary, who is smarter than me and who I can always call on for math help. I also really appreciate the love and support of the rest of my family, especially my Nana.

Peter Jensen, thank you for everything you've done for me over the years. From making me delicious food, to comforting me after a bad day, to driving with me to lab at 3 am when I'm panicking about getting things done, you have been there to support me. I love you so much, and I can't wait to see where our next move takes us together.

Table of Contents

Chapter 1: Research objectives and chapter summaries

1.1 Research objectives

On-line microdialysis sampling coupled to microchip electrophoresis with electrochemical detection is a powerful combination of techniques that can be used for near-real time *in vivo* monitoring of neurotransmitters or drug metabolism. Excitingly and importantly for this dissertation, due to the small overall size of these devices and associated instrumentation, on-animal monitoring is also a possibility. The ability to monitor analytes, especially neurotransmitters, on-line and in near-real time in a freely-roaming animal that is in no way tethered or constrained allows for the correlation of these neurochemicals with true behavior. This information can be used to better understand the neurochemical basis behind various behaviors, or in drug development.

The goal of this dissertation is therefore to achieve on-line monitoring of neurotransmitters *in vivo*. This dissertation is a subset of the larger "lab-on-a-sheep" project in the Susan Lunte Lab, which has the goal of developing a system capable of on-line monitoring of neurotransmitters in freely roaming and behaving animals (initially sheep). The eventual goal is to enable the correlation between levels of neurotransmitters and behavior in these freely roaming animals. In order to accomplish this goal, separation-based sensors are being developed employing microdialysis sampling coupled, on-line, to microchip electrophoresis with electrochemical detection. These separation-based sensors can be placed on-animal and controlled remotely to allow free range of movement in natural environments. This dissertation describes work towards *in vivo* monitoring of neurochemicals in rat brains, for future on-animal work involving sheep.

1.2 Chapter summaries

1.2.1 Chapter 2

Microchip electrophoresis with electrochemical detection is a powerful technique that is introduced in this chapter. The basic principles of microchip electrophoresis, including separation mechanisms, common microchip designs and sample injection strategies, and principles of amperomeric electrochemical detection are described in this chapter. Importantly for this dissertation, considerations when implementing microchip electrophoresis with electrochemical detection are detailed; the effect of the separation voltage on the working electrode and electrode placements employed to mitigate this effect are described. Common working electrode materials and configurations in microchip electrophoresis are also described, with a focus on the carbon electrode types used in this dissertation. Lastly, representative biological applications are discussed.

1.2.2 Chapter 3

Microchip electrophoresis with electrochemical detection was used to separate and detect analytes in the dopamine metabolic pathway. Initially, a PDMS/PDMS microchip with integrated carbon fiber electrode was employed for separation optimization; however, it was determined that a PDMS/glass hybrid device exhibited much more reproducible separations. The optimized separation and detection method was then used to monitor the conversion of L-DOPA to dopamine over time by a rat brain slice *in vitro*.

1.2.3 Chapter 4

While microchip electrophoresis lends itself well to the analysis of microdialysis samples, there are some considerations for coupling the two techniques. In this chapter, basic principles of microdialysis are presented, along with some practical considerations unique to on-

line microdialysis-microchip electrophoresis. A review of the current microdialysis-microchip electrophoresis literature is discussed, including describing the three different interface designs and current applications.

1.2.4 Chapter 5

This chapter develops a device capable of on-line monitoring using microdialysis coupled to microchip electrophoresis with electrochemical detection (MD-ME-EC). A novel fabrication procedure is described to allow for the integration of a reuseable carbon electrode into the device. The separation of dopamine, norepinephrine, and ascorbic acid was optimized using the developed device, with the goal of monitoring dopamine and norepinephrine release from PC-12 cells. Additionally, the length of the injection time was investigated with the goal of increasing the signal. Increasing the injection time from 1.0 s to 50.0 s did result in a 100-fold increase in peak area for dopamine; however, while analytes were separated under these conditions when dissolved in 15 mM phosphate, the separation collapsed when analytes were dissolved the cell stimulation buffer. Future work for this application of the on-line MD-ME-EC device will focus on alternative PC-12 cell stimulation protocols.

1.2.5 Chapter 6

The overall goal of this thesis is on-line monitoring of neurochemicals *in vivo* and on-animal. This chapter details the progress towards *in vivo* monitoring of neurochemicals in the brain of an anesthetized rat. This chapter combines the MD-ME-EC device detailed in Chapter 5 with the separation of analytes in the dopamine metabolic pathway described in Chapter 3. The *in vivo* monitoring of the dopamine metabolic pathway was achieved after a L-DOPA perfusion. Additionally, some considerations and limitations of the device are described.

1.2.6 Chapter 7

This chapter summarizes all progress on this project to date. Future directions, both immediate and long term, are described. Future directions include correlating behaviors of animals with the on-animal monitoring of neurotransmitters and monitoring biomarkers of traumatic brain injury in the clinic.

1.2.7 Appendix

The appendix of this thesis is primarily for the use of future researchers who wish to fabricate and use MD-ME-EC devices with carbon-based electrodes. In this appendix, the fabrication of carbon fiber and pyrolyzed photoresist film carbon electrode substrates is described.

Chapter 2: Principles and strategies for coupling microchip electrophoresis with electrochemical detection

Adapted selections from: D.B. Gunasekara, M.B. Wijesinghe, R.A. Saylor, S.M. Lunte, Principles and Strategies for Microchip Electrophoresis with Amperometric Detection, in: D.W.M. Arrigan (Ed.), Electrochemical Strategies in Detection Science, The Royal Society of Chemistry (2016) p. 84-124.

2.1 Introduction

Microchip electrophoresis (ME) is a powerful separation technique that has been extensively employed in many lab-on-a chip devices since its introduction in the mid-1990s [1,2]. Electrophoretic separations in microchip electrophoresis are based on the same principles and strategies that are employed for the more traditional capillary-based separations. These separations are performed in channels of micron or submicron dimensions on planar substrates, allowing for new applications in areas where traditional capillary-based electrophoresis (CE) is difficult to apply.

Most detection methods employed with capillary electrophoresis have been successfully adapted to the microchip format. Laser-induced fluorescence (LIF) is the most commonly applied detection strategy in microchip electrophoresis due to the relative ease of focusing the laser beam in the separation channel and detecting the resulting fluorescence using a microscope. However, LIF has two main disadvantages when used as a detection strategy in microchip electrophoresis. The first is that fluorescence detection normally requires analyte derivatization with a fluorophore prior to analysis. Secondly, the associated optics and instrumentation for LIF detection are much larger than the chip used for analysis, negating some of the benefits of miniaturization that are characteristic of the microchip format, such as portability. Other optical techniques, such as absorbance detection, that is widely used in capillary electrophoresis, are impractical to implement in the microchip format due to the small dimensions of the channel resulting in a limited path length.

Electrochemical detection (EC) methods, based on either conductivity or amperometry, are popular for detection in microchip electrophoresis, and this pairing offers many advantages. A major advantage of electrochemical methods is that the electrodes used for both detection and

separation can be directly integrated into the microchip. When incorporating electrodes into microchip electrophoresis devices, microelectrodes can be employed as working electrodes without a loss in sensitivity. Another advantage is that, unlike LIF detection, substrates do not need to be optically transparent. In addition, the associated electronics (potentiostats) can be easily miniaturized and battery powered, making portable analysis systems possible. Lastly, many analytes of interest, including many biologically relevant molecules, are electroactive and do not require derivatization prior to their detection. Microchip electrophoresis coupled to electrochemical detection (ME-EC) has been employed for a wide variety of applications, and there are several excellent reviews on the topic [3-10].

This chapter focuses specifically on amperometric detection for microchip electrophoresis, as that is the most common form of electrochemistry used in microchip electrophoresis and was employed in the work described in this thesis. The basic principles of electrophoretic separations in the microchip format will be presented first, followed by a discussion of theoretical and practical considerations of coupling microchip electrophoresis to amperometric detection. The use of different electrode materials and configurations to increase the selectivity of microchip electrophoresis will be described as well as some representative applications of the technique.

2.2 Principles of microchip electrophoresis separations

2.2.1 Electrophoretic separation within a microchip

For electrophoresis experiments, a channel is filled with a conductive buffer and, following sample injection, separations are accomplished by applying a voltage across the channel. Glass and silica are the most common substrates for microchip electrophoresis-based separations. When run buffers of a pH greater than 3 are employed in these substrates, the

surface of the channels become negatively charged due to the presence of ionized silanol groups. Upon application of an electric field (for simplicity positive high voltage is considered here), this results in the production of electroosmotic flow (EOF), which moves all analytes regardless of charge toward the cathode. In the case of polymer substrates, the surface is often chemically modified to generate a negative surface charge to obtain EOF.

The production of EOF in a channel is due to the generation of a potential field at the surface of the channel known as the zeta potential (Figure 2.1A). As a result of this zeta potential cations in the buffer, such as H^+ and Na^+, will electrostatically adhere to the surface of the channel in an attempt to neutralize the negative charge at the channel surface. However, these adsorbed ions cannot completely neutralize the charge and a second diffuse layer, consisting of cations that are closely associated with the surface, is formed to balance the remaining surface charge [11,12]. This results in an electrical double layer as shown in Figure 2.1A. Once a positive high voltage is applied, the positively charged hydrated ions in the diffuse layer are drawn toward the cathode (negative/ground electrode), creating electroosmotic flow. The zeta potential profile of this phenomenon can be seen in Figure 2.1B. The EOF carries all analytes, regardless of charge, toward the cathode. In addition, since the flow is generated along the channel surface, it creates a plug flow profile (Figure 2.1C) that exhibits significantly less band broadening than pressure-driven flows [11,12].

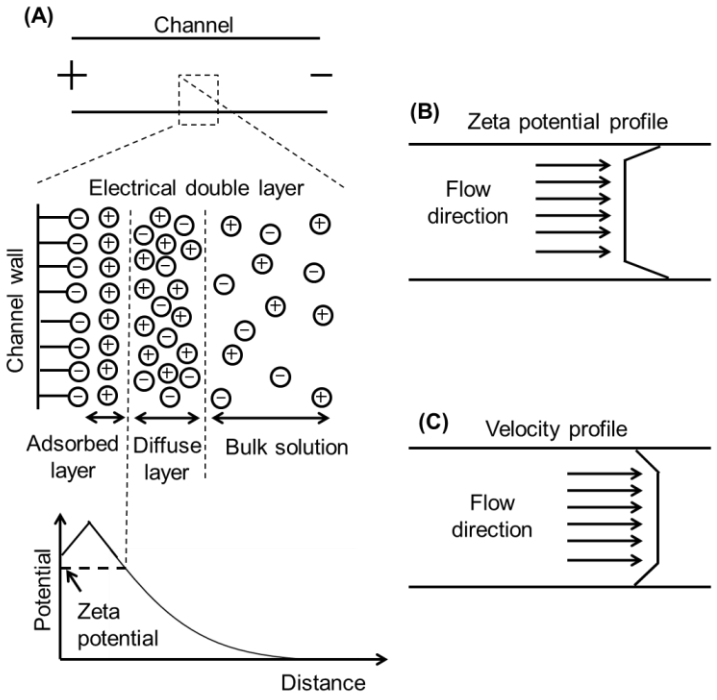

Figure 2.1 Electroosmotic flow in a channel. (A) The charged wall in a glass/silica channel, schematic of the electric double layer, and potential distribution as a function of distance. (B) Zeta potential distribution and (C) EOF velocity distribution across the separation channel.

In microchip electrophoresis, the separation potential is applied across a channel by placing electrodes (normally Pt) into two buffer-filled reservoirs at either end of the channel. A high voltage is applied to one electrode while the other electrode is held at ground. This produces a linear voltage drop across the channel that is dependent on the resistance of the run buffer and the channel dimensions. Since current flows between the electrodes, redox reactions occur at both the anode and cathode [8]. In aqueous run buffers, these reactions are usually the reduction and oxidation of water at the cathode and anode, respectively [13].

Cathode: $2H_2O + 2e \rightleftharpoons H_2 + 2OH^-$ (–0.828 vs. NHE)

Anode: $O_2 + 4e + 4H^+ \rightleftharpoons 2H_2O$ (+1.229 vs. NHE)

To achieve a separation in microchip electrophoresis, it is necessary to produce differences in analyte migration within the electric field. In the simplest form of microchip electrophoresis, free-zone electrophoresis, analytes are separated based on differences in the ratio of their charge-to-hydrodynamic radii. This separation is dependent on a combination of two different forces on a charged molecule in an electric field: the electrostatic and frictional force. The electrostatic force (Eq) is a force experienced by the molecule toward the electrode of opposite charge, which is balanced by the frictional force ($6\pi\eta a v_{ep}$) of the solution. The ion quickly reaches a steady-state velocity based on these two opposing forces, and the velocity of the analyte (v_{ep}) can be described by:

$$v_{ep} = Eq/6\pi\eta a$$

where E is the electric field gradient, q is the charge of the analyte, η is the viscosity of the run buffer, and a is the hydrodynamic radius of the analyte. In this equation, the factor $q/6\pi\eta a$ is defined as the electrophoretic mobility (μ_{ep}) and is a constant for a specific analyte in a given buffer system (where η is constant) [12]. Therefore, μ_{ep} depends only on the ratio of charge-to-hydrodynamic radius, as mentioned above. Analytes must exhibit different electrophoretic mobilities under the separation conditions in order to be adequately resolved. The speed of analysis is partly dependent on the velocity of an ion in the channel (v_{ep}) which is a function of the electric field strength (E) and the electrophoretic mobility, as seen in the equation below [12].

$$v_{ep} = \mu_{ep} E_{ep}$$

Separations accomplished through the application of a positive voltage gradient across the negatively charged channel are referred to as “normal polarity” separations (Figure 2.2A,C).

In normal polarity, the electrophoretic mobility of a cation is positive, and it is attracted to the cathode. The electroosmotic flow is also in the direction of the cathode. Therefore, positive ions will migrate out of the capillary first, with their migration time a being a function of the combination of their electrophoretic mobility and the magnitude of the electroosmotic flow [11,12].

$$\mu_{app} = \mu_{ep} + \mu_{eo}$$

In this equation, μ_{app} is the apparent (observed) electrophoretic mobility, μ_{ep} is the actual electrophoretic mobility (+), and μ_{eo} is the electroosmotic mobility (+). Anions, on the other hand, are attracted to the anode and exhibit negative electrophoretic mobilites. In most cases, using positive polarity, the EOF (+) is stronger than the μ_{ep} (–) for large anions, so they still migrate toward the cathode. Exceptions are very small anions that have high negative electrophoretic mobilities or separations that are performed under conditions of low electroosmotic flow. In free-zone electrophoresis, neutral species migrate with the EOF and are not separated from one another.

For small negative ions with high negative electrophoretic mobilities, "reverse polarity" is often used (Figure 2.2B,D). To accomplish a reverse polarity separation, the electrophoresis channel is modified with a positive charge either by covalent modification or adsorption of a positively charged surfactant such as tetradecyltrimethylammonium bromide (TTAB) (Figure 2.2D). In this separation mode, the order of migration is opposite that of normal polarity separations, and the buffer anions in the diffusive layer move toward the anode (ground electrode) following the application of a negative high voltage gradient between the two channel ends [11,12]. Therefore, the EOF is in the opposite direction and anions will migrate first, followed by neutrals and then cations.

Microchip electrophoresis separations can be performed using a variety of materials including glass, polydimethylsiloxane (PDMS), polymethylmethacrylate (PMMA), and ceramics [14]. As indicated above, glass surfaces generate significant EOF at pH values greater than 3. However, many polymer chips, such as PDMS, do not natively possess a high, uniform surface charge, so the substrate is often modified to generate an EOF. This can be accomplished by plasma oxidation, dynamic modification by run buffer components (Figure 2.2 C and D), or the introduction of charged functional groups into the polymer itself [15].

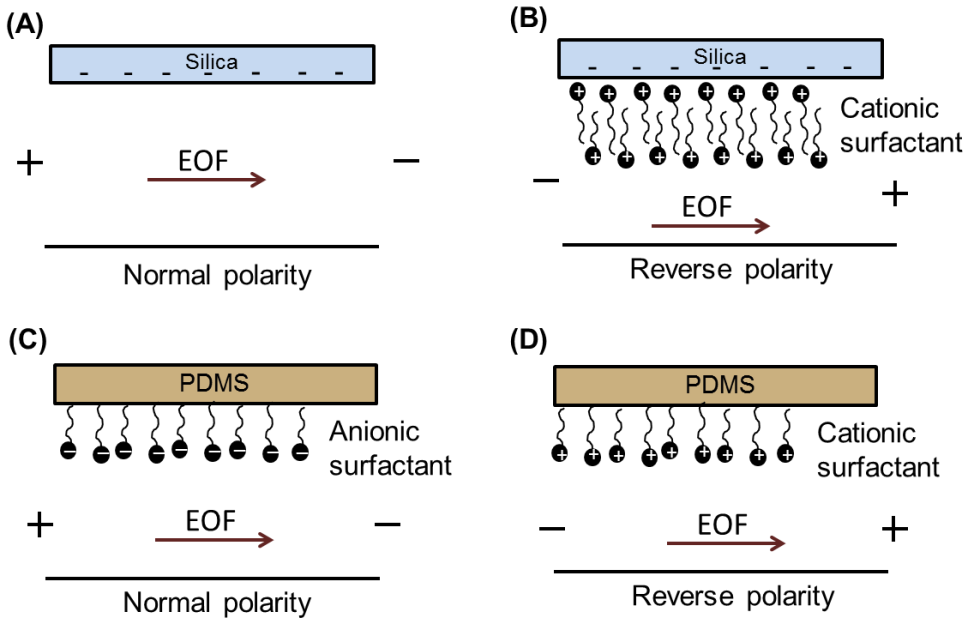

Figure 2.2 The charge at the surface of channels within a microchip (A) unmodified glass or silica channel for normal polarity separation, (B) surfactant-modified glass or silica channel for reverse polarity separations, (C) PDMS or polymer channel modified with an anionic surfactant for normal polarity separations, and (D) PDMS or polymer channel modified with a cationic surfactant in reverse polarity separations.

2.2.2 Microchip designs

A significant advantage of the microchip format is the ability to integrate multiple functions, including sample preparation, preconcentration, and detection into a single chip. The simple-t microchip configuration is the most common design used for ME. However, double-t, offset-t, serpentine channels, and dual-channel microchip designs have also been developed (Figure 2.3). In most devices, fluid is manipulated within the chip using electroosmotic flow.

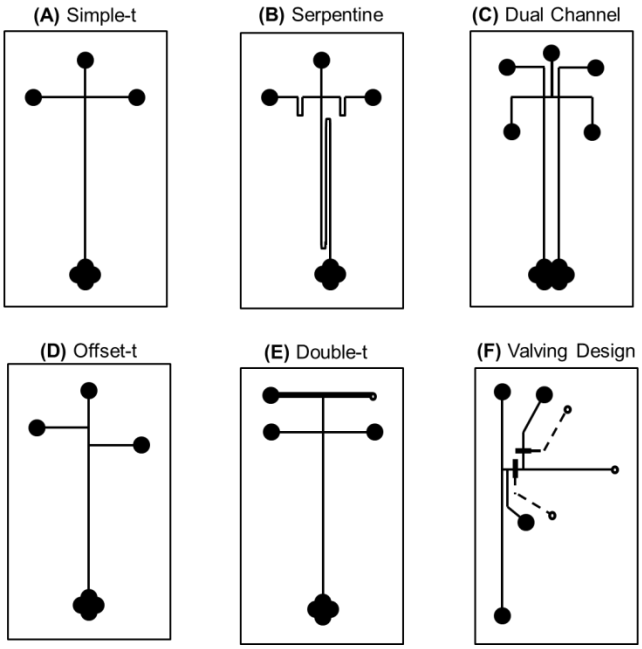

Figure 2.3 Microchip designs commonly employed in ME-EC.

In the simple-t (Figure 2.3A), serpentine (Figure 2.3B), and dual-channel (Figure 2.3C) designs, sample introduction into the separation channel is normally achieved using an electrokinetically gated injection as shown in Figure 2.4A [16-18]. In this injection format, the high voltage applied at the buffer reservoir is floated for a short amount of time, allowing sample to enter the separation channel. When the voltage is reestablished across the separation channel, analytes are separated. While this injection strategy is simple to employ, as only applied

voltages are manipulated, there can be an electrokinetic bias on analytes entering the separation channel. For example, in positive polarity, smaller cations will be preferentially injected into the channel. The number of moles of each species that is injected in this mode is also dependent on the electrophoretic mobility of the compound due to the electrokinetic bias. This can sometimes be used to an advantage to selectively enhance species of a specific charge in the presence of interferences with an opposite charge or larger mass but the same charge. Additionally, the volume of sample that is injected depends on the injection time, applied voltages, and buffer ionic strength; therefore, slight changes in conditions result in differing amounts of sample introduced into the channel. The volume of the sample injected can be calculated using the velocity of EOF, injection time, and the area of the channel.

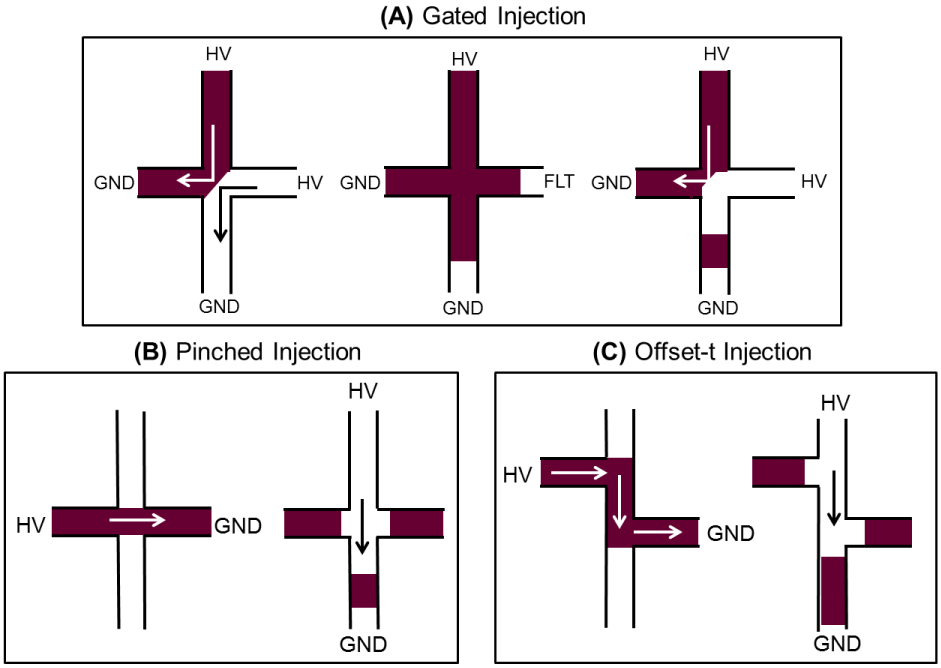

Figure 2.4 Injection strategies in microchip electrophoresis. (A) Gated injection in a simple-t, serpentine, or dual-channel device, (B) pinched injection in a simple-t or serpentine device, and (C) offset-t injection for injecting known sample volumes.

Another benefit of this injection strategy for ME is that application of the electric fields during the injection process generates a reproducible signature in the electropherogram, due to charging current on the electrode. This can conveniently be used to mark time zero in the electropherogram. The field strength can be calculated using the junction voltage, or voltage at the channel intersection. Using Kirchoff's Laws and modeling the channels as resistors, the junction potential can be determined [19].

The pinched injection mode (Figure 2.4B) can also be used in the simple-t and simple-t serpentine device designs. In this case, sample is placed in one of reservoirs in the channel perpendicular to the separation channel and a high voltage is applied across that channel, causing sample to fill the entire channel. For separation, the run buffer is placed in the separation channel and the high voltage is then applied across this channel. This permits a plug of sample corresponding to the size of the intersection to enter into the separation channel. One advantage of this injection approach is that one high voltage power supply is adequate to perform both injection and separation, while in gated injection two separate high voltage power supplies are required.

Offset-t microchip designs (Figure 2.3D) also allow the injection of a finite and known volume into the separation channel. The volume that is injected depends on the length of the offset of the perpendicular channel in relation to the separation channel. In this injection scheme, the offset channel is filled by applying high voltage between two ends of the channel as shown in Figure 2.4C. The volume trapped in the offset portion of the channel is then injected by applying a voltage across the separation channel.

The serpentine design microchip (Figure 2.3B) arose out of a need for a longer separation channel to achieve better resolution of complex mixtures while still conforming to manufacturing

constraints. Many devices are designed around the 4 inch silica wafers that are used in microelectronic device manufacturing; thus, it is not possible to fabricate long, straight channel configurations using conventional photolithographic methods. In designing serpentine microchips for gated injection, care must be taken to extend not only the separation channel itself but also the side arms to enable good electrokinetic gating. A possible problem with serpentine channels is that using a separation channel that has the same width in the straight part as for the turns can cause band-broadening due to the "race track effect," leading to decreased resolution. This can be mitigated by using serpentine chips in which there is a decrease in channel width around the turns [20].

The dual-channel design shown in Figure 2.3C has been used with in-channel amperometric detection. In this design, reference and working electrodes are placed in isopotential positions within the two separate channels for background subtraction [21,22]. This dual-channel design uses two electrokinetically gated intersections that allow the same amount of sample to be introduced into two distinct separation channels. This approach is discussed in more detail in section 2.5.2.2.

To integrate continuous flow streams with microchip electrophoresis separations, the double-t design was developed [23,24]. This design has been modified for continuous analysis of microdialysis samples by ME (Figure 2.3E) [25]. A plug of sample is introduced into the separation channel by means of a flow-gated interface, which is established by the hydrodynamic pressure of microdialysis sampling and the electrokinetic flow from the application of a voltage. For sample introduction, as in the electrokinetic gating, the high voltage is floated and then reestablished. This design allows the integration of microdialysis sampling with microchip electrophoresis, permitting both *in vivo* and *in vitro* monitoring [4].

Alternatively, valves have been employed to couple continuous-flow streams, such as microdialysis sampling, to microchip electrophoresis (Figure 2.3F) [26,27]. These PDMS-based valves are pneumatically driven and allow discrete sample injection into the separation channel. In contrast to the flow-gated design discussed above, the valving devices do not have an electrokinetic bias on sample introduction. Electrochemical detection has been integrated into these devices, in fact, the first application of microdialysis sampling coupled to microchip electrophoresis with electrochemical detection employed pneumatic valves [28].

2.3 Electrochemical detection

The most popular electrochemical detection method for microchip electrophoresis is amperometric detection, where a constant potential is applied to the working electrode and the current resulting from the oxidation or reduction of analytes is measured [7,10]. Amperometry is generally preferred over potential scanning methods such as cyclic voltammetry due to lower background currents, ease of operation, lower LODs, and higher sensitivity; however, amperometry at a single electrode does not provide voltammetric characterization or redox information on the analyte. This information can be obtained through use of multiple electrode configurations (section 2.5.2) or running the same sample multiple times and using different detection potentials.

In amperometry, the optimal applied potential is normally just above the peak potential (on the current-limiting plateu) for the analyte of interest. The peak potential (E_p) for the analyte can be determined in one of two ways: running a cyclic voltammogram or constructing a hydrodynamic voltammogram. Cyclic voltammetry can be performed in bulk solution using the same electrode material and run buffer that will be used in the chip, allowing for the E_p of a specific analyte to be estimated. A better, but much more tedious method is to construct a

hydrodynamic voltammogram for the analyte of interest. This is accomplished by measuring the peak height (current) obtained for a given analyte (following the electrophoretic separation) at several different working electrode potentials. A plot of peak current vs. potential is then plotted for each analyte of interest. Using an applied potential that is on the current limiting plateau will improve the precision of the current response because a slight decrease in potential will not dramatically change the current output; however, applying a potential that is much higher than the peak potential for the specific analyte can result in detecting additional interferents in the sample matrix. Judicious choice of working electrode potential in this manner can allow for optimal detection while potentially eliminating interferents.

In ME, typically only 20–30% of the total molecules in the sample plug are oxidized or reduced [29]. The maximum current that can be achieved under these hydrodynamic conditions can be calculated using a modified version of the Faraday equation, below [30].

$$I_{limit} = nF(C_i - C_f)u$$

In this equation, I_{limit} is the current at the current-limiting plateau, n is the number of electrons transferred in the oxidation or reduction, F is the Faraday constant, C_i is the initial analyte concentration or the concentration before oxidation/reduction, C_f is the analyte concentration after the oxidation/reduction takes place, and u is the linear velocity of the analyte. As evident by the equation above, it is necessary to know the concentration of analyte after the oxidation or reduction to calculate I_{limit}. This concentration can be determined using the conversion efficiency of the electrode. To calculate the conversion efficiency, the actual current or charge of species observed due to oxidation/reduction of a species at the electrode is divided by the total current or charge that can be theoretically generated for the same amount of analyte, which can be calculated using the Faraday equation, below, where Q is the charge, n is the number of electrons

in the oxidation/reduction reaction, F is the Faraday constant, and N is the number of moles oxidized or reduced [30].

$$Q = nFN$$

The conversion efficiency depends on many factors, including electrode type and alignment, type of injection and reproducibility, and changes in flow. Therefore, care needs to be taken when calculating the conversion efficiency for different microchip configurations.

Under ideal conditions, the analyte signal can be directly related to analyte concentration without the need for a calibration curve or standards. By integrating peaks generated from current vs. time profiles (i-t curves), the charge is obtained. Using Faraday's equation, knowing how many electrons are transferred in the oxidation/reduction, as well as taking into account to the conversion efficiency, the number of moles of analyte that was injected into the system and then detected can be calculated [30]. If the volume of the injection plug is known, concentration can then be easily determined.

Amperometric detection for ME-EC is normally conducted in the oxidative mode, although the reductive mode has also been employed. The potential window that can be used for amperometric detection is highly dependent on the electrode material and the buffer pH [13,31]. The width of this potential window is usually defined by both the reduction of oxygen and the oxidation and reduction of water. Additionally, since aqueous buffers are most commonly employed for microchip electrophoresis, the width of this potential window is pH dependent. In reductive analysis, one challenge is the increase in background current due to the reduction of oxygen in the run buffer. This problem can be avoided by thoroughly deoxygenating the run buffer and sample prior to analysis. Lastly, the potential window can be expanded using nonaqueous buffers for the separation.

2.4 Interaction of separation field with the working electrode

2.4.1 Theory and considerations

In the case of ME-LIF, the laser beam can be focused directly onto the separation channel to excite the analytes of interest as they pass by. An advantage of this approach is that detection can be performed virtually anywhere within the separation channel. However with ME-EC, the electrodes cannot be placed deep inside the channel due to interactions of the separation field with the detection electrodes. Therefore, several different electrode configurations have been developed, as well as specialized potentiostats, to avoid and/or minimize interaction of the separation voltage with amperometric detection in microchip electrophoresis. Before discussing these configurations and how they work, it is important to understand the theoretical basis of the interaction of an external (separation) field with a working electrode placed in that field. For this reason, the best available model to explain these interactions is presented prior to the more practical discussion of electrode configurations.

An electric field is required to accomplish separations in microchip electrophoresis with typical field strengths between 100 and 1500 V/cm. In addition, the electrophoretic process normally generates microamperes of current, while only nano- or picoamperes of current are measured by the potentiostat [22,32]. The electric field and resulting current can affect the working electrode when it is placed in the separation channel. It is this interaction that places fundamental constraints on implementation of electrochemical detection for microchip electrophoresis [33,34]. Fluctuations in the voltage, and hence the separation current, as well as improper grounding of the high voltage lead to the main source of noise in ME-EC [22,32,35,36]. These fluxuations in potential and improper grounding result in increased background noise at the detector and higher LODs. Additionally, when a high voltage is applied

across a thin film metal electrode deposited on glass, the currents and heat generated by the separation voltage can damage the electrode. Even more importantly, if the high currents generated by the electrophoretic separation ground through the working electrode, the potentiostat electronics can be destroyed.

In addition to the above nontrivial considerations, the separation voltage will also induce a shift in the apparent potential of the working electrode if it is placed inside the separation channel. These half-wave potential shifts have been reported for both CE-EC and ME-EC [33,34], and must be taken into consideration especially when employing in-channel alignment (section 2.4.2.3). Both the Wightman and Bohn groups have developed models for describing the effect of an applied electric field on the apparent potential of an electrode placed within the field [37,38]. Figure 2.5 shows a potential versus distance diagram for normal (A) and reverse (B) polarity separations using the Bohn model [37]. As can be seen in this figure, the separation voltage decreases linearly across the separation channel as a function of the solution resistance. In these theoretical configurations, the separation ground and reference electrodes are assumed to be parallel to one another (in the detection reservoir) so that there is no effect of the separation field on the reference electrode. Additionally, the oxidative mode is considered and, therefore, the positive potential represents lower energy and the negative potential represents higher energy [37,38].

In normal polarity (Figure 2.5A), the separation voltage causes a decrease in the energy of the molecules near the electrode surface. Therefore, the electrode needs to drive to a more positive potential for electron transfer from molecules to the electrode (oxidation) to occur. That is, the apparent half-wave potential for analytes is shifted in a positive direction when the electrode is placed inside the channel [33,37,38], and a higher potential must be applied to the

working electrode for oxidation. In the case of reverse polarity (Figure 2.5B), the separation voltage causes an increase in the energy of the molecules near the electrode surface. Therefore, less positive potentials need to be applied to the working electrode for oxidation to occur [34].

This model is based on the premise that heterogeneous electron transfer occurs between the solution and the electrode; the solution and working electrode potential are distinct. Therefore, the effective potential of the electrode can be defined as the sum of both of these components [37,38]:

$$E_{eff,\,WE} = E_{app,\,WE} + E_{shift}$$

where $E_{eff,\,WE}$ is the effective working electrode potential, E_{shift} is the potential across the buffer above the electrode, and $E_{app,\,WE}$ is the potential applied to the working electrode by the potentiostat. E_{shift} is dependent both on the voltage (iR) drop across the channel and the location of the working electrode within the channel [37,38]. In positive polarity separations, E_{shift} is positive because this is the extra potential necessary at the working electrode (since molecules in the solution have lower energy under these conditions). Therefore, the in-channel hydrodynamic voltammogram is shifted in the positive direction compared to the end-channel hydrodynamic voltammogram (Figure 2.5A). The potential of the solution above the electrode is then defined by the following equations:

$$E_{shift} = \theta iR$$

$$\theta = \frac{d_{WE}}{d_{total}}$$

In these equations, i is the separation current, R is the resistance in the microchannel, d_{WE} is the distance between the separation ground electrode and the working electrode, and d_{total} is the total

distance between the high voltage electrode and ground. Using these parameters, the half-wave potential shift experienced by the working electrode can be defined as:

$$E_{1/2,\ with\ HV} = E_{1/2,\ without\ HV} + E_{shift}$$

The energy diagram for reverse polarity is shown in Figure 2.6B and in this case E_{shift} is negative because molecules in the solution have higher energy under these conditions. Therefore the in-channel hydrodynamic voltammogram is shifted in the negative direction compared to the end-channel hydrodynamic voltammogram (Figure 2.5B).

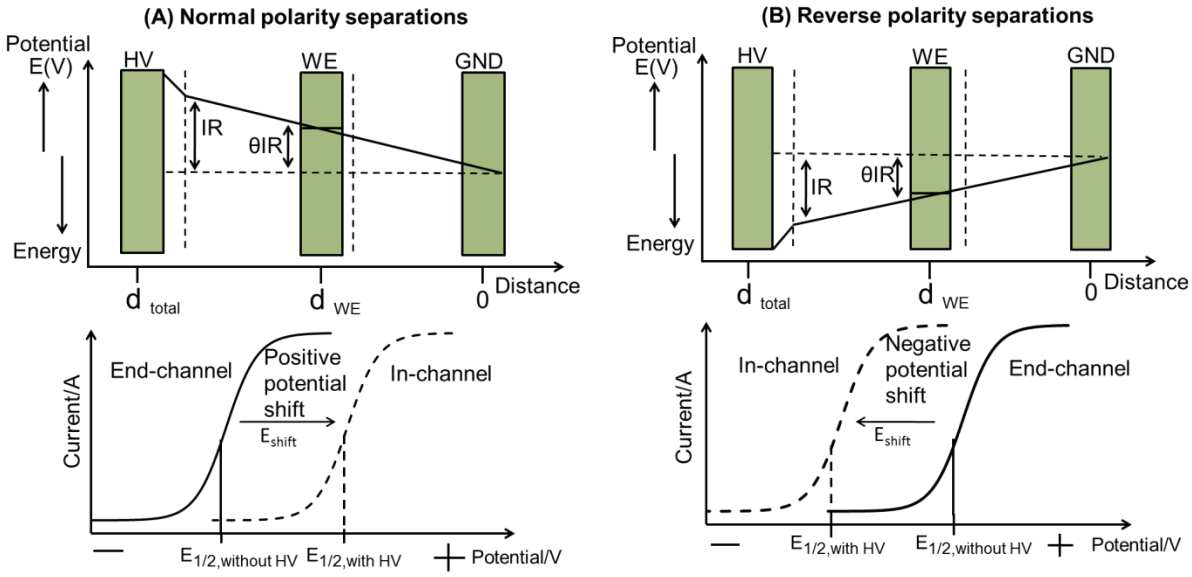

Figure 2.5 The potential vs. distance diagram for normal and reverse polarity separations. The potential drop across the channel and representative potential shift in the HDV for (A) a normal polarity and (B) reverse polarity separation. Reproduced (adapted) from reference [37].

2.4.2 Electrode alignment

Electrode alignment in microchip electrophoresis is categorized into three different configurations depending on the placement of the electrode relative to the separation channel. This categorization also shows the different strategies for preventing or minimizing the interaction of the separation field with the working electrode. The main three electrode configurations are end-, off- and in-channel electrode alignments; these can be visualized in Figure 2.6 and were directly compared previously [39].

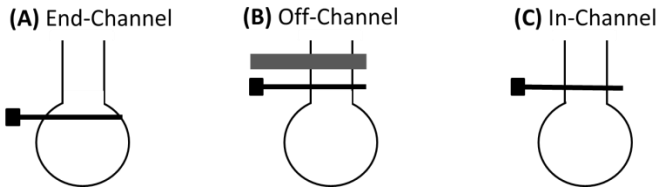

Figure 2.6 Electrode alignments in microchip electrophoresis. (A) end-channel detection, (B) off-channel detection using a decoupler (shown in grey), and (C) in-channel detection using an isolated potentiostat.

2.4.2.1 End-channel detection

A common strategy to prevent the interaction of separation field with the electrochemical detector is to place the electrode in the ground reservoir 5–15 μm away from the end of the separation channel, where the electric field from the separation has dissipated [9,39]. This strategy is known as the end-channel electrode configuration (Figure 2.6A). In this configuration, analytes diffuse into the waste reservoir as they exit the channel prior to their detection, which can lead to band broadening [39]. This band broadening leads to a loss of separation efficiency and a reduction in sensitivity. However, the noise due to separation field is minimized, leading

to lower limits of detection than for some of the other configurations. To more effectively dissipate the separation field and minimize the amount of analyte dispersion, Henry's group developed a "bubble cell." In this microchip, the channel is widened at the end prior to the waste reservoir, and the working electrode is placed in this wider channel where the separation field is significantly decreased compared to the separation channel [40]. Major advantages of the end-channel approach are that it is compatible with commercially available (grounded) potentiostats and no additional fabrication steps are needed to decouple the separation field from the working electrode; however, there is a loss in separation efficiency in this configuration.

2.4.2.2 Off-channel detection

Off-channel detection involves placing the working electrode inside the channel, but the separation field is grounded prior to the working electrode using a metal decoupling electrode (Figure 2.6B) [9,41]. Band electrodes fabricated from Pd or Pt are commonly employed for this purpose, as they can adsorb the hydrogen gas produced at the cathode, minimizing bubble formation [41,42]. However, this approach has not been successfully employed in the reverse polarity mode because O_2 is produced under these conditions, which is not as actively adsorbed by the metal electrodes. Another challenge with the off-channel configuration is that the microfabricated metal band electrodes are not always stable in the presence of high separation fields. Additionally, it can be difficult to simultaneously fabricate the Pt or Pd electrodes for the decoupler and different materials for detection electrodes (such as carbon) into the same device. To circumvent both of these problems, metal wire electrodes embedded in an epoxy or polystyrene substrate have been used as a decoupler instead of microfabricated electrodes [43,44].

In addition to metal-based decouplers, a cellulose acetate decoupler has been reported for ME-EC. This method is similar to the CE method in which a fracture is created on the capillary, which is then covered by an ion-permeable membrane such as cellulose acetate or nafion, and placed in the ground reservoir [45-47]. Using the cellulose acetate decoupler in either CE or ME devices, separation current is then grounded through this fracture. Analyte is pushed from the fracture (decoupler) to the working electrode by the EOF that is produced in the separation part of the capillary. In the ME-EC report, a cellulose acetate decoupler was is placed over a part of the separation channel that has been etched to provide an ion path. Using this configuration, very low noise good LODs were observed [48].

The primary advantage of using the off-channel configuration is that the detector is isolated from the noise induced from fluctuations in the separation field, which can result in lower LODs. However, this approach also requires a strong EOF so that the analytes are pushed to the detection electrode with minimum band broadening. If low pH run buffers are employed with glass or fused silica substrates, band broadening can occur at the detection electrode because the flow profile changes from plug to parabolic flow after the decoupler [39]. The distance between the decoupler and the working electrode should also be kept to a minimum.

2.4.2.3 In-channel detection

The third approach to performing amperometric detection in ME, in-channel detection, requires an isolated or "floating" potentiostat that is not electrically grounded. If an ungrounded "floating" potentiostat is available, it is possible to place the working electrode directly inside the channel (Figure 2.6C). However, it is important to note that most common commercially available potentiostats are grounded and cannot be employed in this configuration, since the high

voltage will ground through the working electrode and potentiostat, destroying the electronic components of the potentiostat.

In-channel amperometric detection using an isolated potentiostat has been reported for both normal and reverse polarity separations [33,34]. The advantage of this configuration is that it minimizes band broadening because there is no band dispersion in the channel and, therefore, high separation efficiencies and sensitivity can be obtained. However, because the electrode is placed in the separation field, there can be both potential shifts and noise due to separation voltage fluctuations, which can affect the LODs that can be achieved (as discussed in section 2.4.1). To address the LODs concern, a dual channel/dual electrode approach has been reported for background subtraction [22,49]. The microchip contains two separation channels: one is used as a separation channel and the second is used as a reference channel. The symmetry of dual-channel microchips allows symmetrical voltage distribution through the two channels and, therefore, a similar volume of sample and buffer can be injected into each channel. A reference and working electrode are placed inside the separation and reference channels, respectively. The noise due to fluctuations in the separation voltage will be the same at both electrodes and thus can be cancelled out [22,49].

2.5 Electrode configurations

Analytical performance of an amperometric detector that is integrated with microchip electrophoresis is highly dependent on the working electrode composition (*e.g.*, carbon- or metal-based), electrode size, the number of electrodes (*e.g.*, single electrode versus electrode array), alignment (*e.g.*, in-channel, end-channel, or off-channel), and whether a two- or three-electrode system is used.

2.5.1 Microelectrodes

For ME-EC measurements, many different types and sizes of microelectrodes have been employed. The current response obtained in any electrochemical system depends on the dimensions of the electrodes used for the measurements. Width is the most critical dimension for the band electrodes that are more commonly employed with ME-EC. When the width of a band electrode is smaller than 12.5 μm, the electrode is considered to an ultramicroelectrode, while electrodes with widths of less than or equal to 100 nm are termed nanoelectrodes. As the size of the electrode decreases, mass transport to the electrode surface increases but the geometric area of the electrode decreases and therefore the signal decreases. The IR drop, along with the background currents, is also significantly decreased [50]. Compared to the signal, noise decreases at a higher rate as the electrode becomes smaller, resulting in improved S/N ratios when using micro- or nanoelectrodes [51].

2.5.2 Multiple electrodes

Multiple electrode detection systems using micro- or nanoelectrodes can be used in an array format for signal enhancement or for peak identification using dual electrodes. These systems can provide additional information about the identity of the analyte and/or enhance sensitivities.

2.5.2.1 Electrode arrays

Microelectrodes as working electrodes for microchip electrophoresis are of considerable importance because of their ultrafast mass transport due to small electrode dimensions, reduced IR drop, and improved S/N ratio. If a collection of microelectrodes is used in an array, it has a higher S/N than does a single electrode of total geometric area equal to that of the array. This is due to the fact that capacitive currents (overall noise) are proportional to the active surface (sum

of the area of individual electrodes) of the electrode array while the overall response is proportional to the geometric area (area of the electrode array). Arrays using carbon ink electrodes were employed in ME-EC by the Martin group to enhance the LOD obtained for catecholamines [44,52].

2.5.2.2 Dual electrodes

There are two types of dual electrode configurations that are commonly employed for amperometric detection: dual-parallel and dual-series. Dual-parallel electrodes are configured so that solution flows over both electrodes simultaneously. In the series configuration, one electrode follows the other, so solution "sees" the first electrode before the second.

Both dual-series and dual-parallel electrode configurations have been widely employed in LC and CE with electrochemical detection for voltammetric identification of analytes [53-56]. Dual-series electrodes have also been employed in microchip electrophoresis in the generation-collection mode, where analytes are identified based on chemically reversible redox processes [57-59]. In this mode, the first electrode is commonly utilized for generation of the oxidation product of a reduced compound. The product is then reduced back to the original reduced species at the second electrode. The reduction usually occurs at a more selective detection potential than the oxidation since there are few reducible compounds in biological samples. Determination of catecholamines is a common application of this approach [57-59]. Catechol-containing compounds are oxidized to their corresponding orthoquinones at the first electrode, and then reduced back to the catechol at the second electrode. Selectivity is obtained at the second electrode due to the low reduction potential necessary to detect the orthoquionone product.

Collection efficiency between electrodes, or the percentage of species reduced at the second electrode compared to the amount of species oxidized at the first electrode, can also be

used for identification of analytes. This is due to the fact that the collection efficiency is different for different species and is dependent on the reversibility of the electrochemical reaction. For example, phenol, catechol, and trihydroxyphenol all display different degrees of chemical reversibility and, therefore, different current ratios. The dual-series configuration has been used extensively for the identification of phenolic acids and catecholamines after microchip electrophoresis separations [57-59].

Even though the dual-parallel configuration has been successfully employed for voltammetric characterization of analytes through current ratios in capillary elecrophoresis [60], this configuration has not been used in ME-EC. This is due to difficulties in the fabrication and design of two microelectrodes in a parallel configuration in the narrow electrophoresis channel. Recently, Gunasekara *et al.* developed a dual-parallel electrode configuration using a dual-channel microchip design (Figure 2.3C). They used this dual-parallel configuration to identify contaminating species in peroxynitrite samples and macrophage cell lysates [61].

Voltammetry could potentially be used for identification of compounds; however, potential scanning techniques such as cyclic voltammetry and square wave voltammetry are difficult to implement in microchip electrophoresis. Some of the challenges include the high background noise that results from the voltage scanning due to capacitance (charging current), low temporal resolution of slow scanning techniques, high LODs, and reduced sensitivity [62-64].

2.6 Electrode materials

As stated earlier, the selection of electrode material is an important consideration in ME-EC. Most electrodes can be classified into two types: carbon-based electrodes and metal-based electrodes, and both types are discussed in more detail in this section.

2.6.1 Carbon-based electrodes

Carbon-based electrodes have many advantages over metal-based electrodes, and have been used extensively in microchip electrophoresis systems. Practically, carbon electrodes are relatively inexpensive and are simple to fabricate. Electrochemically, carbon electrodes have a large potential window, low background noise, low over-potential, and less fouling than their metal-based counterparts [13]. Additionally, many biologically relevant analytes are organic compounds and, therefore, generate a better response at carbon-based electrodes. Many different types of carbon have been integrated into microchip electrophoresis devices, including carbon fiber, carbon paste, carbon ink, pyrolyzed photoresist film carbon, carbon nanotubes, and boron-doped diamond electrodes. While carbon electrodes are an excellent choice for microchips made from PDMS and other polymers, plastics, or hybrid chips, they are not currently compatible with fabrication of an all-glass chip.

Carbon fiber electrodes are often employed for amperometric detection in microchip electrophoresis [65]. The primary method for integrating carbon fibers into ME is by placing the fiber into a PDMS substrate. A trench that is the width of the fiber is typically created in a PDMS substrate supported on a glass backing. The carbon fiber is then laid on the trench and pushed into it, taking extreme care not to break the fiber. To make connections to the fiber, a copper wire is epoxied onto the glass backing, and the fiber and wire are connected using colloidal silver. The process for making these electrodes can be seen in Figure 2.7. While this procedure produces a fairly rugged electrode substrate that can, with care, last for months or years, the process for inserting the fiber into the trench can be difficult and time consuming for a novice. Additionally, these electrodes are limited in size by what is commercially available, generally 7 and 33 μm in diameter.

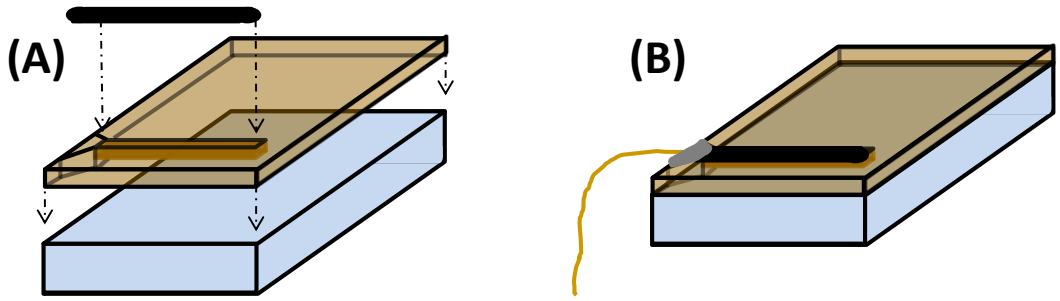

Figure 2.7 Fabrication of a carbon fiber electrode into a PDMS substrate. (A) A PDMS slab with a trench is placed onto a glass plate for stability and a carbon fiber is rolled into the trench. (B) Electrode substrate, complete with silver colloidal and copper wire connections.

An alternative method to integrate both carbon and metal (section 2.6.2) electrodes into microchip electrophoresis devices is to embed the electrode into epoxy or polystyrene. This fabrication method was developed by the Martin group [28,43,44,66], and allows for the electrode to be polished (and the surface cleaned) prior to each use. In this procedure, an electrode is placed into a mold than is then filled with powdered polystyrene. The polystyrene is then melted, cooled, and the electrode-containing polystyrene substrate is removed from the mold. The substrate is then polished using a wet grinder to create a useable substrate. The procedure for this fabrication method can been seen in Figure 2.8.

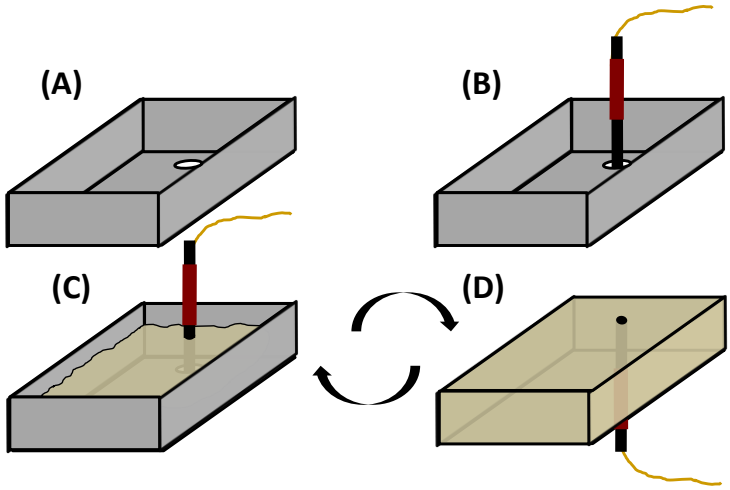

Figure 2.8 Epoxy or polystyrene embedded electrode fabrication. (A) Mold for eventual substrate with hole in the bottom for electrode. (B) Electrode with connections is placed into the hole in the mold. (C) Powdered epoxy or polystyrene is placed into the mold and melted to create the electrode substrate. (D) Substrate is removed from the mold and polished to create a useable electrode substrate.

Following their introduction by Ralph N. Adams in the 1950s [67], carbon paste electrodes have been employed for many years for electrochemical applications and were first integrated into microchip electrophoresis devices in 2001 by the Lunte group [68]. These electrodes are more easily fabricated than carbon fibers; however, they also cannot be produced by classic lithographic techniques. To create a carbon paste electrode for microchip electrophoresis, a trench is built in a substrate (PDMS, PMMA, glass) and a mixture of a carbon-based material (graphite, carbon nanotubes, etc.), and a binding agent (oil) is pressed into the trench [69]. This procedure can be visualized in Figure 2.9. One of the benefits of this procedure is that the carbon paste can also be integrated into more rigid substrates, such as plastics or glass, whereas carbon fibers can only be placed in the more malleable PDMS. For

example, carbon paste electrodes have been integrated into PMMA substrates for the detection of dopamine and catechol following microchip electrophoresis using a PDMS/PMMA hybrid simple-t device [69].

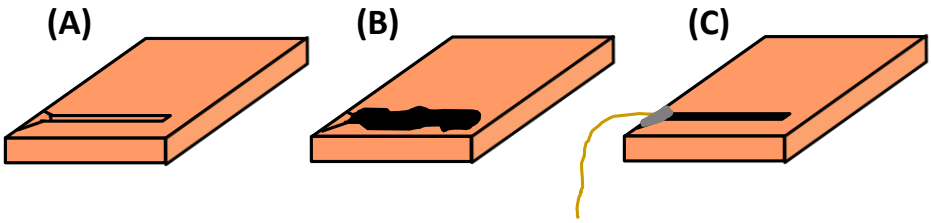

Figure 2.9 Carbon paste electrode fabrication. (A) PDMS, PMMA, or glass substrate with a trench, (B) carbon material and binding agent pressed into trench, (C) electrode polished with excess paste removed and silver colloidal and copper wire attached.

Carbon ink electrodes have also been employed with ME-EC. These electrodes are fabricated by micromolding or screen printing and can be integrated into a variety of substrates, including PDMS [39], glass [70], and epoxy [44]. Wang's group employed an external screen-printed carbon ink electrode for end-channel detection in an all-glass microchip [71].

Pyrolyzed photoresist film carbon electrodes offer the sizeable advantage that they can be manufactured using classic photolithography techniques [72,73]. These electrodes are manufactured by depositing photoresist in the pattern of the desired electrode onto a glass plate using photolithography. The glass plates with photoresist are placed under inert conditions in temperatures up to 1100°C to create the final electrode. The procedure can be seen in Figure 2.10. These electrodes have been shown to have near-atomic flatness and good electrochemical properties similar to those of traditional glassy carbon electrodes; however, they do have a lower

oxygen/carbon ratio, leading to slower electron transfer kinetics for some analytes such as dopamine [72]. These electrodes have been employed previously in ME-EC devices [57].

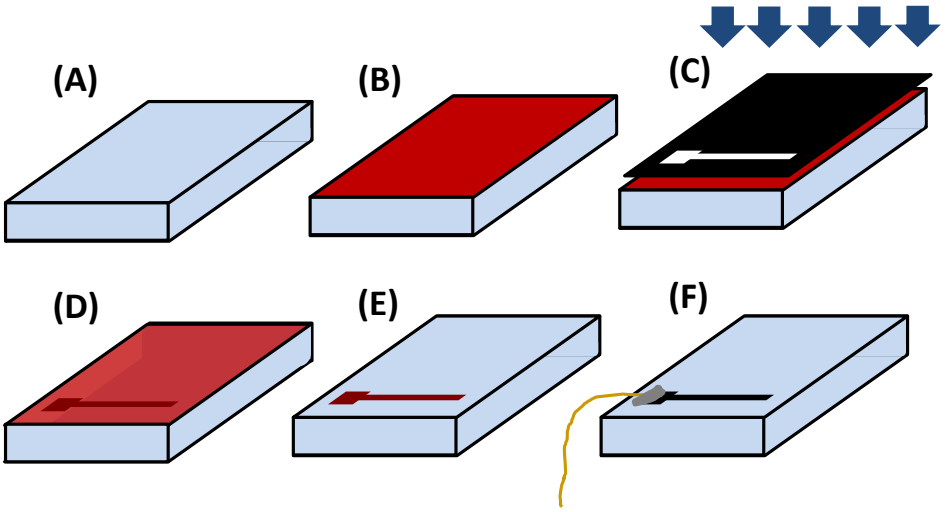

Figure 2.10 Pyrolyzed photoresist film (PPF) carbon electrode fabrication. (A) Fused silica glass electrode substrate. (B) Positive photoresist is deposited on the electrode substrate. (C) A mask with desired features is placed over the substrate and is exposed to UV light. (D) Substrate is placed in photoresist developer and (E) Only the electrode (in photoresist) remains after development. (F) After pyrolysis in a tube furnace, a carbon electrode remains on the substrate. Connections are made with silver colloidal and copper wire.

Surface electron transfer kinetics with carbon electrodes is highly dependent on the arrangement of carbon atoms in different planes [74]. Carbon nanotubes, one of the important allotropes of carbon, generate a large surface area, exhibit reduced surface fouling, and have significant electrocatalytic activity. Signal enhancement is possible with carbon nanotubes due

to the large surface area available for the redox process. In general, the use of carbon nanotubes in ME-EC leads to low limits of detection by increasing the signal more than the noise [75].

Boron-doped diamond electrodes are also important for electrochemical detection as they offer less capacitive currents, decreased surface fouling, and a broad potential window [76-78]. Preparation of these electrodes is accomplished by depositing a thin film of boron-doped diamond on silicon wafers using a high pressure plasma-assisted chemical vapor deposition system with both carbon and boron sources. After the deposition, chemical etching is used to dissolve the silicon wafer substrate to obtain a boron doped-diamond thin film electrode. This thin film can then be attached to substrates with an adhesive [78]. Boron-doped diamond electrodes have been used for ME-EC analysis of nitroaromatic explosives, organophosphate nerve agents, and phenols. The main advantage of this electrode material for ME-EC is its ruggedness and reproducibility [79].

2.6.2 Metal-based electrodes

Pt, Pd, Au, Cu, and Ag electrodes have all been employed in ME-EC devices. Metal electrodes have the advantage over carbon electrodes in that they can be fabricated using classic lithography techniques, are amenable to mass production commercially (MicruX Technologies and MicroLIQUID are two examples), their fabrication is well described in the literature, and they can be used in all-glass devices [80-82]. However, these electrodes can be fairly expensive to purchase or fabricate. Additionally, depending on the metal employed, a major disadvantage of these electrodes for ME-EC is that most metals require an adhesion layer (typically titanium, tantalum, or nichrome) to adhere to glass. This adhesion layer can generate an insulating oxide layer through grain boundary diffusion and limit the lifetime of the electrode when exposed to

the separation field. Undesired reactions such as adsorption of gases, formation of oxide layers, and adsorption of organics are also drawbacks of metal electrodes.

To fabricate a metal electrode on a glass substrate, glass substrates coated with chrome and positive photoresist are generally used as a substrate. The desired electrode geometry is patterned onto the substrate using a transparency mask and a UV flood source. The photoresist is developed, and the underlying chrome layer is etched away using chrome etchant. Using a buffered oxidant, the glass is etched to produce a trench. Lastly, a thin layer of an adhesion metal is deposited in the trench followed by the desired electrode material using a metal deposition system. The excess metal, photoresist, and chrome layer are removed to obtain a metal electrode supported on glass [80]. This procedure can be seen in Figure 2.11.

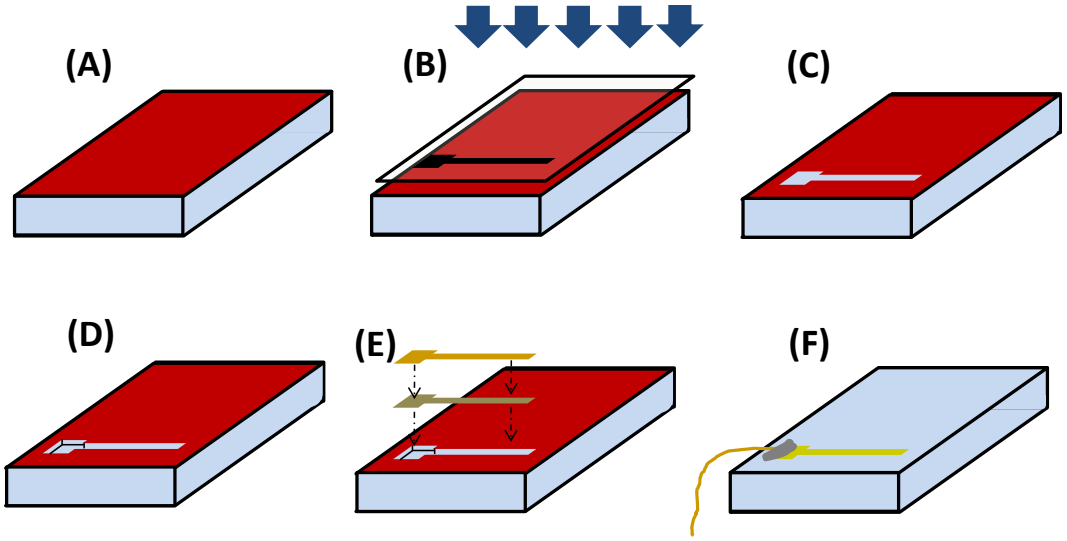

Figure 2.11 Fabrication of metal electrodes onto a glass substrate. (A**)** Glass substrate covered with a layer of photoresist and chrome. (B) A mask with the desired features is placed over the substrate and exposed with UV light. (C) The photoresist is developed, and the underlying chrome layer is removed to show bare glass in the design of the desired feature. (D) The glass is etched down to produce a trench. (E) An adhesion metal and the desired electrode metal are deposited onto the substrate. (F) After excess photoresist and chrome are removed, and electrical connections are made, a substrate with a metal electrode remains.

As a substitute for metal deposition, a trench on a PDMS substrate similar to that used for integration of carbon fiber electrodes can also be employed to integrate metal wires or the electrodes can simply be glued into the substrate [83]. Also, metal wire electrodes embedded in an epoxy or polystyrene substrate (as described in section 3.6.1 for carbon fiber electrodes) have been used in microchip electrophoresis [43].

2.7 Biological applications of ME-EC

Microchip electrophoresis with electrochemical detection has been employed for a variety of applications. Many features of ME-EC such as its small size, portability, availability and ability to obtain specific designs, low reagent consumption, and the ability to perform analysis with limited sample volume are difficult or impossible to achieve using traditional benchtop analytical instrumentation. ME-EC has therefore found widespread use in biological, environmental, and food-based applications. In this chapter, representative biological applications involving cellular analyses, and amino acid analysis are presented. Chapter 3 will describe the applications of ME-EC involving the analysis of microdialysis samples.

2.7.1 Cellular analysis

Cellular analysis has been performed using ME-EC, and was reviewed previously [3]. In addition to cellular analysis using MD-ME-EC (highlighted in Chapter 4), the Martin group also developed a microchip device that was capable of immobilization of PC-12 cells in a collagen-coated micropallet, cell stimulation, sample injection and separation, and detection of dopamine and norepinephrine at a carbon ink microelectrode, all on-chip [84]. An integrated polystyrene and PDMS hybrid device was recently developed by the same group and has the ability to perform on-chip cell culture and detection of cellular release with ME-EC [66].

The quantification of pro-oxidants and antioxidants in cells reveals the cellular redox status and thus facilitates the understanding of diseases and disorders caused by the imbalance between pro-oxidants and antioxidants. The short channels and fast separations characteristic of ME allows for the detection of reactive species such as peroxynitrite and nitric oxide before they degrade significantly [34,85,86]. Microchip electrophoresis also permits the separation of the metabolites of these reactive species and cell antioxidants. Recently ME-EC was used for the

analysis of NO_2^-, NO, and antioxidants in macrophage cells employing a simple-t device with in-channel detection and a Pt working electrode [87].

2.7.2 Amino acid and carbohydrate analysis

Amino acid analysis, while generally performed by precolumn derivatization and ME-LIF, has also been accomplished using ME-EC. One strategy for the detection of amino acids by ME-EC is to derivatize the compounds with an electroactive tag. The products of both o-phthaldialdehyde (OPA) and naphthalene-2,3-dicarboxaldehyde (NDA) are isoindoles that are electrochemically active. This strategy has been used, along with ME-EC, to separate NDA/CN^- derivativized citrulline and glycine, which were then detected using the end-channel configuration with a carbon paste electrode [65]. Wang and coworkers employed on-chip derivatization using (OPA)/2-mercaptoethanol and separation and detection using microchip electrophoresis at a gold screen-printed working electrode in the end-channel configuration to detect histidine, valine, isoleucine, leucine, glutamic acid, aspartic acid, arginine, and lysine [88].

Carbohydrates have also been separated with microchip electrophoresis and detected directly with electrochemistry. Garcia et. al. employed pulse amperometric detection at a gold electrode after microchip electrophoresis separation to detect both amino acids and carbohydrates [89]. Swartz et al. successfully separated and detected galactose, fructose, and sucrose, using microchip electrophoresis and direct electrochemical detection with a copper-coated Pt electrode [90].

2.8 Conclusions

Microchip electrophoresis with electrochemical detection is a powerful technique that is being employed for fast, near real-time, on-site analysis of many different compounds. However, as discussed in this chapter, care must be taken to integrate electrochemical detection

into microchip electrophoresis platforms. When performed well, the microchip format allows multiple processes to be integrated on-chip prior to separation and detection. Additionally, the small format permits portable analysis. In the future, these benefits will continue to be exploited for applications such as cell cytometry, on-animal sensing, and portable diagnostics. Microchip electrophoresis with electrochemical detection will be employed in the next chapter for the separation of analytes in the dopamine metabolic pathway, with the eventual goal of on-line analysis of these analytes.

2.9 References

[1] A. Manz, N. Graber, H.M. Widmer, Miniaturized total chemical analysis systems: a novel concept for chemical sensing, Sens. Actuators, B 1 (1990) 244-248.

[2] S.C. Jacobson, R. Hergenroder, L.B. Koutny, J.M. Ramsey, High-Speed Separations on a Microchip, Anal. Chem. 66 (1994) 1114-1118.

[3] A.S. Johnson, A. Selimovic, R.S. Martin, Microchip-based electrochemical detection for monitoring cellular systems, Anal. Bioanal. Chem. 405 (2013) 3013-3020.

[4] R.A. Saylor, S.M. Lunte, A review of microdialysis coupled to microchip electrophoresis for monitoring biological events, J. Chromatogr. A 1382 (2015) 48-64.

[5] G. Chen, Y. Lin, J. Wang, Microchip capillary electrophoresis with electrochemical detection for monitoring environmental pollutants, Curr. Anal. Chem. 2 (2006) 43-50.

[6] A. Martin, D. Vilela, A. Escarpa, Food analysis on microchip electrophoresis: An updated review, Electrophoresis 33 (2012) 2212-2227.

[7] J.J.P. Mark, R. Scholz, F.-M. Matysik, Electrochemical methods in conjunction with capillary and microchip electrophoresis, J. Chromatogr. A 1267 (2012) 45-64.

[8] P. Kuban, P.C. Hauser, Fundamentals of electrochemical detection techniques for CE and MCE, Electrophoresis 30 (2009) 3305-3314.

[9] N.A. Lacher, K.E. Garrison, R.S. Martin, S.M. Lunte, Microchip capillary electrophoresis/electrochemistry, Electrophoresis 22 (2001) 2526-2536.

[10] W.R.I.V. Vandaveer, S.A. Pasas-Farmer, D.J. Fischer, C.N. Frankenfeld, S.M. Lunte, Recent developments in electrochemical detection for microchip capillary electrophoresis, Electrophoresis 25 (2004) 3528-3549.

[11] H. Whatley, in: J.R. Petersen, A.A. Mohammad (Eds.), Clinical and Forensic Applications of Capillary Electrophoresis, Humana Press Inc., 2001, p. 21-58.

[12] J.C. Giddings, Unified Separation Science, John Wiley & Sons, Inc, New York, 1961.

[13] A.J. Bard, L.R. Faulkner, Electrochemical Methods: Fundamentals and Applications, John Wiley & Sons, Inc., Hoboken, NJ, 2002.

[14] P.N. Nge, C.I. Rogers, A.T. Woolley, Advances in Microfluidic Materials, Functions, Integration, and Applications, Chem. Rev. 113 (2013) 2550-2583.

[15] H. Makamba, J.H. Kim, K. Lim, N. Park, J.H. Hahn, Surface modification of poly(dimethylsiloxane) microchannels, Electrophoresis 24 (2003) 3607-3619.

[16] B.E. Slentz, N.A. Penner, F. Regnier, Sampling BIAS at channel junctions in gated flow injection on chips, Anal Chem 74 (2002) 4835-4840.

[17] S.V. Ermakov, S.C. Jacobson, J.M. Ramsey, Computer Simulations of Electrokinetic Injection Techniques in Microfluidic Devices, Anal. Chem. 72 (2000) 3512-3517.

[18] J.M. Karlinsey, Sample introduction techniques for microchip electrophoresis: A review, Anal. Chim. Acta 725 (2012) 1-13.

[19] K. Seiler, D.J. Harrison, A. Manz, Planar glass chips for capillary electrophoresis: repetitive sample injection, quantitation, and separation efficiency, Anal. Chem. 65 (1993) 1481-1488.

[20] S.K. Griffiths, R.H. Nilson, Low-Dispersion Turns and Junctions for Microchannel Systems, Anal. Chem. 73 (2001) 272-278.

[21] C. Chen, J. Hahn, Enhanced aminophenols monitoring using in-channel amperometric detection with dual-channel microchip capillary electrophoresis, Environmental Chemistry Letters 9 (2011) 491-497.

[22] C. Chen, J.H. Hahn, Dual-Channel Method for Interference-Free In-Channel Amperometric Detection in Microchip Capillary Electrophoresis, Anal. Chem. 79 (2007) 7182-7186.

[23] S. Attiya, A.B. Jemere, T. Tang, G. Fitzpatrick, K. Seiler, N. Chiem, D.J. Harrison, Design of an interface to allow microfluidic electrophoresis chips to drink from the fire hose of the external environment, Electrophoresis 22 (2001) 318-327.

[24] Y.-H. Lin, G.-B. Lee, C.-W. Li, G.-R. Huang, S.-H. Chen, Flow-through sampling for electrophoresis-based microfluidic chips using hydrodynamic pumping, J. Chromatogr. A 937 (2001) 115-125.

[25] B.H. Huynh, B.A. Fogarty, R.S. Martin, S.M. Lunte, On-Line Coupling of Microdialysis Sampling with Microchip-Based Capillary Electrophoresis, Anal. Chem. 76 (2004) 6440-6447.

[26] M.W. Li, B.H. Huynh, M.K. Hulvey, S.M. Lunte, R.S. Martin, Design and Characterization of Poly(dimethylsiloxane)-Based Valves for Interfacing Continuous-Flow Sampling to Microchip Electrophoresis, Anal. Chem. 78 (2006) 1042-1051.

[27] M.W. Li, R.S. Martin, Integration of continuous-flow sampling with microchip electrophoresis using poly(dimethylsiloxane)-based valves in a reversibly sealed device, Electrophoresis 28 (2007) 2478-2488.

[28] L.C. Mecker, R.S. Martin, Integration of Microdialysis Sampling and Microchip Electrophoresis with Electrochemical Detection, Anal. Chem. 80 (2008) 9257-9264.

[29] M.K. Hulvey, S.M. Lunte, D.J. Fischer, C.D. Kuhnline, Electrochemical Detection Methods Following Liquid Chromatography, Capillary Electrophoresis, and Microchip Electrophoresis Separations, Encyclopedia of Analytical Chemistry.

[30] P.T. Kissinger, W.R. Heineman, Laboratory techniques in electroanalytical chemistry, Marcel Dekker, Inc, New York, 1996.

[31] S. Creager, in: C.G. Zoski (Ed.), Handbook of Electrochemistry, Elsevier, San Diego, 2007, p. 57-72.

[32] D. Meneses, D.B. Gunasekara, P. Pichetsurnthorn, J.A.F. da Silva, F.C. de Abreu, S.M. Lunte, Evaluation of in-channel amperometric detection using a dual-channel microchip electrophoresis device and a two-electrode potentiostat for reverse polarity separations, Electrophoresis 36 (2015) 441-448.

[33] R.S. Martin, K.L. Ratzlaff, B.H. Huynh, S.M. Lunte, In-channel electrochemical detection for microchip capillary electrophoresis using an electrically isolated potentiostat, Anal. Chem. 74 (2002) 1136-1143.

[34] D.B. Gunasekara, M.K. Hulvey, S.M. Lunte, In-channel amperometric detection for microchip electrophoresis using a wireless isolated potentiostat, Electrophoresis 32 (2011) 832-837.

[35] R. Kuldvee, M. Kaljurand, H. Smit, Improvement of Signal-to-Noise Ratio of Electropherograms and Analysis Reproducibility with Digital Signal Processing and Multiple Injections, Journal of High Resolution Chromatography 21 (1998) 169-174.

[36] W. Lu, R.M. Cassidy, Background noise in capillary electrophoretic amperometric detection, Analytical Chemistry 66 (1994) 200-204.

[37] N.M. Contento, P.W. Bohn, Electric field effects on current-voltage relationships in microfluidic channels presenting multiple working electrodes in the weak-coupling limit, Microfluid. Nanofluid. 18 (2015) 131-140.

[38] S.P. Forry, J.R. Murray, M.L.A.V. Heien, L.E. Locascio, R.M. Wightman, Probing Electric Fields Inside Microfluidic Channels during Electroosmotic Flow with Fast-Scan Cyclic Voltammetry, Anal. Chem. 76 (2004) 4945-4950.

[39] D.J. Fischer, M.K. Hulvey, A.R. Regel, S.M. Lunte, Amperometric detection in microchip electrophoresis devices: Effect of electrode material and alignment on analytical performance, Electrophoresis 30 (2009) 3324-3333.

[40] Q. Guan, C.S. Henry, Improving MCE with electrochemical detection using a bubble cell and sample stacking techniques, Electrophoresis 30 (2009) 3339-3346.

[41] N.A. Lacher, S.M. Lunte, R.S. Martin, Development of a microfabricated palladium decoupler/electrochemical detector for microchip capillary electrophoresis using a hybrid glass/poly(dimethylsiloxane) device, Anal. Chem. 76 (2004) 2482-2491.

[42] C.-C. Wu, R.-G. Wu, J.-G. Huang, Y.-C. Lin, H.-C. Chang, Three-Electrode Electrochemical Detector and Platinum Film Decoupler Integrated with a Capillary Electrophoresis Microchip for Amperometric Detection, Anal. Chem. 75 (2003) 947-952.

[43] A.S. Johnson, A. Selimovic, R.S. Martin, Integration of microchip electrophoresis with electrochemical detection using an epoxy-based molding method to embed multiple electrode materials, Electrophoresis 32 (2011) 3121-3128.

[44] A. Selimovic, A.S. Johnson, I.Z. Kiss, R.S. Martin, Use of epoxy-embedded electrodes to integrate electrochemical detection with microchip-based analysis systems, Electrophoresis 32 (2011) 822-831.

[45] D.M. Osbourn, C.E. Lunte, Cellulose acetate decoupler for on-column electrochemical detection in capillary electrophoresis, Analytical Chemistry 73 (2001) 5961-5964.

[46] S. Park, S.M. Lunte, C.E. Lunte, A perfluorosulfonated ionomer joint for capillary electrophoresis with on-column electrochemical detection, Anal. Chem. 67 (1995) 911-918.

[47] T.J. O'Shea, R.D. Greenhagen, S.M. Lunte, C.E. Lunte, M.R. Smyth, D.M. Radzik, N. Watanabe, Capillary electrophoresis with electrochemical detection employing an on-column Nafion joint, J. Chromatogr. 593 (1992) 305-312.

[48] D.M. Osbourn, C.E. Lunte, On-column electrochemical detection for microchip capillary electrophoresis, Anal. Chem. 75 (2003) 2710-2714.

[49] C.-P. Chen, W. Teng, J.-H. Hahn, Nanoband electrode for high-performance in-channel amperometric detection in dual-channel microchip capillary electrophoresis, Electrophoresis 32 (2011) 838-843.

[50] P.S. Cahill, Q.D. Walker, J.M. Finnegan, G.E. Mickelson, E.R. Travis, R.M. Wightman, Microelectrodes for the Measurement of Catecholamines in Biological Systems, Anal. Chem. 68 (1996) 3180-3186.

[51] R.M. Wightman, Probing Cellular Chemistry in Biological Systems with Microelectrodes, Science 311 (2006) 1570-1574.

[52] L.C. Mecker, L.A. Filla, R.S. Martin, Use of a Carbon-Ink Microelectrode Array for Signal Enhancement in Microchip Electrophoresis with Electrochemical Detection, Electroanalysis 22 (2010) 2141-2146.

[53] C.E. Lunte, P.T. Kissinger, R.E. Shoup, Difference mode detection with thin-layer dual-electrode liquid chromatography/electrochemistry, Anal. Chem. 57 (1985) 1541-1546.

[54] C.E. Lunte, T.H. Ridgway, W.R. Heineman, Voltammetric-amperometric dual-electrode detection for flow injection analysis and liquid chromatography, Anal. Chem. 59 (1987) 761-766.

[55] D.A. Roston, R.E. Shoup, P.T. Kissinger, Liquid chromatography/electrochemistry: thin-layer multiple electrode detection, Anal. Chem. 54 (1982) 1417A-1418A, 1422A, 1424A, 1428A, 1430A, 1432A, 1434A.

[56] M. Zhong, S.M. Lunte, Tubular-Wire Dual Electrode for Detection of Thiols and Disulfides by Capillary Electrophoresis/Electrochemistry, Anal. Chem. 71 (1999) 251-255.

[57] D.J. Fischer, W.R.I.V. Vandaveer, R.J. Grigsby, S.M. Lunte, Pyrolyzed photoresist carbon electrodes for microchip electrophoresis with dual-electrode amperometric detection, Electroanalysis 17 (2005) 1153-1159.

[58] R.S. Martin, A.J. Gawron, S.M. Lunte, C.S. Henry, Dual-Electrode Electrochemical Detection for Poly(dimethylsiloxane)-Fabricated Capillary Electrophoresis Microchips, Anal. Chem. 72 (2000) 3196-3202.

[59] L.C. Mecker, R.S. Martin, Use of micromolded carbon dual electrodes with a palladium decoupler for amperometric detection in microchip electrophoresis, Electrophoresis 27 (2006) 5032-5042.

[60] M.K. Dorris, E.W. Crick, C.E. Lunte, A parallel dual-electrode detector for capillary electrophoresis, Electrophoresis 33 (2012) 2725-2732.

[61] D.B. Gunasekara, Departmet of Chemistry, University of Kansas, 2014.

[62] S.S. Ferris, G. Lou, A.G. Ewing, Scanning electrochemical detection in capillary electrophoresis, J. Microcolumn Sep. 6 (1994) 263-268.

[63] F.D. Swanek, G. Chen, A.G. Ewing, Identification of Multiple Compartments of Dopamine in a Single Cell by Scanning Electrochemical Detection, Anal. Chem. 68 (1996) 3912-3916.

[64] H. Fang, T.L. Vickrey, B.J. Venton, Analysis of Biogenic Amines in a Single Drosophila Larva Brain by Capillary Electrophoresis with Fast-Scan Cyclic Voltammetry Detection, Anal. Chem. 83 (2011) 2258-2264.

[65] A.J. Gawron, R.S. Martin, S.M. Lunte, Fabrication and evaluation of a carbon-based dual-electrode detector for poly(dimethylsiloxane) electrophoresis chips, Electrophoresis 22 (2001) 242-248.

[66] A.S. Johnson, B.T. Mehl, R.S. Martin, Integrated hybrid polystyrene-polydimethylsiloxane device for monitoring cellular release with microchip electrophoresis and electrochemical detection, Anal. Methods 7 (2015) 884-893.

[67] R.N. Adams, Carbon paste electrodes, Anal. Chem. 30 (1958) 1576.

[68] R.S. Martin, A.J. Gawron, B.A. Fogarty, F.B. Regan, E. Dempsey, S.M. Lunte, Carbon paste-based electrochemical detectors for microchip capillary electrophoresis/electrochemistry, Analyst 126 (2001) 277-280.

[69] A. Regel, S. Lunte, Integration of a graphite/poly(methyl-methacrylate) composite electrode into a poly(methylmethacrylate) substrate for electrochemical detection in microchips, Electrophoresis 34 (2013) 2101-2106.

[70] M.L. Kovarik, N.J. Torrence, D.M. Spence, R.S. Martin, Fabrication of carbon microelectrodes with a micromolding technique and their use in microchip-based flow analyses, Analyst (Cambridge, U. K.) 129 (2004) 400-405.

[71] J. Wang, B. Tian, E. Sahlin, Micromachined electrophoresis chips with thick-film electrochemical detectors, Anal Chem 71 (1999) 5436-5440.

[72] S. Ranganathan, R.L. McCreery, Electroanalytical Performance of Carbon Films with Near-Atomic Flatness, Anal. Chem. 73 (2001) 893-900.

[73] S. Ranganathan, R. McCreery, S.M. Majji, M. Madou, Photoresist-derived carbon for microelectromechanical systems and electrochemical applications, J. Electrochem. Soc. 147 (2000) 277-282.

[74] M. Pumera, A. Escarpa, Nanomaterials as electrochemical detectors in microfluidics and CE: Fundamentals, designs, and applications, Electrophoresis 30 (2009) 3315-3323.

[75] J. Wang, Electrochemical detection for capillary electrophoresis microchips: A review, Electroanalysis 17 (2005) 1133-1140.

[76] J.W. Strojek, M.C. Granger, G.M. Swain, T. Dallas, M.W. Holtz, Enhanced Signal-to-Background Ratios in Voltammetric Measurements Made at Diamond Thin-Film Electrochemical Interfaces, Anal. Chem. 68 (1996) 2031-2037.

[77] G.M. Swain, R. Ramesham, The electrochemical activity of boron-doped polycrystalline diamond thin film electrodes, Anal. Chem. 65 (1993) 345-351.

[78] D. Shin, D.A. Tryk, A. Fujishima, A. Muck, Jr., G. Chen, J. Wang, Microchip capillary electrophoresis with a boron-doped diamond electrochemical detector for analysis of aromatic amines, Electrophoresis 25 (2004) 3017-3023.

[79] J. Wang, G. Chen, M.P. Chatrathi, A. Fujishima, D.A. Tryk, D. Shin, Microchip Capillary Electrophoresis Coupled with a Boron-Doped Diamond Electrode-Based Electrochemical Detector, Anal. Chem. 75 (2003) 935-939.

[80] D.E. Scott, R.J. Grigsby, S.M. Lunte, Microdialysis Sampling Coupled to Microchip Electrophoresis with Integrated Amperometric Detection on an All-Glass Substrate, ChemPhysChem 14 (2013) 2288-2294.

[81] A.T. Woolley, K. Lao, A.N. Glazer, R.A. Mathies, Capillary Electrophoresis Chips with Integrated Electrochemical Detection, Anal. Chem. 70 (1998) 684-688.

[82] R.P. Baldwin, T.J. Roussel, Jr., M.M. Crain, V. Bathlagunda, D.J. Jackson, J. Gullapalli, J.A. Conklin, R. Pai, J.F. Naber, K.M. Walsh, R.S. Keynton, Fully integrated on-chip electrochemical detection for capillary electrophoresis in a microfabricated device, Anal. Chem. 74 (2002) 3690-3697.

[83] C.S. Henry, M. Zhong, S.M. Lunte, M. Kim, H. Bau, J.J. Santiago, Ceramic microchips for capillary electrophoresis-electrochemistry, Anal. Commun. 36 (1999) 305-307.

[84] A.L. Bowen, R.S. Martin, Integration of on-chip peristaltic pumps and injection valves with microchip electrophoresis and electrochemical detection, Electrophoresis 31 (2010) 2534-2540.

[85] D.B. Gunasekara, M.K. Hulvey, S.M. Lunte, J.A. Fracassi da Silva, Microchip electrophoresis with amperometric detection for the study of the generation of nitric oxide by NONOate salts, Anal. Bioanal. Chem. 403 (2012) 2377-2384.

[86] M.K. Hulvey, C.N. Frankenfeld, S.M. Lunte, Separation and Detection of Peroxynitrite Using Microchip Electrophoresis with Amperometric Detection, Analytical Chemistry 82 (2010) 1608-1611.

[87] D.B. Gunasekara, J.M. Siegel, G. Caruso, M.K. Hulvey, S.M. Lunte, Microchip electrophoresis with amperometric detection method for profiling cellular nitrosative stress markers, Analyst 139 (2014) 3265-3273.

[88] J. Wang, M.P. Chatrathi, B. Tian, Micromachined separation chips with a precolumn reactor and end-column electrochemical detector, Anal. Chem. 72 (2000) 5774-5778.

[89] C.D. Garcia, C.S. Henry, Direct determination of carbohydrates, amino acids, and antibiotics by microchip electrophoresis with pulsed amperometric detection, Anal. Chem. 75 (2003) 4778-4783.

[90] M.A. Schwarz, B. Galliker, K. Fluri, T. Kappes, P.C. Hauser, A two-electrode configuration for simplified amperometric detection in a microfabricated electrophoretic separation device, Analyst (Cambridge, U. K.) 126 (2001) 147-151.

Chapter 3: Microchip electrophoresis with electrochemical detection for the determination of analytes in the dopamine metabolic pathway

Adapted from: Saylor, R.A., Reid, E.A., and Lunte, S.M., "Microchip electrophoresis with electrochemical detection for the determination of analytes in the dopamine metabolic pathway," Electrophoresis 36 (2015) 1912-1919.

3.1. Introduction

Dopamine is an important neurotransmitter [1,2] that has been implicated in reward, social behavior, movement, mood, and addiction, as well as neurological disorders such as Parkinson's and Huntington's diseases [3]. The most popular method for monitoring dopamine release *in vivo* is fast scan cyclic voltammetry [4,5]. However, it is not possible to measure dopamine and its metabolites simultaneously with this technique, making it impossible to investigate the effect of drugs or other treatments on the dopamine metabolic pathway (Figure 3.1). Specifically, L-DOPA, the precursor to dopamine, has been the gold-standard treatment for Parkinson's disease for over half a century, and, therefore, much research has been performed regarding its role in neurotransmission and neuromodulation [6,7]. Methods for the simultaneous measurement of dopamine and L-DOPA along with their metabolites are important to understanding the roles of these compounds in biological processes and drug metabolism. Methods such as capillary electrophoresis with laser-induced fluorescence or electrochemical detection [8-11] and liquid chromatography with electrochemical detection [12] have been previously employed to analyze dopamine and/or related compounds in microdialysis samples and brain tissue.

Microchip electrophoresis (ME) is an excellent separation method for the analysis of biologically important molecules. Separations employing microchip electrophoresis are fast (sub-minute), highly efficient, and require low sample volumes (pL-to-nL) [13,14]. These qualities make microchip electrophoresis ideal for the analysis of time-sensitive, small volume, and precious biological samples. Additionally, microchip electrophoresis operates on a planar, chip-based platform, allowing integration of multiple steps (sampling, separation, detection) all onto a single device.

Many different substrate materials have been employed in microchip electrophoresis, including glass, PDMS, PMMA, and paper [15]. For many applications, the material of choice is glass as it has the same properties as the fused silica used in traditional capillary electrophoresis—strong EOF, low analyte adsorption, and good optical clarity. PDMS is also widely used for microchip electrophoresis due to its low cost, ease of fabrication, and the fact that electrodes can be easily incorporated into the device. However, PDMS devices have several disadvantages, including low EOF, analyte adsorption, and inconsistent analyte migration times [16]. Glass/PDMS hybrid devices can be an effective compromise in an attempt to combine the consistencies of glass with the ease of fabrication of PDMS devices.

Electrochemical detection (EC), especially amperometry, has long been employed as a detection strategy in microchip electrophoresis, due, in part, to the ability to integrate electrodes directly into the microchip format [17-19]. Additionally, many important biological molecules are natively electroactive and do not require derivatization prior to their detection. Both metal and carbon-based electrodes have been incorporated directly in-chip for a variety of applications [18,19]. However, integrating electrodes for electrochemical detection into an all-glass microchip electrophoresis device can be difficult and has not been reported for carbon electrodes. The procedure for creating all-glass microchip electrophoresis devices with integrated electrodes involves high temperatures and pressures and requires a complete seal around the electrodes and channel, which can be challenging to accomplish [20,21]. For the detection of catecholamines and related compounds, various types of carbon electrodes integrated in polymer and plastic substrates have been employed, including carbon fiber [22], carbon paste [23], carbon ink [24], and pyrolyzed photoresist film [25,26], as they generate good responses for many biological, carbon-containing analytes.

In this study, the separation and detection of compounds in the L-DOPA metabolic pathway (Figure 3.1) were optimized using microchip electrophoresis with electrochemical detection. Additionally, the performance of an all-PDMS device with a carbon fiber electrode was compared to that of a PDMS/glass hybrid device with a pyrolyzed photoresist film carbon electrode. As this method will be used in the future for on-line monitoring of brain microdialysis samples, maintaining biological and injection compatibility with the run buffer was paramount. The optimized method was then employed *in vitro* to study the metabolism of L-DOPA by a brain slice. In the future, this method will be coupled on-line to microdialysis sampling for on-animal analysis of drug metabolism *in vivo*.

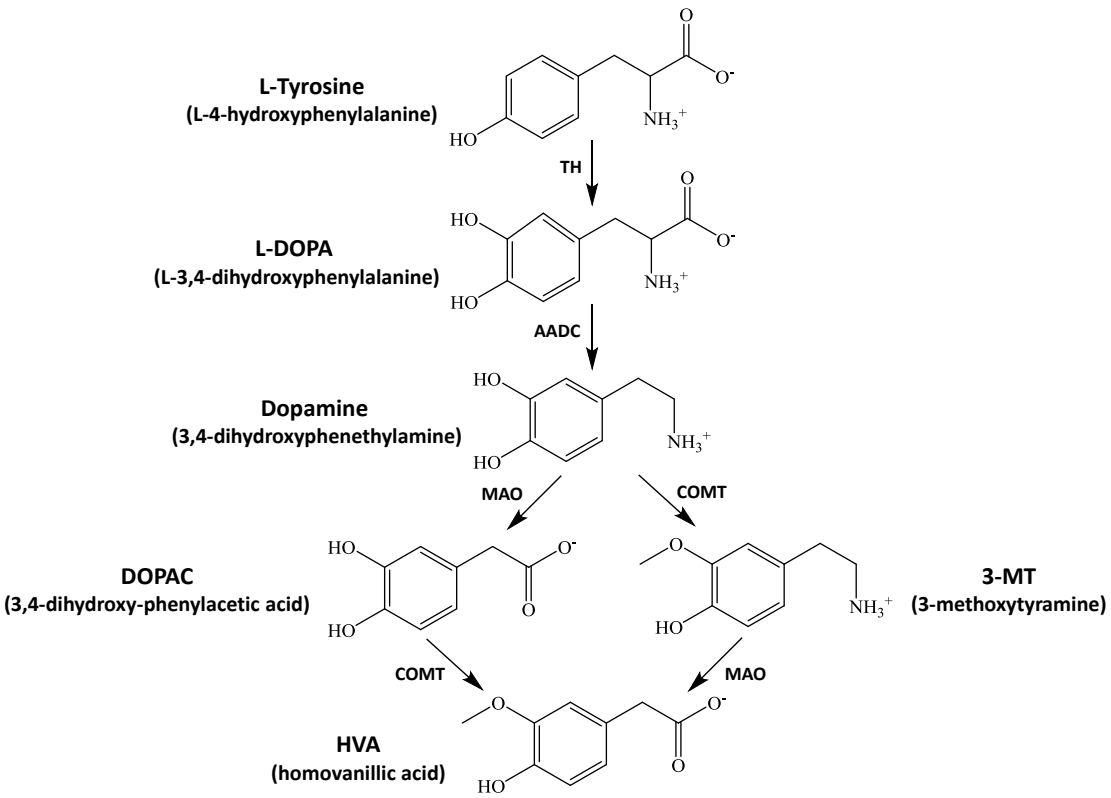

Figure 3.1 Compounds in the dopamine metabolic pathway (at pH 7.4). Enzymes are: TH (tyrosine hydroxylase), AADC (aromatic L-amino acid decarboxylase), MAO (monoamine oxidase) and COMT (catechol-o-methyltransferase).

3.2. Materials and methods

3.2.1. Reagents

The following chemicals were used as received: AZ 1518 positive photoresist and AZ 300 MIF developer (AZ Electronic Materials, Sommerville, NJ, USA); SU-8 10 and SU-8 developer (Micro-Chem, Newton, MA, USA); L-tyrosine (L-Tyr), 3,4-dihydroxy-L-phenylalanine (L-DOPA), homovanillic acid (HVA), 3,4-dihydroxyphenylacetic acid (DOPAC), dopamine hydrochloride, 3-methoxytyramine hydrochloride (3-MT), 3-nitrophenylboronic acid (3-NPBA) sodium phosphate dibasic, sodium phosphate monobasic, and boric acid (Sigma-Aldrich, St. Louis, MO, USA); NaOH and 2-propanol (IPA) (Fisher Scientific, Fairlawn, NJ, USA); sodium dodecyl sulfate (SDS) (Thermo Scientific, Waltham, MA, USA); and PDMS and curing agent (Sylgard 184 silicon elastomer base and curing agent, Dow Corning Corp., Midland, MI, USA). Additionally, the following were also used: high temperature fused silica glass plates (4 in × 2.5 in × 0.085 in, Glass Fab, Rochester, NY, USA); 33 μm diameter carbon fibers (Avco Specialty Materials, Lowell, MA, USA); copper wire (22 gage, Westlake Hardware, Lawrence, KS, USA); epoxy (J-B Weld, Sulphur Springs, TX, USA); colloidal silver liquid (Ted Pella, Inc., Redding, CA, USA); and 18.2 MΩ water (Millipore, Kansas City, MO, USA).

3.2.2. Fabrication of PDMS channels

The fabrication of PDMS microchips has been described elsewhere [27]. Briefly, a silicon master was created using SU-8 10 negative photoresist spun onto a 4 in diameter silicon wafer to a thickness of 15 μm using a Cee 100 spin coater (Brewer Science, Rolla, MO, USA). The wafer was then heated to 65°C for 2 min and ramped to 95°C for 5 min as the soft bake procedure on a programmable hotplate (Thermo Scientific, Waltham, MA, USA). After the soft bake, the coated wafer was covered with a negative transparency mask created using AutoCad

(Autodesk, San Rafael, CA, USA) and printed onto transparencies (Infinite Graphics, Minneapolis, MN, USA) of the fluidic channels and exposed at 344 mJ/cm^2 using a UV flood source (ABM Inc., Scotts Valley, CA, USA). After exposure, the wafer was again transferred to a programmable hotplate for the post-bake at 65°C for 1 min, then 95°C for 2 min. The master was then developed in SU-8 developer, rinsed with isopropyl alcohol, and dried with nitrogen. Finally, a hard bake was performed at 200°C for 2 h. This procedure produced a master with 15 µm raised channels that were 40 µm wide as measured by an Alpha Step-200 surface profiler (KLA-Tencor, Milpitas, CA). In this simple-t device, the separation channel was 5.0 cm and the side and top arms were 0.75 cm in length. To create the PDMS microchip from the silicon master, PDMS/curing agent was mixed at a 10:1 ratio and poured onto the master to a form a thickness of about 2 mm. The PDMS was cured overnight at 70°C, after which the PDMS channels were peeled from the Si wafer. Reservoirs for buffer and pump waste were punched into the PDMS using a 4 mm biopsy punch (Harris Uni-Core, Ted Pella, Inc., Redding, CA, USA).

3.2.3. Electrode fabrication

3.2.3.1. Carbon fiber electrode in PDMS

The placement of carbon fiber electrodes into PDMS has been described previously [28] and can be seen in Chapter 2 (Figure 2.7). Briefly, a 5 in silicon master wafer containing a raised structure with the dimensions 35 µm × 40 µm was created using the same procedure outlined in section 2.2. PDMS was poured over the master to create a trench with the same dimensions. Once hardened, the PDMS was placed on a glass plate to add structural stability, and a 33 µm carbon fiber was placed into the trench. The carbon fiber was connected to detection electronics through silver colloidal liquid and copper wire.

3.2.3.2. Pyrolyzed photoresist film electrode on quartz glass

Pyrolyzed photoresist film (PPF) electrode fabrication has been described previously [25,29] and can be seen in Chapter 2 (Figure 2.10). Briefly, a 2.5 × 4 in plate of quartz glass was cleaned using acid and base piranha. After drying the substrate for 2 h at 200°C on a programmable hotplate, AZ 1518 positive photoresist was spun onto the substrate using a Cee 100 spin coater. Photoresist (4 mL) was dynamically deposited on the substrate while at 100 rpm for 10 s. The spin coater was then ramped at 500 R/s to 2,000 rpm and held for 20 s. The substrate was then heated to 100°C for 1.5 min on a programmable hotplate. Positive mask designs for the electrodes were created using AutoCad software and printed onto transparencies. The coated substrate was placed on a reflective surface, covered with the transparency mask, and exposed at 21.5 mW/cm^2 for 4 s using a UV floodsource. Post exposure, the substrate was developed in MIF 300 for about 10 s and rinsed with nanopure water.

Substrates with photoresist were then placed in a Linden-BlueM 3 Zone Tube furnace (Cole-Parmer, Vernon Hills, IL, USA), with a constant flow of nitrogen gas at about 5 psi throughout the pyrolysis procedure. The temperature program was ramped from room temperature to 925°C at 5.5°C/min and held there for 1 h. The furnace was then allowed to cool to room temperature. Final electrode dimensions after pyrolysis, as measured using a surface profiler, were 35 μm wide and 0.5 μm in height.

3.2.4. Electrophoresis procedure

Complete microchips for microchip electrophoresis were constructed by placing the PDMS channel layer in conformal contact with the electrode containing substrate (either PDMS with a carbon fiber electrode or glass with a PPF electrode), creating a reversible bond between

the two. Care was taken to align the electrode at the very end of the separation channel (Figure 3.2).

Prior to electrophoresis, the channels in the device were flushed with isopropyl alcohol, 0.1 M NaOH, and the separation buffer for about 5 min each. All electrophoresis procedures were accomplished using two Spellman CZE 1000R (Hauppauge, NY, USA) high voltage power supplies controlled using LabView (National Instruments, Austin, TX, USA) programs written in-house. A gated injection scheme was utilized for sample introduction and separation in the simple-t device. A gate was accomplished by applying 1900 V at the sample reservoir, 1600 V at the buffer reservoir, and holding the sample waste and detection reservoirs at ground (Figure 3.2). All injections were accomplished by floating the buffer voltage for 1.0 s, then reapplying the voltages for the separation. Standard stock solutions (10 mM) were prepared daily in 18.2 mΩ water and diluted into 15 mM phosphate buffer (pH 7.4) at the time of analysis. Unless otherwise noted, 100 μM standard solutions were employed.

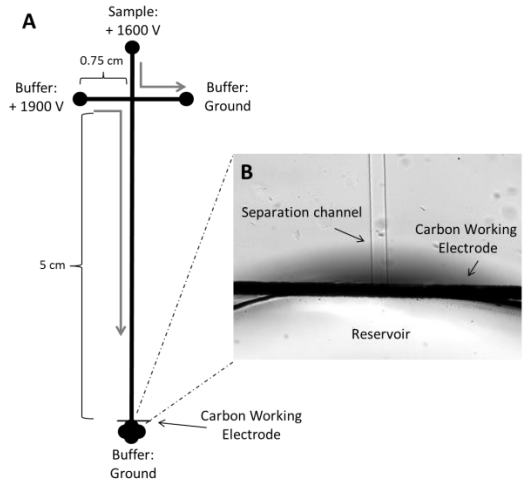

Figure 3.2. Simple-t microchip electrophoresis with electrochemical detection device. (A) Applied voltages and channel dimensions. (B) Electrode alignment at the end of the separation channel with a 35 μm PPF carbon electrode.

3.2.5. Electrochemical detection and data analysis

In experiments determining optimal electrode potential, a CHI (CH Instruments, Austin, TX, USA) potentiostat was employed using a three electrode configuration (carbon fiber working, Ag/AgCl reference, and Pt auxiliary). Cyclic voltammetry of each analyte in sodium phosphate buffer (pH 7.4) was performed, scanning from -0.3 V to 1 V and then back to -0.3 V at a scan rate of 0.1 V/s. The resultant half wave and peak potentials were determined using CHI software.

For electrophoresis experiments, electrochemical detection was accomplished using a two electrode system (carbon working, Ag/AgCl reference (BASi, West Lafayette, IN, USA)) with an electrically isolated potentiostat (Pinnacle Technology, Inc., Lawrence, KS, USA). The sampling rate for this device was 10 Hz, and data acquisition was performed through wireless transmission and visualized with Pinnacle Acquisition Laboratory (PAL 8400) software. This potentiostat has been used previously in our group for in-channel amperometric detection [30]. For all separation optimization and characterization experiments, the working electrode (carbon fiber or PPF) potential was held at 0.8 V (vs. Ag/AgCl). For brain slice experiments, the working electrode potential was held at 1.0 V (vs. Ag/AgCl), as that potential is further along the current limiting plateau. The working electrode was placed at the channel outlet (Figure 3.2). This electrode alignment has been employed previously in our lab and yields higher efficiency separations than other detection configurations with minimal interference between the separation and detection voltages [31].

All data were analyzed using Origin 8.6 software (OriginLab, Northhampton, MA, USA) after baseline subtraction. In calculating performance parameters for the PDMS/PDMS device, three different microchips were employed and the migration times, resolution values, and

number of theoretical plates/meter for up to 25 total injections (across the three chips) were averaged. However, due to occasional co-migration between both dopamine and DOPAC and dopamine and HVA in this device (section 3.2.1), theoretical plate values for those analytes were based on only 23 total injections. With the PDMS/glass device, performance parameters were calculated based on a total of 30 injections across three different microchips (10 injections per chip). Resolution values for both devices were calculated between the stated analyte and the following peak/analyte.

3.2.6. Brain slice

A brain from a male Wistar rat weighing 385 g was obtained postmortem and used in this experiment. The rat was previously used for a seizure trial [32], and 50 mg/kg 3-mercaptoproponic acid was administered to the rat i.p. over 48 h prior to its death. All experiments were performed in accordance with regulations of the Institutional Animal Care and Use Committee (IACUC) at the University of Kansas, which operates with accreditation from the Association for Assessment and Accreditation of Laboratory Animal Care (AAALAC). The day of the experiment, the brain was removed postmortem and immediately placed in a specimen container surrounded and immersed in liquid nitrogen. Prior to the microchip electrophoresis experiments, the brain was partially thawed in ice-cold aCSF, and sagittal slices (~ 3 mm thick) were prepared by hand using a razor blade. The brain slices were allowed to thaw completely in aCSF. An individual brain slice was then placed in 515 µL of 15 mM phosphate (pH 7.4) in a 2 mL centrifuge tube. Using a water bath, the temperature was maintained at 37°C for the entire experiment. An initial baseline aliquot (25 µL) was removed immediately and 10 µL of a 10 mM stock solution of L-DOPA was added to the liquid surrounding the slice so that the brain

slice was surrounded by 200 µM L-DOPA in 15 mM phosphate (pH 7.4). Subsequent aliquots (25 µL) were removed from the supernatant and analyzed at indicated time points.

3.3. Results and discussion

3.3.1. Detection optimization

Cyclic voltammetry was employed to determine the oxidation potentials of each of the analytes of interest, and therefore the detection potential, to apply during electrophoresis experiments. A cyclic voltammogram of each analyte in phosphate buffer was taken and analyzed. Figure 3.3 depicts the half wave to peak potential for each analyte. A working electrode potential of 0.8 V (vs. Ag/AgCl) or above ensures detection on the current-limiting plateau for all analytes of interest; therefore, 0.8 V or above was used in all subsequent studies.

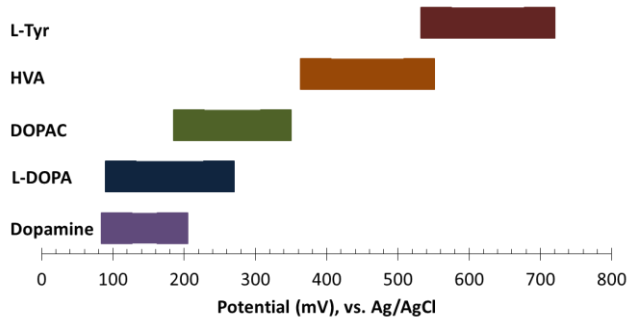

Figure 3.3 Determination of optimal detection potential. The half wave-to-peak potential was graphed for each analyte. A potential of 800 mV (vs. Ag/AgCl) or above is high enough to be on the current-limiting plateau for all analytes of interest.

3.3.2. Separation optimization (PDMS/PDMS device)

3.3.2.1. Background electrolyte

The initial separation optimization of five compounds in the dopamine metabolic pathway was performed using an all-PDMS 5 cm simple-t device (Figure 3.2). In these studies, the working electrode was a 33 μm carbon fiber electrode. The ultimate goal is to use this separation for on-line analysis of brain microdialysis samples on-animal, where artificial cerebrospinal fluid will be employed as the perfusate. Therefore, a 15 mM sodium phosphate buffer at pH 7.4 was chosen as the background electrolyte to maintain injection compatibility. Additionally, better electrochemical responses were observed in this system with sodium phosphate acting as the background electrolyte when compared to boric acid. To establish a strong, consistent gate and sample injection, separation voltages and injection times were optimized using the 15 mM sodium phosphate buffer (pH 7.4). These parameters are key to both inhibiting sample leakage into the separation channel during separation and injecting an adequate amount of sample to detect. Voltages of 1900 V and 1600 V applied to the sample and buffer reservoirs, respectively, produced a stable gate with a separation field strength of ~220 V/cm, as calculated using Kirchhoff's laws [33]. These voltages enabled the highest field strength possible, while still maintaining a prolonged chip lifetime when using phosphate as the background electrolyte. These voltages, combined with an injection time of 1.0 s, allowed adequate sample introduction into the channel. While sodium phosphate concentrations higher than 15 mM were also investigated, the high ionic strength lead to excessive Joule heating, resulting in rapid deterioration of the PDMS and a reduction in electroosmotic flow (for example, a 25 mM phosphate buffer resulted in enough Joule heating to boil the solution in the

channels in under 7 minutes). A concentration of 15 mM sodium phosphate allowed for prolonged chip life while still maintaining a good buffering capacity.

3.3.2.2. Addition of SDS

A strong, stable EOF is necessary in microchip electrophoresis to establish a consistent gate and reproducible sample injection and to enable all analytes to reach the detector. Unfortunately, PDMS does not possess a high negative surface charge as does glass, so SDS was added to the background electrolyte in the PDMS-based device to generate a negative charge at the channel walls [34]. With the low SDS concentrations in this system, dopamine co-migrated with other analytes of interest. However, if the SDS concentration was increased to concentrations above the critical micellar concentration [35], the positively charged dopamine interacted electrostatically with the negatively charged SDS micelles, causing it to migrate later, as seen in Figure 3.4. The other analytes, which are not positively charged at pH 7.4, were unaffected by the negative micelles and their migration times remained unchanged. At an SDS concentration of 15 mM, the migration time of dopamine was substantially increased, permitting it to be resolved from the other analytes of interest.

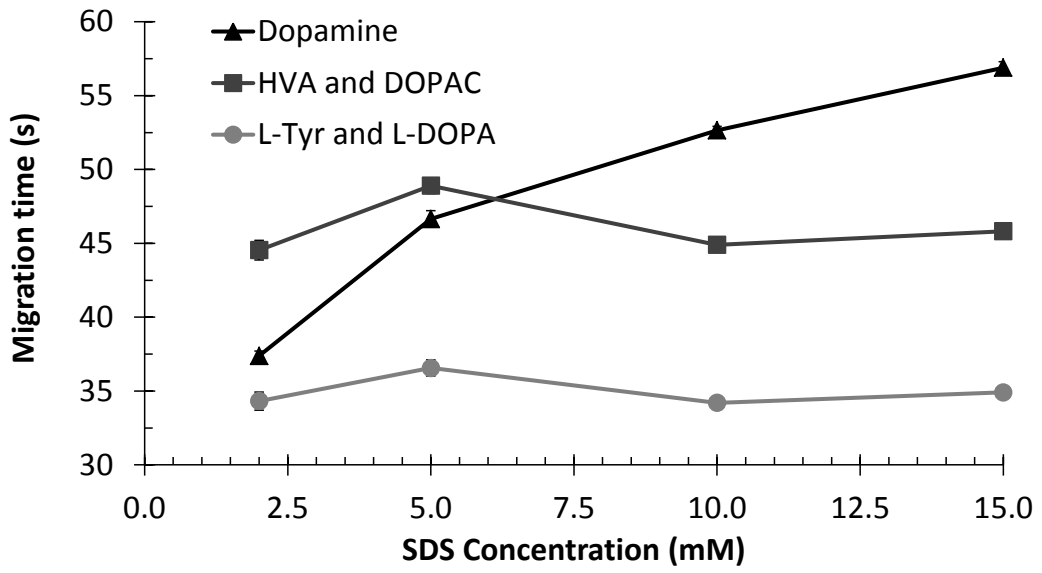

Figure 3.4. Effect of SDS concentration on analyte migration times. Run buffer is indicated SDS concentration and 15 mM phosphate (pH 7.4). Separation performed on an all-PDMS device with a carbon fiber working electrode at 0.8 V (vs. Ag/AgCl). Each point corresponds to the average of three sequential injections.

3.3.2.3. Addition of boric acid

Due to the similarity in the chemical structures and charges of L-Tyr and L-DOPA as well as that of HVA and DOPAC, their separation was initially challenging. Both L-Tyr and L-DOPA possess amine and carboxylic acid functional groups, and the only difference in their structures is that L-DOPA contains a catechol moiety while L-Tyr does not. The same is true for HVA and DOPAC. In order to resolve these pairs of analytes, an additional separation strategy was employed. Borate has long been used as a background electrolyte in microchip electrophoresis, and it is well known that it complexes with catechol moieties [36]. Because L-DOPA and DOPAC are catechols, while L-Tyr and HVA are not, boric acid was added to the separation buffer as a complexation reagent to resolve the compounds (Figure 3.5). A

concentration of 2.5 mM boric acid was sufficient to provide good resolution for five analytes. Therefore, the optimal separation buffer was determined to be 15 mM phosphate, 15 mM SDS, and 2.5 mM boric acid at pH 7.4. These conditions resulted in separation efficiencies between 60,000 and 290,000 theoretical plates/meter for the range of analytes, resolutions of 1.2 or better, and a complete separation in under 60 s.

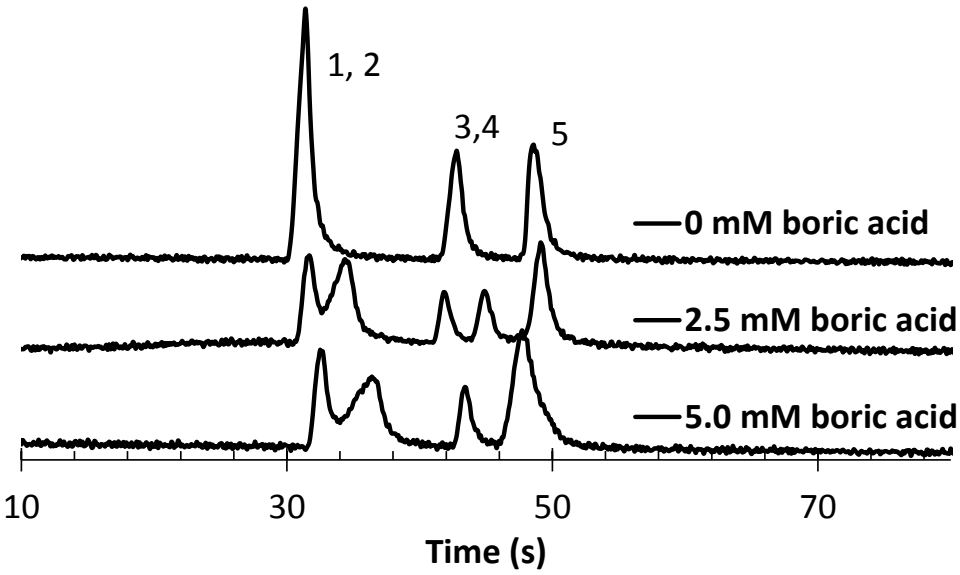

Figure 3.5. Effect of boric acid concentration on analyte migration times. Analyte identities: (1) L-Tyr, (2) L-DOPA, (3) HVA, (4) DOPAC (5) dopamine. Run buffer is indicated boric acid concentration and 15 mM phosphate (pH 7.4) and 15 mM SDS. Separation was performed on an all-PDMS device with a carbon fiber working electrode at 0.8 V (vs. Ag/AgCl).

3.3.2.4. 3-nitrophenylboronic acid

An alternative buffer modifier, 3-nitrophenylboronic acid (3-NPBA) was also investigated to enhance the separation. This molecule consists of a benzene core with nitro and boric acid functional groups in the meta position. Previous researchers investigated the affinity for various boronic acids, including 3-NPBA, towards a catechol dye, Alizarin Red S, as part of a project to develop a oligosaccharide sensor [37]. These researchers found that 3-NPBA had a relatively high affinity towards the dye (K_a = 6110 ± 75 M^{-1}) in 100 mM phosphate buffered saline (pH 7.5) when compared to other tested boronic acids.

As 3-NPBA is a larger molecule than boric acid, and may therefore increase the resolution between L-Tyr and L-DOPA as well as DOPAC and HVA a greater amount, it was investigated here. In initial studies, varying concentrations (1 mM to 15 mM) of 3-NPBA were added to a run buffer comprised of 15 mM phosphate and 15 mM SDS, to determine the effect on analyte migration times. While 3-NPBA did separate L-Tyr from L-DOPA and DOPAC from HVA, under all conditions dopamine comigrated with the other analytes. Next, ratios of boric acid: 3-NPBA were investigated to further enhance the separation, with the goal of further separating dopamine from the other analytes without having to increase the concentration of SDS. This strategy was only a partial success, with a ratio of 20:1 boric acid: 3-NPBA increasing the migration time of dopamine slightly, but not enough to completely resolve it from the other peaks. Higher concentrations of SDS was then added to the run buffer, and a run buffer consisting of 15 mM phosphate (pH 7.4), 40 mM SDS, and a ratio of 20:1 boric acid:3-NPBA (concentrations of 5 mM boric acid and 0.25 mM 3-NPBA) was sufficient to give a separation in under 70 s with resolutions of 2.0 or better for all analytes. However, the extremely high SDS concentration necessary to separate dopamine from the other analytes of interest under these

conditions made the migration time of dopamine highly irreproducible. Therefore, these separation conditions were not employed in subsequent experiments.

3.3.3. Microchip material optimization

3.3.3.1. PDMS/PDMS microchip with carbon fiber electrode

For the separation optimization experiments described in the previous section (section 3.1), an all-PDMS device was employed. However, it quickly became apparent that reproducibility of analyte migration times injection-to-injection and chip-to-chip was problematic with this device. Previous researchers have reported that PDMS-based devices suffer from migration time irreproducibility caused by inconsistences in the EOF over time due to a changing channel surface [38]. As can be seen in Table 3.1, this was also the case for the separation of the analytes in this study. When using the PDMS/PDMS device, the migration times deviated by 10-15% intra-day (data not shown) and 14-21% overall (Table 3.1). Dopamine was especially problematic, with a migration time of 56 ± 9 s for all experiments. Additionally, in some experiments the dopamine peak would slowly decrease in migration time over multiple injections on the same microchip and begin to co-migrate with the other peaks (data not shown). While the resolution between the other analytes remained relatively constant or increased, the resolution between dopamine and the other analytes deteriorated. This is evident from the high standard deviation in resolution number for DOPAC and dopamine (1.7 ± 2.4). It is believed that this inconsistency in the migration of dopamine was due to the high SDS concentration in the run buffer, as dopamine was the only analyte affected by the SDS micelles. This effect may have been caused by the dynamic equilibria between the PDMS and SDS, as well as between dopamine and SDS, changing over time. There is also the possibility that this

effect is due to continuous SDS adsorption by PDMS. Because dopamine is a critical analyte in this system, reducing its migration time variability was important in these studies.

Table 3.1. Separation performance parameters

	PDMS/PDMS microchip[a]			PDMS/glass microchip[b]		
Analyte	t_m (s)	R	$N \cdot 10^3$/meter	t_m (s)	R	$N \cdot 10^3$/meter
L-Tyr	36 (± 5)	1.2 (± 0.4)	100 (± 26)	38 (± 3)	1.1 (± 0.2)	99 (± 20)
L-DOPA	39 (± 6)	4.4 (± 1.0)	60 (± 30)	41 (± 3)	3.3 (± 0.6)	30 (± 12)
HVA	50 (± 10)	1.8 (± 0.4)	290 (± 90)	52 (± 4)	1.6 (± 0.3)	180 (± 50)
DOPAC	53 (± 11)	1.7 (± 2.4)	230 (± 50)	56 (± 5)	2.4 (± 0.4)	130 (± 30)
Dopamine	56 (± 9)	-	190 (± 100)	65 (± 5)	-	70 (± 30)

[a]PDMS/PDMS values were calculated using 3 different microchips and n > 23 total injections
[b]PDMS/glass values were calculated using 3 different microchips and n = 30 total injections

3.3.3.2. PDMS/glass microchip with pyrolyzed photoresist film electrode

In contrast to devices made from PDMS, those made of glass exhibit a strong, reproducible EOF and, therefore, more reproducible migration times. However, carbon electrodes are unfortunately not currently compatible with the bonding procedures used to make all-glass devices, so in this study a PDMS/glass hybrid device was employed. This device consisted of three walls of PDMS (channel substrate) and one wall of glass (electrode substrate). The use of a PDMS/glass hybrid device made it possible to substitute a pyrolyzed photoresist film (PPF) carbon electrode for the carbon fiber electrode. PPF electrodes have been shown to display higher sensitivities and lower LODs than carbon fiber electrodes, due to a decrease in background noise [29]. In the PDMS/glass hybrid device, the migration time of all analytes increased relative to that in the PDMS/PDMS device. While the EOF values for PDMS/glass devices have been shown to be faster than that in PDMS/PDMS devices [38], these previous

studies were performed without the use of a surfactant in the run buffer. The addition of high amounts of surfactants in PDMS microchips have been shown to generate a much faster EOF [34]. We believe that the faster migration times in the PDMS/PDMS device are due to this effect. With regards to the separation reproducibility, the migration time reproducibility was dramatically improved (*e.g.*, 65 ± 5 s for dopamine) due to the stabilizing presence of just one wall of glass when using the hybrid microchip. The RSD for migration times in the PDMS/glass device ranged from 4-6% intra-day (data not shown) and 7-9% overall (Table 3.1). However, the separation efficiencies and resolution were decreased compared to those in the all-PDMS device (Table 3.1). This trend is in agreement with previous studies by our group using laser-induced fluorescence detection to compare PDMS, glass, hybrid PDMS/glass, and polyester toner devices [38]. Using the PDMS/glass hybrid device, efficiencies between 30,000 and 180,000 theoretical plates/meter and resolutions of 1.1 or better in under 65 s were still achieved. Although there was decreased efficiency and resolution with the hybrid device, it was used for all further studies due to the dramatic improvement in migration time reproducibility. Prior to the brain slice studies, the migration time of another possible dopamine metabolite, 3-MT, was investigated. 3-MT was completely resolved from other analytes under the optimal separation conditions (Figure 3.6).

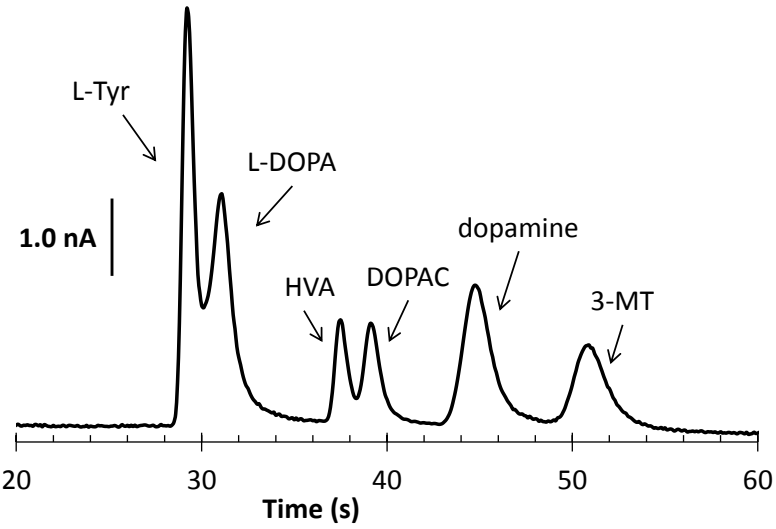

Figure 3.6 Optimized separation of analytes in the dopamine metabolic pathway. Analyte identities are indicated in the figure. Run buffer was 15 mM phosphate, 15 mM SDS and 2.5 mM boric acid. Separation was performed on a PDMS/glass hybrid device with a PPF working electrode at 1.0 V (vs. Ag/AgCl).

3.3.4. Analysis of L-DOPA metabolism in brain slice

To investigate the conversion of L-DOPA into dopamine *in vitro*, a brain slice was incubated in 15 mM phosphate (pH 7.4) buffer at 37°C. The solution surrounding the brain slice was then spiked with L-DOPA at t = 0, and the total solution volume surrounding the brain slice at this time was 500 µL. Every 10 min, a 25 µL aliquot of the brain slice solution was removed and analyzed by microchip electrophoresis with electrochemical detection. Following the addition of L-DOPA to the brain slice, several additional peaks appeared in the electropherogram, as can be seen in Figure 3.7A. At the 10 min mark, a peak appeared that could correspond to either HVA or DOPAC. Unfortunately, the definitive identity of this peak could not be elucidated based solely on the migration times. Later, at t = 30 min, another peak

appeared, corresponding to dopamine; its appearance over time can be seen in Figure 3.7B. After its appearance, the dopamine peak continued to increase over time, reaching a maximum at 50 minutes. The appearance of the dopamine peak at a later time than the HVA/DOPAC metabolite peak was expected, as the concentration of these metabolites is higher than that of dopamine due to the fast reuptake and metabolism of dopamine in the brain [39]. In the future, dual-series electrodes will be incorporated into the device to further confirm analyte identity through voltammetric characterization [22,28].

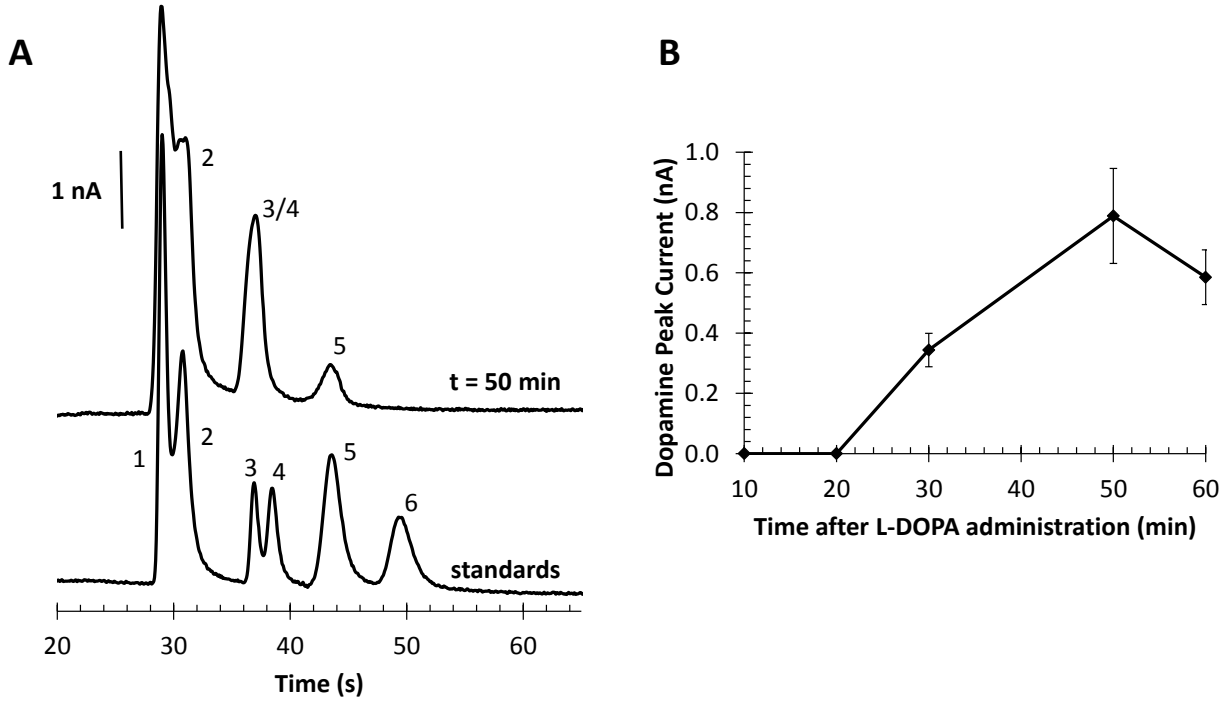

Figure 3.7 Microchip electrophoresis with electrochemical detection analysis of L-DOPA metabolism by a rat brain slice. (A) Electropherograms of standards and L-DOPA metabolism at 50 min aligned at L-DOPA peak. Peak identities are: (1) L-Tyr, (2) L-DOPA, (3) HVA, (4) DOPAC, (5) dopamine, and (6) 5-MT. (B) Appearance of dopamine after L-DOPA administration, monitored over time. Each point corresponds to three sequential injections of the same sample.

3.4. Conclusions

The separation and detection of six analytes in the dopamine metabolic pathway was accomplished in under 65 s with microchip electrophoresis and electrochemical detection using a separation buffer consisting of 15 mM phosphate, 15 mM SDS, and 2.5 mM boric acid at pH 7.4. This separation was characterized with both all-PDMS and PDMS/glass hybrid devices and, while the all-PDMS devices did generate a more efficient separation, the PDMS/glass hybrid device exibited much better migration time reproducibility. This method was then used to monitor L-DOPA metabolism in a rat brain slice over time using microchip electrophoresis with electrochemical detection. To accomplish on-line monitoring of these analytes *in vivo*, this method must be coupled to microdialysis sampling. The next chapter reviews the development and approach behind methods for coupling microdialysis sampling to microchip electrophoresis.

3.5. References

[1] A. Carlsson, Occurrence, distribution, and physiological role of catechol amines in the nervous system, Pharmacol. Rev. 11 (1959) 490-493.

[2] A. Carlsson, M. Lindqvist, T. Magnusson, B. Waldeck, On the presence of 3-hydroxytyramine in brain, Science 127 (1958) 471.

[3] J.R. Cooper, F.E. Bloom, R.H. Roth, The Biochemical Basis of Neuropharmacology, Oxford University Press, New York, 2003.

[4] P.T. Kissinger, J.B. Hart, R.N. Adams, Voltammetry in brain tissue--a new neurophysiological measurement, Brain Res 55 (1973) 209-213.

[5] R.M. Wightman, Probing Cellular Chemistry in Biological Systems with Microelectrodes, Science 311 (2006) 1570-1574.

[6] M.A. Mena, M.J. Casarejos, R.M. Solano, J. Garcia de Yebenes, Half a century of L-DOPA, Curr. Top. Med. Chem. 9 (2009) 880-893.

[7] A.C. Whitfield, B.T. Moore, R.N. Daniels, Classics in Chemical Neuroscience: Levodopa, ACS Chem. Neurosci. 5 (2014) 1192-1197.

[8] M. Shou, C.R. Ferrario, K.N. Schultz, T.E. Robinson, R.T. Kennedy, Monitoring Dopamine in Vivo by Microdialysis Sampling and On-Line CE-Laser-Induced Fluorescence, Anal. Chem. 78 (2006) 6717-6725.

[9] H. Fang, M.L. Pajski, A.E. Ross, B.J. Venton, Quantitation of dopamine, serotonin and adenosine content in a tissue punch from a brain slice using capillary electrophoresis with fast-scan cyclic voltammetry detection, Anal. Methods 5 (2013) 2704-2711.

[10] H. Fang, T.L. Vickrey, B.J. Venton, Analysis of Biogenic Amines in a Single Drosophila Larva Brain by Capillary Electrophoresis with Fast-Scan Cyclic Voltammetry Detection, Anal. Chem. 83 (2011) 2258-2264.

[11] M.E. Denno, E. Privman, B.J. Venton, Analysis of Neurotransmitter Tissue Content of Drosophila melanogaster in Different Life Stages, ACS Chem. Neurosci. 6 (2015) 117-123.

[12] J.D. Cooper, K.E. Heppert, M.I. Davies, S.M. Lunte, Evaluation of an osmotic pump for microdialysis sampling in an awake and untethered rat, J. Neurosci. Methods 160 (2007) 269-275.

[13] D. Wu, J. Qin, B. Lin, Electrophoretic separations on microfluidic chips, J. Chromatogr. A 1184 (2008) 542-559.

[14] L.A. Legendre, J.P. Ferrance, J.P. Landers, in: J.P. Landers (Ed.), Handbook of Capillary and Microchip Electrophoresis and Associated Microtechniques, CRC Press, New York, 2008, p. 335-358.

[15] P.N. Nge, C.I. Rogers, A.T. Woolley, Advances in Microfluidic Materials, Functions, Integration, and Applications, Chem. Rev. 113 (2013) 2550-2583.

[16] G. Ocvirk, M. Munroe, T. Tang, R. Oleschuk, K. Westra, D.J. Harrison, Electrokinetic control of fluid flow in native poly(dimethylsiloxane) capillary electrophoresis devices, Electrophoresis 21 (2000) 107-115.

[17] P. Kuban, P.C. Hauser, Fundamentals of electrochemical detection techniques for CE and MCE, Electrophoresis 30 (2009) 3305-3314.

[18] N.A. Lacher, K.E. Garrison, R.S. Martin, S.M. Lunte, Microchip capillary electrophoresis/electrochemistry, Electrophoresis 22 (2001) 2526-2536.

[19] J.J.P. Mark, R. Scholz, F.-M. Matysik, Electrochemical methods in conjunction with capillary and microchip electrophoresis, J. Chromatogr. A 1267 (2012) 45-64.

[20] R.S. Keynton, T.J. Roussel, M.M. Crain, D.J. Jackson, D.B. Franco, J.F. Naber, K.M. Walsh, R.P. Baldwin, Design and development of microfabricated capillary electrophoresis devices with electrochemical detection, Anal. Chim. Acta 507 (2004) 95-105.

[21] R.P. Baldwin, T.J. Roussel, Jr., M.M. Crain, V. Bathlagunda, D.J. Jackson, J. Gullapalli, J.A. Conklin, R. Pai, J.F. Naber, K.M. Walsh, R.S. Keynton, Fully integrated on-chip electrochemical detection for capillary electrophoresis in a microfabricated device, Anal. Chem. 74 (2002) 3690-3697.

[22] R.S. Martin, A.J. Gawron, S.M. Lunte, C.S. Henry, Dual-Electrode Electrochemical Detection for Poly(dimethylsiloxane)-Fabricated Capillary Electrophoresis Microchips, Anal. Chem. 72 (2000) 3196-3202.

[23] R.S. Martin, A.J. Gawron, B.A. Fogarty, F.B. Regan, E. Dempsey, S.M. Lunte, Carbon paste-based electrochemical detectors for microchip capillary electrophoresis/electrochemistry, Analyst 126 (2001) 277-280.

[24] L.C. Mecker, R.S. Martin, Use of micromolded carbon dual electrodes with a palladium decoupler for amperometric detection in microchip electrophoresis, Electrophoresis 27 (2006) 5032-5042.

[25] D.J. Fischer, W.R.I.V. Vandaveer, R.J. Grigsby, S.M. Lunte, Pyrolyzed photoresist carbon electrodes for microchip electrophoresis with dual-electrode amperometric detection, Electroanalysis 17 (2005) 1153-1159.

[26] N.E. Hebert, B. Snyder, R.L. McCreery, W.G. Kuhr, S.A. Brazill, Performance of pyrolyzed photoresist carbon films in a microchip capillary electrophoresis device with sinusoidal voltammetric detection, Anal. Chem. 75 (2003) 4265-4271.

[27] D.C. Duffy, J.C. McDonald, O.J.A. Schueller, G.M. Whitesides, Rapid Prototyping of Microfluidic Systems in Poly(dimethylsiloxane), Anal. Chem. 70 (1998) 4974-4984.

[28] A.J. Gawron, R.S. Martin, S.M. Lunte, Fabrication and evaluation of a carbon-based dual-electrode detector for poly(dimethylsiloxane) electrophoresis chips, Electrophoresis 22 (2001) 242-248.

[29] D.J. Fischer, M.K. Hulvey, A.R. Regel, S.M. Lunte, Amperometric detection in microchip electrophoresis devices: Effect of electrode material and alignment on analytical performance, Electrophoresis 30 (2009) 3324-3333.

[30] D.B. Gunasekara, M.K. Hulvey, S.M. Lunte, In-channel amperometric detection for microchip electrophoresis using a wireless isolated potentiostat, Electrophoresis 32 (2011) 832-837.

[31] D.B. Gunasekara, J.M. Siegel, G. Caruso, M.K. Hulvey, S.M. Lunte, Microchip electrophoresis with amperometric detection method for profiling cellular nitrosative stress markers, Analyst 139 (2014) 3265-3273.

[32] E.W. Crick, I. Osorio, N.C. Bhavaraju, T.H. Linz, C.E. Lunte, An investigation into the pharmacokinetics of 3-mercaptopropionic acid and development of a steady-state chemical seizure model using in vivo microdialysis and electrophysiological monitoring, Epilepsy Res. 74 (2007) 116-125.

[33] K. Seiler, Z.H.H. Fan, K. Fluri, D.J. Harrison, Electroosmotic pumping and valveless control of fluid flow within a manifold of capillaries on a glass chip, Analytical Chemistry 66 (1994) 3485-3491.

[34] G.T. Roman, K. McDaniel, C.T. Culbertson, High efficiency micellar electrokinetic chromatography of hydrophobic analytes on poly(dimethylsiloxane) microchips, Analyst 131 (2006) 194-201.

[35] E. Fuguet, C. Rafols, E. Bosch, M. Roses, Characterization of the Solvation Properties of Sodium n-Dodecyl Sulfate Micelles in Buffered and Unbuffered Aqueous Phases by Solvatochromic Indicators, Langmuir 19 (2003) 55-62.

[36] J.P. Landers, R.P. Oda, M.D. Schuchard, Separation of boron-complexed diol compounds using high-performance capillary electrophoresis, Anal. Chem. 64 (1992) 2846-2851.

[37] H.R. Mulla, N.J. Agard, A. Basu, 3-Methoxycarbonyl-5-nitrophenyl boronic acid: high affinity diol recognition at neutral pH, Bioorg. Med. Chem. Lett. 14 (2004) 25-27.

[38] W.K.T. Coltro, S.M. Lunte, E. Carrilho, Comparison of the analytical performance of electrophoresis microchannels fabricated in PDMS, glass, and polyester-toner, Electrophoresis 29 (2008) 4928-4937.

[39] A.P. Newton, J.B. Justice, Jr., Temporal Response of Microdialysis Probes to Local Perfusion of Dopamine and Cocaine Followed with One-Minute Sampling, Anal. Chem. 66 (1994) 1468-1472.

Chapter 4: A review of microdialysis coupled to microchip electrophoresis for monitoring biological events

Adapted from: R.A. Saylor, S.M. Lunte, A review of microdialysis coupled to microchip electrophoresis for monitoring biological events, Journal of Chromatography A 1382 (2015) 48-64.

4.1 Introduction

Continuous monitoring of biomolecules in living systems is important for understanding neurological disorders, evaluation of drug delivery systems, determination of pharmacological responses to drugs and environmental factors, and bioreactor monitoring. Sensors provide a popular approach for monitoring biomolecules *in vivo* and *in vitro*, and commercially available sensors have been developed for many bioactive analytes [1-3]. These include sensors for glucose, nitric oxide, glutamate, and dopamine [4]. However, a major drawback of these sensors is that they are generally limited to detection of a single analyte. It is also not possible to monitor a group of structurally related compounds, such as a drug and its metabolites, in a single assay.

Microdialysis sampling was first introduced by Ungerstedt in 1974 as a method for continuous sampling of the extracellular fluid of the brain [5-9]. This sampling technique has enjoyed wide applicability and has been extensively employed in both research laboratories and clinics [10-17]. Microdialysis sampling is accomplished based on diffusion of molecules across a size-selective membrane. Therefore, microdialysis acts as a "generic" sampling system, in that the dialysate includes all the small molecules present in the extracellular fluid of the tissue that is being interrogated. The resulting dialysate is then collected and can be analyzed by a variety of techniques optimized for the compounds of interest. A major advantage of microdialysis sampling is that it makes it possible to monitor multiple analytes simultaneously (within a single analysis) as long as these analytes can be detected individually. Separation-based analytical systems, in particular, can provide the ability to monitor multiple analytes from a single microdialysis sample. These "separation-based sensors" (Figure 4.1) have been used to continuously monitor multiple neurotransmitters in the brain, drug metabolism, and biomarkers of disease.

Analysis of microdialysis samples can be performed either off-or on-line. The most common method used for off-line separation-based analysis is liquid chromatography [15,18]. However, over the past twenty years, capillary electrophoresis has become increasingly popular [15,18-20]. An advantage of capillary electrophoresis for off-line analysis is that, because this technique requires only nanoliter amounts of sample, a single 1–10 μL microdialysis sample can be analyzed for several different classes of analytes by multiple capillary electrophoresis methods [21-23]. However, a major drawback of off-line analysis is that fairly large volume samples (1–10 μL) need to be collected to be compatible with the instrumentation and avoid evaporation during sample handling.

In order to avoid the issues with the manipulation and analysis of sub-microliter samples and provide a method for near real-time continuous monitoring, on-line separation-based systems have been developed (Figure 4.1). Microdialysis has been coupled to liquid chromatography [14,15,18,24-27] and capillary liquid chromatography [28] for continuous monitoring of drug metabolism and neuropeptides. In 1994, microdialysis was first coupled to capillary electrophoresis and used to monitor the metabolism of an anticancer drug [29]. Later, it was coupled with on-line derivatization to monitor the release of aspartate and glutamate with 1 min temporal resolution [30].

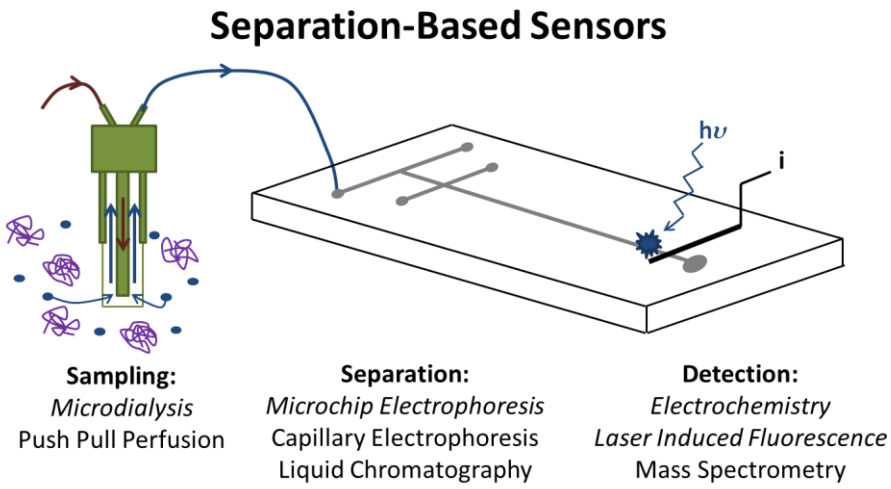

Figure 4.1 Separation-based sensor. Key components are (1) microdialysis probe (2) separation method and (3) detection approach.

Lab-on-a-chip devices were introduced in the early 1990s as a way to integrate multiple chemical processes into a single device [31]. Microchip electrophoresis was initially described by Harrison and Manz in 1992 [32-35], and the first high speed separations were published by Ramsey's group in 1994 [36,37]. The microchip format has all the advantages of capillary electrophoresis for on-line analysis of microdialysis samples, including efficient separations and ease of fluid handling, as well as the unique ability to integrate components such as mixers and detection directly on-chip. The first report of microdialysis coupled to microchip electrophoresis was demonstrated by monitoring an enzyme reaction in 2004 [38]. Since that time, there have been many papers describing new approaches and applications of this technique for monitoring biomolecules *in vivo* and *in vitro*. This chapter will describe the different approaches that have been developed for coupling microdialysis to microchip electrophoresis, as well as applications of this approach for on-line monitoring.

4.2 Microdialysis sampling

The key system components required to perform microdialysis (MD) sampling include connecting tubing, the sampling probe, and a perfusion pump. The probe consists of a semipermeable membrane that is attached to inlet and outlet tubing. In the case of animal studies, the probe is surgically placed into the tissue or organ of interest and perfusate is pumped through the tubing and into the probe. In most cases, the composition of the perfusate is as similar as possible to that of the extracellular fluid in the area of interest so as not to disrupt the biological system being interrogated. Compounds outside the probe diffuse across the semipermeable membrane based on their concentration gradient and are pumped to a fraction collector or on-line analysis system (Figure 4.2). There are many membrane materials available for the fabrication of microdialysis probes, including polyacrylonitrile (PAN), polyarylethersulfone (PAES), cuprophan (CUP), and polyethersulfone (PES) [39]. These materials differ in charge and hydrophobicity and, therefore, impart some selectivity in the sampling process. The probes are also manufactured with a specific molecular weight cut-off (MWCO), which allows only molecules smaller than the cut-off to diffuse across the membrane. Commercially available probes have molecular weight cut-offs ranging from 6 to 100 kDa.

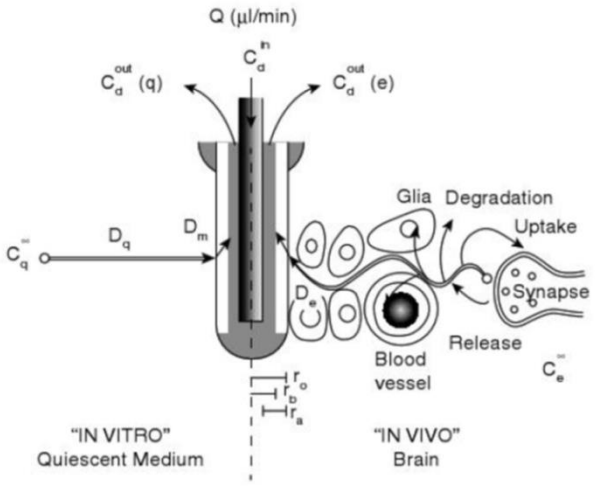

Figure 4.2 Microdialysis sampling. Microdialysis sampling considerations *in vitro* (left) and *in vivo* (right). Reprinted from Kehr [40].

Microdialysis sampling is an ideal "generic" sampling system for on-line separation-based sensors. Because only small molecules pass through the dialysis membrane, it is not necessary to remove proteins or other macromolecules, and the sample can be directly injected into the analysis system. In addition, because analytes migrate into and/or out of the probe via diffusion, there is no net fluid loss, making this technique amenable to long-term *in vivo* monitoring. Furthermore, it is possible to monitor drug metabolism in specific tissues by adding the drug to the perfusate. The drug will then diffuse into the tissue based on its concentration gradient, and metabolites will diffuse in the opposite direction into the probe. This sampling procedure creates a continual flow of sample, in which the analyte concentrations change over time corresponding to concentration changes occurring *in vivo*. Multiple compounds are sampled simultaneously, increasing the ability to understand complex biological processes.

4.2.1 Theory and considerations

4.2.1.1 Probe designs

When performing microdialysis sampling, it is important to choose the appropriate probe design for the tissue or sample that is being interrogated. Several different designs are available, and the choice of probe is dependent on the specific application. Key parameters include the heterogeneity and malleability of the sample or tissue as well as the recovery of the analyte of interest across the probe membrane. The most common probe designs are discussed below. More detailed discussions of the different probe designs are available [18,41], and some of the commercially available options are highlighted in Table 4.1.

Table 4.1. Commercially available microdialysis probes

Probe Type	Selected areas sampled	Membrane (MWCO)
Linear	*in vitro*, homogenous tissue	CUP (6 kDa), PES (55 kDa), PAN (30 kDa),
Ridged cannula	Brain	PAES (20 kDa), PES (100 kDa), CUP (6 kDa), PAN (30 kDa), Cellulosic (38 kDa)
Flexible cannula	Vasculature, soft tissue	PAES (20 kDa), PES (100 kDa), PAN (30 kDa)
Shunt	Bile	PAN (30 kDa)

Linear probes are most often used for the interrogation of homogenous tissues, such as skin [42,43], muscle [44], and liver [45], as well as bioreactor monitoring [46,47]. The linear probe consists of a dialysis membrane suspended between two pieces of capillary tubing (Figure 4.3A). The membrane is typically up to 10 mm in length, although longer membranes (1–5 cm) are commercially available. This probe is threaded through the tissue of interest or can be placed directly into a bioreactor. These probes are flexible, enabling their use in the peripheral tissue of awake, freely moving animals. In addition, because the membrane length can be relatively long compared to the other types of probes, recoveries of analyte using this probe are generally higher

than in other designs. Shunt probes are a modified version of the linear probe for the sampling of flowing streams that are high in salt concentration (Figure 4.3C). The first application of this probe design was reported by Scott and Lunte for sampling bile in rats without altering its normal flow [48]. These probes have also been used extensively for desalting sample streams prior to mass spectrometric analysis [49].

Cannula-type probes typically provide better spatial resolution than linear probes, but are much more rigid (Figure 4.3B). The probe body is generally made of stainless steel, and the probe membrane has a diameter of 220–500 μm and a length of 1–4 mm. These types of probes are used extensively to sample brain tissue due to its high degree of heterogeneity [5,7]. A guide cannula can be used to immobilize the probe on the skull of the experimental animal to ensure that it stays in place throughout the experiment and allow for easy probe removal after experimentation. The MetaQuant probe, a specific type of rigid cannula microdialysis probe, provides two separate flow streams, one for ultra-low flow rate sampling and another make-up flow to increase total collected volume [50]. Due to the rigid nature of cannula-type probes, they are generally not used for sampling soft tissue because they can cause tissue damage. For soft tissue and blood sampling, a flexible cannula-type microdialysis probe has been described [51]. This probe is constructed from fused silica or polyimide tubing and can be used to perform intravenous sampling in awake, freely moving animals [51].

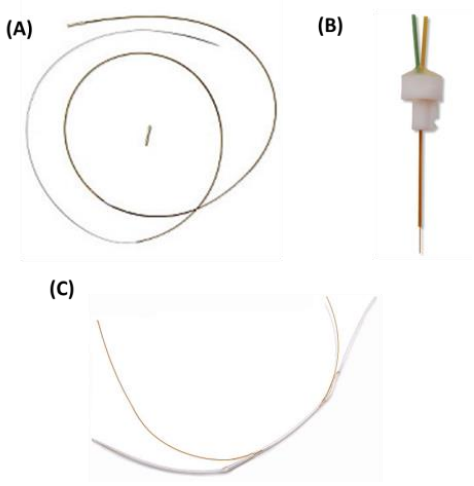

Figure 4.3 Microdialysis probe types. (A) Linear probe design for sampling in homogenous tissues. (B) Rigid cannula probe design for sampling within the brain. (C) Shunt probe design for sampling from bile fluid. Images reprinted from Bioanalytical Systems, Inc.

4.2.1.2 Recovery and calibration

Because microdialysis sampling is based on diffusion of an analyte to and across a semipermeable membrane, there are many factors that can affect extraction efficiency and analyte recovery. Extraction efficiency of a microdialysis system can be defined by the following equation, where $C_{perfusate}$, $C_{dialysate}$, and C_{sample} are the concentration of analyte in the perfusate, collected dialysate, and sample (or tissue), respectively.

$$Extraction\ efficiency = \frac{C_{perfusate} - C_{dialysate}}{C_{perfusate} - C_{sample}}$$

For many experiments, the perfusate contains no analyte ($C_{perfusate} = 0$), therefore, the extraction efficiency equation simplifies to the recovery expression below:

$$Relative\ recovery = \frac{C_{dialysate}}{C_{sample}}$$

There are many experimental variables that affect the extraction efficiency. These include temperature (of the perfusate and tissue), type of tissue and degree of tissue perfusion by blood, metabolism and degradation of the analyte, pH, probe membrane composition and molecular weight cut-off, flow rate, as well as physical and chemical characteristics of the analyte (Figure 4.2) [40,52,53]. In particular, flow rate has a very large impact on extraction efficiency. At high flow rates, perfusate is constantly being pushed through the microdialysis probe, giving analytes little time to diffuse across the probe and reach equilibrium; therefore, relative recovery is low under these conditions. In contrast, very low flow rates give much higher relative recoveries, with flow rates of 0.1 µL/min approaching 100% recovery [54]. These extremely low flow rates can be problematic, however, due to the extremely small sample volumes that are generated and the long time necessary to generate a sample with enough volume to be analyzed with traditional analytical methods. For example, at 0.1 µL/min it would take 100 minutes to acquire a 10 µL sample. Theoretically, this factor could be exploited when employing microchip electrophoresis, as very small sample volumes are required (nL–pL); however, most researchers performing microdialysis coupled to microchip electrophoresis currently use flowrates of ~1.0 µL/min.

Calibration of microdialysis probes for each experiment is important for quantitation because recovery is highly dependent on a number of factors, as discussed above. There are four main methods for microdialysis probe calibration: (1) determining recovery *in vitro* and assuming that it is the same *in vivo*, (2) delivering an internal standard in the perfusate and accounting for its loss [55-57], (3) using the no-net-flux and dynamic no-net-flux methods [58-61], and (4) employing ultra-low flow rates (~0.1 µL/min) [54] or the MetaQuant probe [50,62] and assuming 100% recovery. For additional information on these methods, the reader is directed to excellent reviews on the topic [52,63].

4.2.1.3 Spatial and temporal resolution

Temporal and spatial resolution are two important considerations when developing a separation-based sensor using microdialysis sampling. The significance of these two parameters is dependent on the tissue or organ that is being interrogated and the biological process under study.

4.2.1.3.1 Spatial resolution

Spatial resolution, or the region of tissue that is addressed by the probe, is affected by the length and diameter of the probe membrane. For homogenous tissues, relatively large probe membranes are used since they permit greater recoveries and high spatial resolution is not necessary. However, when sampling heterogeneous tissues, such as the brain, spatial resolution is extremely important. While typical commercial brain cannula probes are 220–500 μm in diameter, smaller probes for both push–pull perfusion [64-66] and microdialysis [67] are currently being developed. These probes produce less tissue damage and provide better spatial resolution than commercially available probes. Microfabricated microdialysis probes that contain nanoporous membranes produced in silicon have recently been reported by Kennedy's group [67]. These new probes will make it possible to take advantage of the positive attributes of microdialysis sampling (exclusion of larger molecules, no net fluid loss, etc.) while significantly improving the spatial resolution.

4.2.1.3.2 Temporal resolution

An important consideration when designing an on-line microdialysis–microchip electrophoresis system is determining the optimal temporal resolution or the frequency at which the data are collected and analyzed for the application of interest [11]. For example, to monitor *in vivo* neurotransmitter release, a temporal resolution of seconds to milliseconds is often

required. However, for other applications such as drug metabolism, environmental monitoring, and bioreactor sampling, a temporal resolution of several minutes to hours is adequate. Table 4.2 lists additional applications and the temporal resolution that they require. For on-line applications of microdialysis sampling with a separation method, temporal resolution is dependent on three interrelated parameters. These are (1) the detection limits of the analytical method for the analyte of interest, (2) the time required for analysis, and (3) the zone dispersion that occurs within the probe and connecting tubing.

Table 4.2. Temporal resolution necessary for various applications

Application/ compound	Temporal resolution
Neurotransmitters	Milliseconds to seconds
Drug transport and metabolism	Minutes to hours
Energy biomarkers (glucose, lactate, etc.)	Minutes to hours
Peptides	Minutes
Bioreactor monitoring	Minutes to hours
Reactive oxygen and nitrogen species	Minutes
Antioxidants (glutathione, ascorbic acid, etc.)	Minutes to hours
Environmental monitoring	Hours to days

The detection limits, or mass sensitivity, of the analytical method is an important parameter for defining temporal resolution in both on-line and off-line systems [41,68]. Since analyte recovery through the microdialysis probe is usually much less than 100%, the detection limits of the method must be significantly lower than the predicted extracellular concentration of the analyte of interest. The mass of analyte that is collected through the probe, as well as the concentration of analyte in the dialysate, is dependent on the flow rate used for sampling, membrane type, and tissue being sampled (Table 4.3). At high flow rates, there is high absolute recovery of analyte, but the sample concentrations are low. The volume collected per unit time

is also higher in this case. On the other hand, at very low flow rates extraction efficiency can approach 100%, but the sample volume per unit time is much smaller, necessitating a low sample volume analytical method such as capillary electrophoresis or microchip electrophoresis.

Table 4.3. Factors affecting extraction efficiency, temporal resolution, and lag time in MD-ME

Extraction efficiency	Temporal Resolution	Lag Time
Diffusion coefficient in probe membrane	Limits of detection	Dead volume of probe
Diffusion coefficient in tissue (*in vivo*)	Sample volume requirements	Flow rate
Flow rate	Diffusion within probe and tubing	Volume of tubing to sample collection/analysis system
Tissue damage/scar formation	Analysis time (on-line)	
Stirred or unstirred system (*in vitro*)		Sample preparation steps, *e.g.*,derivatization (on-line)
Perfusion of tissue (*in vivo*)		
Metabolism or receptor binding		
Probe membrane area		

The combination of analyte recovery and detection limits of the analytical method defines the smallest volume that must be collected for analysis and, hence, the temporal resolution. However, in cases where the concentration of an analyte is significantly higher than the detection limits of the method, very small sample volumes can be analyzed and the temporal resolution is then dependent on the analysis time for on-line systems. An example is the determination of amino acids, such as glutamate and aspartate, in brain dialysates. These compounds are present at micromolar concentrations in the extracellular fluid of the brain, while their fluorescent derivatives can be detected at low nano- to picomolar concentrations. Therefore, micro- to nanoliter volumes of dialysate can be employed for analysis since there is more than enough sensitivity to detect the analytes of interest. Temporal resolution for these two analytes using on-line systems has been reported as high as 12 s for capillary electrophoresis [69] and 35 s for microchip electrophoresis [70]. In contrast, neuropeptides are present at low picomolar

concentrations in the extracelluar fluid of the brain. Therefore, longer sampling times are required to obtain enough mass to detect them [71].

In cases where the detection limits of the analytical method are sufficient and very fast (subminute) separations can be achieved, Taylor dispersion [72] of the analyte zone in the probe and associated tubing can be the defining parameter for temporal resolution [11]. Lada et al. demonstrated that the response time of a microdialysis probe, with a minimal amount of connecting tubing, was 16 s at a flow rate of 1 μL/min. This increased to 85 s for a flowrate of 0.2 μL/min [11,69]. An additional consideration is that zone dispersion is a bigger problem when working with freely moving rather than anesthetized animals, since additional tubing must be employed to allow for movement in the awake animal system. To mitigate zone dispersion within the connecting tubing, segmented flow has been employed [73]. In this approach, the perfusate flow stream is broken into nanoliter droplets that are separated by oil, and diffusion is restricted to the droplet volume (Section 4.5.3).

An additional parameter that must be considered for on-line systems is the delay between the sampling step and the analytical device. This "lag time" depends on the length and inner diameter of the connecting tubing between the probe and the analytical system as well as the flow rate used for microdialysis sampling. Ideally, to minimize lag time between the event and the analytical signal, high flow rates and very short lengths of very small diameter tubing would be used for the sampling process. As mentioned above, this is most easily accomplished when performing experiments with anesthetized animals, where the instrument can be placed in very close proximity to the animal. However, for freely moving animal experiments using the Raturn® or a similar set-up, the length of the tubing between the animal and the swivel and then the analytical system can be significant, leading to a long delay between the event and the signal.

The additional tubing can also lead to an increase in response time due to Taylor dispersion of the analyte. For large animal sampling, it is possible to place the analytical system on-animal and thereby minimize the amount of tubing that is needed to connect the probe to the analytical system.

4.2.2 On-line/off-line sample analysis

Microdialysis samples can be analyzed on- or off-line. While there are many conventional separation-based analytical methods that lend themselves to off-line analysis, most of these methods require microliter sample volumes and costly instrumentation. They also usually require manual sample manipulation steps that can lead to fluid loss due to surface tension and evaporation. Separations can take several minutes to an hour and, therefore, samples must be stored prior to analysis (or a refrigerated autosampler must be employed). On-line methods negate the need for sample storage and handling and make it possible to analyze sub-microliter samples; however, the separation method must be fast enough to keep up with sample generation to preserve temporal resolution. For on-line analysis using methods such as capillary and microchip electrophoresis in which the sample volume requirement is low (nL–pL), temporal resolution is ideally limited only by the time needed for the separation. On-line methods also allow near real-time analysis, which can be useful to experimenters and clinicians who want to continuously monitor a situation on-site.

4.3 Microchip electrophoresis

Microchip electrophoresis (ME) is a separation technique that is ideally suited to on-line analysis of microdialysis samples due to its high separation efficiencies, low sample volume requirements (nL–pL), and fast separation times [18,20,74,75]. This technique has become

increasingly popular since it was first reported in 1992 [32-37,76]. Additionally, the microchip platform provides the ability to integrate sampling, separation, and detection on-chip.

4.3.1 Separation considerations

Microchip electrophoresis is a liquid-phase separation method in which analytes are separated based on the ratio of their charge-to-hydrodynamic radii. When performing a typical free-zone electrophoresis experiment, a small channel with charged walls is filled with a background electrolyte followed by a sample plug, and a voltage is applied across the channel. When this voltage is applied, analytes in the channel migrate based on both their innate electrophoretic mobilities and the electroosmotic flow. The electrophoretic mobility of an individual analyte depends on its charge and hydrodynamic radius, with small, highly charged analytes moving the fastest and large analytes moving more slowly due to frictional drag forces. The electroosmotic flow, or EOF, is a bulk flow generated by the electric double layer at the charged walls of the channels (as discussed in Chapter 2) [77]. In polydimethylsiloxane (PDMS)-based microchips and others without natively charged walls, a surfactant (for example, sodium dodecyl sulfate (SDS) in normal polarity and tetradecyltrimethylammonium bromide (TTAB) in reverse polarity) is added to help wet the channels and establish an EOF [78].

When analyzing high ionic strength microdialysis samples using microchip electrophoresis, an important consideration is Joule heating in the microchip. Joule heating is a part of any electrophoresis experiment, and occurs due to the current passing through the fluid in the channels generating heat [74,79]. In microchip electrophoresis, better separation efficiencies and faster analysis times are obtained with higher electric fields, therefore small channel lengths and high applied voltages are optimal, which can result in a substantial amount of Joule heating [74,79,80]. Depending on the microchip material and its thermal conductivity, the heat

generated can cause a decrease in separation efficiencies, bubbling or boiling of the liquid in the channels, and/or actual damage to the channels themselves. Care must be taken in choosing buffer type and concentration that is used for the separation, as many buffer systems are high in ionic strength. Additionally, most microdialysis samples must be high in ionic strength (~150 mM salt concentration) to maintain proper osmolality in the tissue being sampled. This can create a situation where Joule heating readily becomes problematic if the sample is manipulated in the chip electrokinetically. Injection strategies that couple microdialysis sampling to microchip electrophoresis attempt to overcome this problem by limiting the amount of electrokinetic manipulation to which the sample is subjected; this is discussed in the interface design section of this chapter (Section 4.5).

The compatibility of the separation buffer with the microdialysis perfusate is also important. If the ionic strength of the sample is much higher than that of the separation buffer, analyte dispersion or destacking can occur in the separation channel due to the lower voltage drop over the injection plug compared to the channel [81]. Destacking results in band broadening, leading to decreased efficiencies and higher limits of detection. Most microdialysis samples obtained from *in vivo* studies are high in ionic strength. Therefore, it can sometimes be difficult to match this ionic strength in the separation buffer without producing substantial Joule heating. On the other hand, the composition of the perfusate can lead to isotachophoretic concentration enhancement of analyte as has been observed for the detection of nitrite using a phosphate-buffered saline as the perfusate [82].

4.3.2 Microchip substrates

An important consideration using microchip electrophoresis for microdialysis sampling is the type of material that is used to create the device. Many different pure [83,84] and modified

materials [85] have been used for microchip electrophoresis; however, we will discuss only those that have been implemented in microdialysis–microchip electrophoresis devices. A summary of the advantages and disadvantages of various microchip materials is given in Table 4.4.

Table 4.4. Material advantages and disadvantages for microchip electrophoresis

Material	Advantages	Disadvantages

PDMS	• Low cost
	• Simple, rapid fabrication
	• Ability to incorporate many electrode materials (including carbon)
	• Easy integration of fluidic connectors
		• Slow, irreproducible EOF in native PDMS
		  ○ Migration time variability
		  ○ Difficult to electrokinetically manipulate fluid flow
		• Adsorption of hydrophobic analytes
		• Short lifetime (hours-days)

Glass	• Strong, consistent EOF • Properties similar to those of fused silica • Long lifetime (months-years) • Optically transparent • Possibility of integrating metal electrodes • Commercially available	• Currently impossible to integrate carbon electrodes • Costly and difficult fabrication (in-house) • Fabrication involves chemical etchants • Expensive commercially (in low quantities)

4.3.2.1 Polydimethylsiloxane microchips

Polydimethylsiloxane (PDMS) has been commonly used for the construction of microchip devices due to its low cost and ease of fabrication. To fabricate a simple all-PDMS device, classic photolithography is used to produce a silicon master with raised features [86]. PDMS and curing agent are mixed together and poured onto the silicon master, allowed to cure, and peeled away. This creates a PDMS substrate containing channels that correspond in dimension to those of the raised features of the silicon master. This substrate can then be placed on a flat substrate (*e.g.*, glass, PDMS) to create a complete device. PDMS is flexible, which makes it forgiving in device fabrication, allowing easier integration of ports for microdialysis coupling and electrodes for electrochemical detection. For on-line MD–ME, it is important to create an irreversible bond between the two substrates (PDMS or PDMS/glass) so that the device

can withstand the pressures created by the hydrodynamic flow used for microdialysis without leaking. To generate the irreversible bond, researchers have used both plasma oxidation [38,86,87] and semi-curing methods [88-90].

While creating microchip electrophoresis devices using PDMS is a simple, low cost approach, there are some disadvantages. Channels produced in native PDMS do not possess the high, uniform charge that is characteristic of glass devices, and this can prove challenging when attempting to generate a reproducible and strong EOF [78,91]. A strong EOF is necessary to move all analytes toward the detector as well as to electrokinetically manipulate fluid flow. Another problem is the adsorption of hydrophobic analytes into native PDMS, creating inconsistencies in migration time or complete disappearance of analyte. To mitigate these problems, the surface of the PDMS can be either dynamically or permanently modified. Modification schemes for PDMS have been reviewed [92] and include dynamic coatings such as SDS [78,93] or TTAB [94], oxidation of channels or PDMS surfaces with plasma [95] or corona [96,97], and covalent modifications [98]. Overall, PDMS-based devices are an excellent prototyping tool for researchers due to their ease of fabrication and use, low cost, and compatibility with electrochemical and fluorescence detection; however, care must be taken to achieve good, reproducible separations.

4.3.2.2 Glass microchips

Glass is the most popular substrate for microchip electrophoresis because it has properties most similar to that of the fused silica capillaries that are used in traditional capillary electrophoresis and it is optically transparent. However, all-glass microchip electrophoresis devices are more difficult to fabricate than PDMS. Glass channels are usually created using classical photolithography techniques followed by wet-etching with hydrofluoric acid (HF) [99-

102]. This process creates anisotropic channels, as areas near the surface of the substrate encounter the HF longer than those in the bottom of the channel. Once channels are created, the glass substrate containing channels is bonded to another glass substrate to create the complete device. Glass chips are also commercially available, and several vendors sell custom-made and prefabricated glass devices for microchip electrophoresis.

Most applications of glass microchips employ fluorescence detection since the laser light can be focused directly on the channel. Electrochemical detection is also employed when using glass microchips; however, the tolerances and the necessity for high-temperature bonding can make electrode integration for amperometric detection challenging. Alternative bonding methods that do not require such high temperatures have been reported, including using UV-curable adhesives, HF and high pressure, and vacuum hot press systems, or employing prebonding steps that will make electrode integration easier [103-107].

All-glass chips have the important benefit of a fast, reproducible EOF ($3.90 \pm 0.08 \times 10^{-4}$ $cm^2/V{\cdot}s$ compared to $1.12 \pm 0.10 \times 10^{-4}$ $cm^2/V{\cdot}s$ in native PDMS) [91]. The surface chemistry of the glass channels is well characterized, and analyte adsorption to the channels is low in these devices (with the exception of basic proteins and peptides). Glass devices are very rugged, and under optimal running and storage conditions can last for months or even years with normal use. Additionally, glass exhibits optical clarity over a wide range of wavelengths, making it ideal for optical detection methods such as fluorescence. Metal electrodes have also been integrated into glass chips for electrochemical detection [99-101,108]. All-glass microchips are attractive devices for microdialysis–microchip electrophoresis, provided one has the necessary equipment and expertise to design and fabricate these devices. Alternatively, all-glass chips can be purchased from various vendors, if fabrication in-house is not viable.

4.3.2.3 Hybrid and other microchip materials

PDMS/glass hybrid design microchips have also been used for microdialysis–microchip electrophoresis applications, as demonstrated in Chapter 3 [88,109]. These devices use channels that have been fabricated in either PDMS or glass with the opposite material used as a base substrate. Hybrid devices are easier to fabricate than all-glass, as irreversible bonding can be accomplished using plasma oxidation or semi-curing methods, thus avoiding high-temperature glass-bonding procedures. Additionally, in PDMS/glass hybrid devices, the separation becomes much more reproducible than in all-PDMS devices due to the stabilizing presence of one (or three) walls of glass; how-ever, efficiencies are lower due to differences in EOF between glass and PDMS, causing band broadening [91].

Other materials have been employed for use in microchip electrophoresis, including poly(methyl methacrylate), polycarbonate, paper, and polyester toner [83,84]. To date, these materials have not been used for on-line microdiaysis–microchip electrophoresis. In the future, it will be interesting to watch the development of these materials for their potential use in MD–ME devices.

4.4 Detection strategies

4.4.1 Laser-induced fluorescence

Laser-induced fluorescence (LIF) is the most commonly used detection strategy in microchip electrophoresis, due to the low limits of detection obtainable and the wide range of potentially detectable analytes after derivatization. Generally, confocal microscopes are used to focus the light onto the micron-sized channel where analytes are excited; the resulting fluorescence is then directed to the detector. An advantage of fluorescence detection is that the laser beam can be focused anywhere in the channel so the effective separation length can be

varied by simply moving the focal point of the laser. The laser also can be tightly focused so that very narrow bands can be detected. The power of ME-LIF was first demonstrated by Jacobson et al. for the separation of two fluorescent dyes in less than 150 ms [36].

Very few biological analytes exhibit native fluorescence, so analytes usually need to be derivatized to render them fluorescent. Many different commercially available reagents react with specific functional groups, including amines, thiols, and carboxylic acids [110]. Several of these have been specifically developed to be compatible with commercially available lasers. The derivatization reagent will also change the electrophoretic mobility of the analytes, which can make resolving analytes more difficult as they become more similar in their charge-to-size ratio.

Most laser-based fluorescence detectors for microchip electrophoresis are fairly large, which limits their portability and applicability for on-animal sensors or point-of-care diagnostics. Over the past ten years, diode lasers and integrated optics have made it easier to miniaturize the instrumentation needed for LIF detection. In 2005, Culbertson et al. developed a stand-alone ME-LIF device for the detection of amino acids [111]. More recently, Peter Willis' lab has developed a microchip electrophoresis system with LIF detection for deployment to other planets [112-114]. Additionally, our lab is currently developing a portable miniature LIF detection system for use with on-line microdialysis–microchip electrophoresis [115].

4.4.2 Electrochemistry

Electrochemistry (EC) has long been employed as a detection strategy for microchip electrophoresis, and was discussed in Chapter 1 of this thesis. When a potential is applied to a working electrode, electroactive analytes are oxidized (or reduced) as they flow past the electrode. This oxidation generates electrons, or a measureable current response [116]. In contrast to spectroscopic methods, electrochemical detection does not suffer from path-length

reduction of signal when miniaturized. In fact, with microelectrodes, the noise decreases faster than the signal, leading to an overall improvement in signal-to-noise ratio until the signal is undetectable [116-118]. Additionally, because many biologically relevant molecules are natively electroactive, there is no derivatization requirement as there is in most applications of fluorescence detection. In general, fabrication of electrodes through classic photolithography techniques allows direct integration into microfluidic devices. Electrochemistry coupled to microchip electrophoresis has been previously reviewed [119-122].

Highly sensitive and selective analyses can be accomplished through judicious choice of electrode type and applied potential. The electrode material that is used is dependent on the fabrication methods available, ease of integration, and electroactivity of the analytes of interest. Many different types of metals have been employed, including platinum, gold, copper, and palladium, which are easily fabricated using lithography and metal sputtering or evaporative techniques. Additionally, many different types of carbon electrodes are utilized with this technique, including carbon fiber, pyrolyzed photoresist film, carbon paste, and carbon ink. Using carbon as an electrode material offers many advantages, and many biologically relevant (organic) analytes generate good responses on carbon-based electrodes.

A variety of different options exist for working electrodes used for electrochemical detection in microchip electrophoresis. Many groups are experimenting with nanoelectrodes [123], multiple electrodes [124-126], and 3D electrodes [101] to enhance selectivity and/or sensitivity. In the future, these increases in sensitivity and selectivity will permit better detection limits of biologically relevant molecules with MD–ME–EC.

Working electrode placement is important when performing microchip electrophoresis with electrochemical detection. Due to the high voltages used for electrophoresis, care must be

taken to isolate the separation voltage from the electrochemical detector. Many problems arise if the separation voltage grounds through the potentiostat, which will occur if these two are not isolated from one another. There are three general methods for isolating the potentiostat from the separation voltage: end-channel detection, off-channel detection using a decoupler, and in-channel detection using an electrically isolated potentiostat, as discussed in detail in Chapter 2 [127]. In the end-channel configuration, the working electrode is placed a few microns from the end of the channel in a detection reservoir. The spacing between the working electrode and the channel end allows the separation field to dissipate so that it has very little effect on the electrode and potentiostat. However, this configuration leads to lower separation efficiencies and decreased resolution compared to the other two approaches, due to the diffusion of the analyte into the detection reservoir prior to electrochemical detection [127].

The other two electrode configurations attempt to mitigate these effects by placing the working electrode within the channel. In the case of the off-channel configuration, a band of metal is placed upstream of the working electrode and connected to ground to act as a decoupler. This method relies on the EOF to push the analyte from the decoupler to the detection electrode; therefore, band broadening can occur in low EOF situations. The decoupler must also adsorb the gas generated at the ground electrode (H_2 or O_2) so that bubbles do not form in the channel. Platinum [128] and palladium [129] have been successfully used as decouplers with normal polarity separations due to their ability to adsorb H_2. However, this configuration cannot be employed in reverse polarity separations, because platinum and palladium do not adsorb the O_2 generated at the anode.

Alternatively, isolated or “floating” potentiostats can be employed for in-channel electrochemical detection. In this configuration, the working electrode is usually placed as close

to the end of the channel as possible. Because the working electrode is kept within the channel, higher separation efficiencies can be achieved as there is no band broadening due to diffusion. In these systems, the electric field due to the separation voltage does interact with the working electrode, shifting the applied potential to more positive or negative values in reverse and normal polarity, respectively [130]. As the electrochemical detector is not grounded, this configuration does not destroy the electronics.

4.5 Microdialysis–microchip electrophoresis interface designs

One of the major challenges associated with the implementation of on-line microdialysis–microchip electrophoresis is the development of a robust interface. Due to the pressure-driven flows used for microdialysis sampling, the interface between the microchip and microdialysis flow stream must be strong to avoid chip delamination. Once the hydrodynamic microdialysis sample flow has been integrated into the chip, care must be taken regarding the manner in which the fluid is manipulated. Because of the high ionic strength perfusate employed for most *in vivo* microdialysis sampling experiments, using only electroosmotically driven flow to manipulate samples within the microchip is not ideal due to Joule heating, as discussed in Section 4.3.1. Additionally, because microdialysis sampling creates a continuous flow stream, one of the main hurdles to overcome with on-line microdialysis-microchip electrophoresis is the ability to inject discrete samples from this stream. There are three main methods that have been used to introduce discrete volumes of microdialysis samples into a microchip electrophoresis system. These are flow-gated injection, pneumatic valving, and segmented flow; their development and use are summarized in Table 4.5. Previous reviews have outlined methods of integrating hydrodynamic injections with microchip electrophoresis [131,132].

Table 4.5. Microdialysis-microchip electrophoresis devices

Interface	Region	Analytes	On- or Off-line	Material(s)	Detection	Comments	Reference
Flow-gated	*in vitro*	Enzymatic reaction monitoring fluorescein and FMG	On-line	Glass	LIF	First report of MD-ME	[38]
Flow-gated	Brain (striatum)	Effect of PDC on glutamate	On-line	Glass	LIF (OPA derivatized)		[135]
Pneumatic valves	*in vitro*	Fluorescein, dichlorofluorescein	On-line	PDMS/glass	LIF	First report of MD-ME with pneumatic valving interface	[88]
Flow-gated	*in vitro*	Amino acids	On-line	Glass	LIF (NDA/2-ME derivatized)		[87]
Pneumatic valves	*in vitro*	Dopamine from PC12 cells	On-line	PDMS/glass	EC (carbon ink electrodes with Pd decoupler)	First report of MD-ME-EC	[109]
Segmented flow	Brain (striatum)	Effect of PDC on amino acids	On-line	Glass	LIF (NDA/CN derivatized)	First report of segmented flow MD-ME	[70]
Flow-gated	Brain (striatum)	Fluorescein and amino acids	Pseudo-on-line	PDMS	LIF (NDA/CN derivatized)		[89]
Pneumatic valves	*in vitro*	Catecholamines	On-line	PDMS/glass	EC (carbon ink microarray with Pd decoupler)		[126]
Segmented flow	Brain (striatum)	Effect of PDC or high K^+ on amino acids	Off-line	Glass	LIF (NDA/CN derivatized)	Droplets formed at MD headpiece	[141]
Segmented flow	Brain (striatum)	Effect of K^+ microinjections on amino acids	Off-line	Glass	LIF (NDA/CN derivatized)		[142]
Pneumatic valves	*in vitro*	Catecholamines	On-line	PDMS/epoxy	EC (Pt electrode and Pd decoupled imbedded in epoxy)		[124]
Flow-gated	*in vitro*	Amino acids and an internal standard	On-line	PDMS	LIF (NDA/CN derivatized)		[90]
Flow-gated	*in vitro*	Enzymatic reaction monitoring hydrogen peroxide	On-line	Glass	EC (Pt electrodes)		[108]
Flow-gated	Subcutaneous	Nitrite	On-line	Glass	EC (Pt electrodes)	On-animal (sheep)	[82]
Flow-gated	*In vitro*, Brain	Catecholamines	On-line	PDMS/glass	EC (PPF electrode)		Present work

4.5.1 Flow-gated injection schemes

Flow-gated injection schemes attempt to balance the pressure-driven hydrodynamic flow of the microdialysis probe with the electrophoretic flow of the separation using a double-t design. In this design, sample flows into the microchip in the larger, top "sampling" channel, which allows hydrodynamic microdialysis pressures without chip delamination. A voltage is applied at the buffer reservoir, and the sample and buffer waste reservoirs are held at ground. These voltages create a stable gate at the sample/buffer intersection. When the applied voltage is allowed to float, the sample enters the intersection and can be separated upon re-application of the separation voltage.

The first report of microdialysis sampling coupled directly to microchip electrophoresis used this flow-gated design in an all-glass device [38]. Huynh et al. based their design on previous reports by the Harrison [133] and Chen [134] groups, who used wide "sample introduction channels" to couple hydrodynamic flows with microchip electrophoresis. Using this approach, Huynh and coworkers demonstrated the double-t design with LIF detection to monitor the fluorescence product of an enzymatic reaction *in vitro* (Figure 4.4). Later, this same design was used to separate and detect primary amines following in-channel derivatization with naphthalene-2,3-dicarboxaldehyde/2-mercaptoethanol (NDA/2-ME) [87]. Placing the derivatization reagents in the buffer reservoir allowed dynamic on-channel derivatization and separation after sample injection.

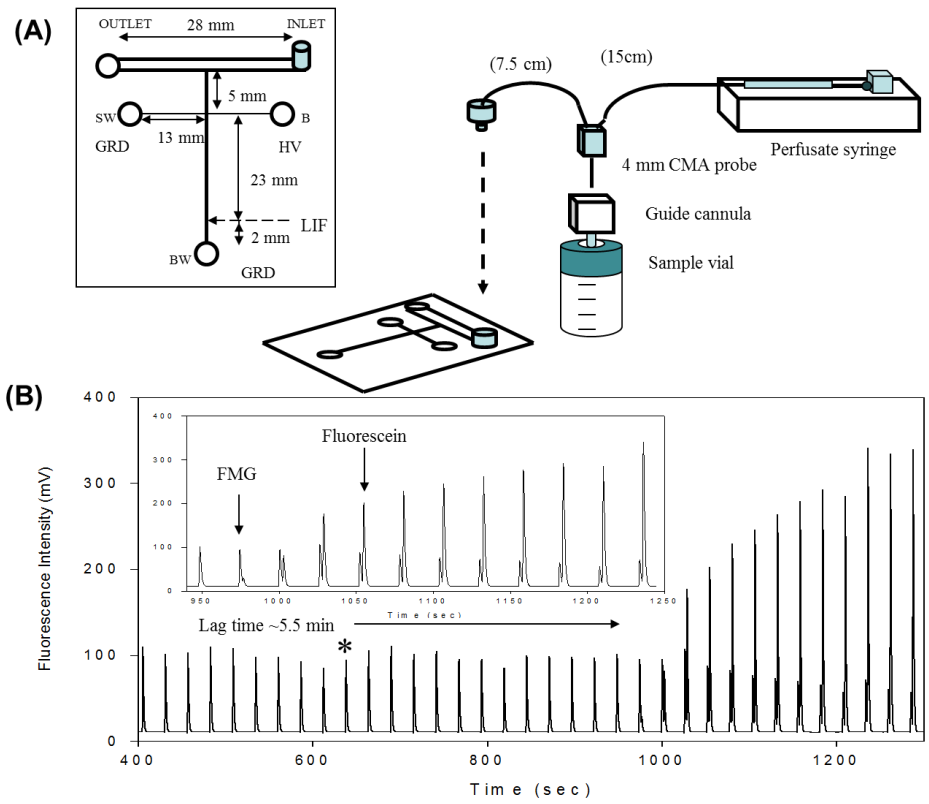

Figure 4.4 Flow-gated injection scheme. (A) Microchip design and experimental set-up. (B) On-line *in vitro* monitoring of an enzymatic reaction. Reprinted (adapted) from Huynh et al. [38].

There have been several modifications and improvements of this original design, permitting more controlled derivatization and the incorporation of electrodes for electrochemical detection. Kennedy's group employed a flow-gated injection scheme and on-line derivatization in an all-glass device to monitor amino acids [135]. Nandi et al. developed a PDMS device that was capable of on-chip derivatization and sample injection following accumulation of analyte in a reservoir [89]. Later, this design was further improved by including pre-channel mixing for on-line derivatization of primary amines with NDA/CN^- (Figure 4.5) [90]. Our group has recently developed an all-glass double-t microchip with in-channel electrochemical detection at

integrated platinum electrodes for MD-ME [108]. This device was used to monitor the production of hydrogen peroxide from the reaction of glucose with glucose oxidase using microdialysis sampling. More recently, it was employed to monitor, subcutaneously on-animal, the production of nitrite from nitroglycerin administered using retrodialysis [82].

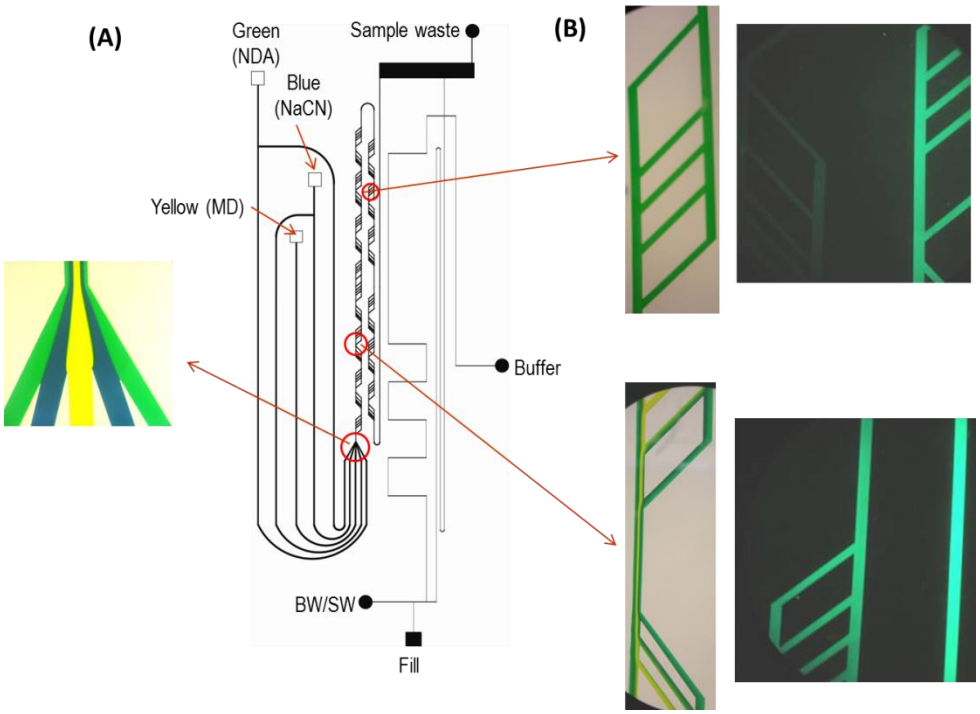

Figure 4.5 On-chip derivatization and flow-gated sample injection. (A) Microchip design. (B) Mixing profiles for various locations in microchip. Reprinted from Nandi et al. [90].

The flow-gated injection scheme is a simple way of introducing pressure-driven microdialysis flow to a microchip and injecting discrete samples from the continuous flow stream into the separation channel. The benefits of this system are in its simplicity; fluid flow is manipulated solely by the pressure from the microdialysate and an applied voltage. However,

there are some challenges associated with this injection scheme. Channel dimensions, flow rates, and applied voltages must all be optimized concurrently to establish a stable gate. Because there is an electrokinetic influence on the injection, some bias may occur during sample injections. In some cases, this can be helpful by eliminating interferences. In addition, the amount of sample injected will depend on the applied field strength and ionic strength of the sample.

4.5.2 Pneumatic valves

Pneumatically driven valves have also been used to couple microdialysis sampling to microchip electrophoresis. These devices are fabricated in two layers (valve and flow layer) using flexible polymers such as PDMS [136,137]. In these devices, flow is controlled using valves that allow discrete sample plugs to enter the electrophoretic channel, which is placed at a right angle to the sample introduction channel.

The first report of the use of pneumatic valves as an interface between microdialysis sampling and microchip electrophoresis was by Li et al. [88]. In their design, a pushback channel was incorporated to eliminate sample diffusion into the separation channel between injections. These researchers demonstrated the operation of the device using fluorescein as a model compound, sampled *in vitro*.

Expanding their original design, Mecker and Martin incorporated valving with electrochemical detection for monitoring dopamine release from PC-12 cells using microdialysis sampling (Figure 4.6) [109]. This was the first report of the incorporation of electrochemical detection with MD–ME. The electrochemical part of the system used a palladium decoupler and carbon ink microelectrodes. The chip was produced using reversible bonding, and the separation electrodes were placed in the chip using an access hole punched into the PDMS layers. This device was able to monitor stimulated dopamine release from preloaded PC-12 cells. Later, the

same group incorporated carbon-ink microelectrode arrays [126] and epoxy-imbedded electrodes [124] into this design.

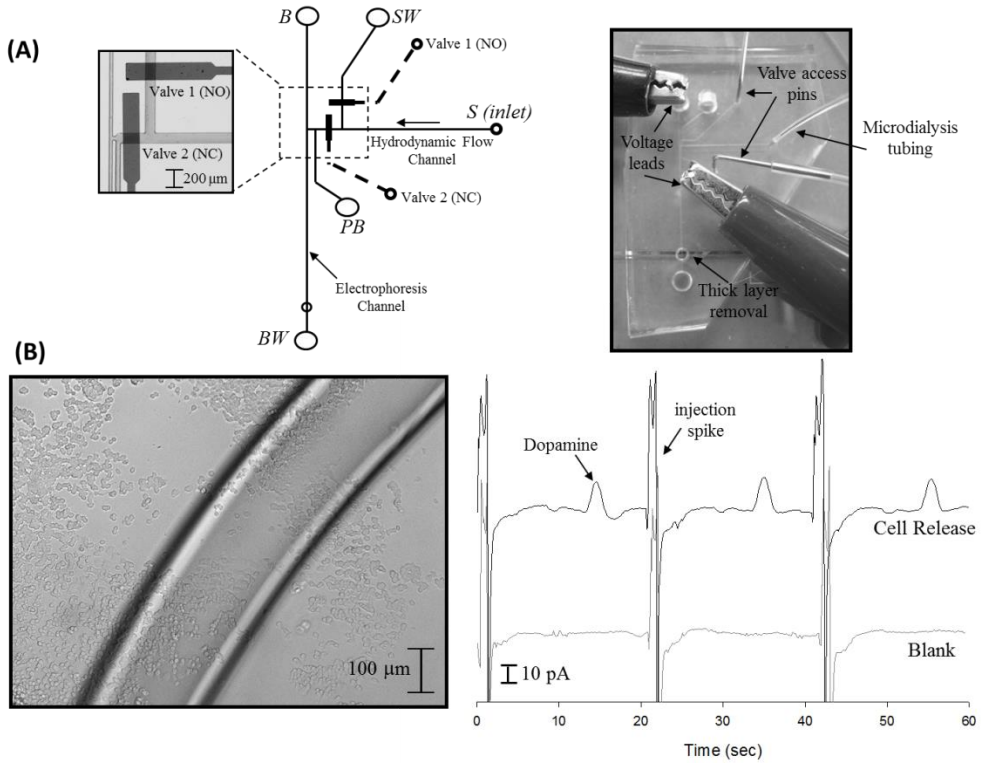

Figure 4.6 Pneumatic valve injection scheme. (A) Microchip design and operation. (B) Micrograph of PC-12 cells and on-line detection of stimulated dopamine release from preloaded PC-12 cells. Reprinted (adapted) from Mecker and Martin [109].

These pneumatic valve-based devices offer several advantages when coupling microdialysis sampling to microchip electrophoresis. As the Martin group has shown, many different electrode materials can be easily incorporated into the device, expanding the range of analytes that can be studied. Additionally, unlike the flow-gated devices, a larger range of field strengths may be used, as there is no voltage compromise needed to establish a gate. There is also no electrokinetic injection bias in these devices. However, these devices require more

technical experience to fabricate. Possibly the largest disadvantage of pneumatic valve-based devices is the limitation in miniaturization and portability of the entire system, due to the bulky gas tanks needed to actuate the device valves unless micropumps are utilized. This limits the development of any point-of-care or on-animal systems using this configuration.

4.5.3 Segmented flow

To overcome losses in temporal resolution due to the diffusion of analyte within connecting tubing, segmented flow-based devices have been developed. These devices segment aqueous sample as droplets within a water-immiscible stream. The size and frequency of these droplets depends on the flow of the sample and water-immiscible stream, two parameters that can be optimized to give ideal droplet sizes.

Building on previous work with segmenting microdialysis flow on a PDMS microchip [138,139] and work by Roman et al. on desegmenting droplets prior to injection and electrophoretic separation [140], Kennedy's group efficiently coupled segmented flow to microchip electrophoresis for *in vivo* monitoring of amino acids from brain microdialysate [70]. In this work, two microchips were employed. A PDMS microchip was used both to segment the microdialysis flow stream and to react the dialysate with NDA/CN^-. This was coupled to a glass chip where the flow was desegmented, the sample injected, and the analytes separated by electrophoresis and detected by LIF (Figure 4.7). Using this device, separation efficiencies of over 200,000 theoretical plates and a temporal resolution of 40 s were obtained [70]. The temporal resolution was controlled by limits imposed by the separation time; faster separation times may further improve this temporal resolution.

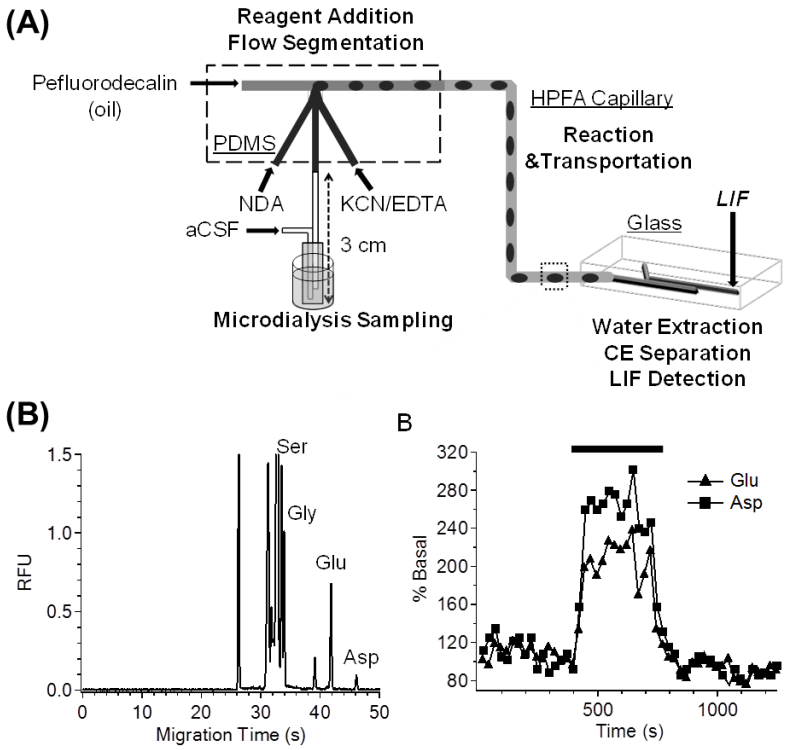

Figure 4.7 Segmented flow-based device. (A) Overal design of flow segmentation and desegmentation for on-line monitoring. (B) *in vivo* monitoring of serine (Ser), glycine (Gly), glutamine (Glu), and aspartate (Asp) using on-line device. Reprinted (adapted) from Wang et al. [70].

More recently, the same group fabricated a device that segments the continuous microdialysis stream into droplets as it is exiting the animal, eliminating any dead volume in connectors that were previously between the animal and segmenting chip. They used this device to sample, create droplets from the microdialysis brain perfusate obtained from an anesthetized rat, and derivatize amino acids in the droplets [141]. After droplet creation on rat, the droplets were collected and immediately analyzed off-line for amino acids using microchip electrophoresis with LIF detection. In a later publication, they reported that droplets created with

this device during MD sampling in awake animals were stored in HPFA collection tubing in a buffer jar filled with hexane at −80°C for up to four days and again analyzed off-line. This process resulted in a temporal resolution of 2 s [142]. Theoretically, this device could be directly coupled to on-line ME for near real-time monitoring, provided the separation time is sufficiently fast.

By segmenting the microdialysis flow into discrete droplets, enhanced temporal resolution can be achieved. Each droplet contains a small sample plug corresponding to a short time period. Because the sample is trapped in the droplet, there is limited analyte dispersion, and temporal resolution is preserved. However, this interface design adds an additional degree of complexity to the final device.

4.6 Applications

Fully integrated, portable, and miniaturized systems using on-line microdialysis–microchip electrophoresis will provide researchers with a very valuable tool for monitoring biological events. While many of these devices are still in the development stage, others are currently being employed in some interesting *in vitro* and *in vivo* applications.

4.6.1 *in vitro* monitoring

Microdialysis coupled to microchip electrophoresis is an excellent tool for the *in vitro* monitoring of cells or bioreactors. Many have employed microdialysis sampling of a mixture of amino acids [87,90] or fluorescein [88] *in vitro* to characterize the device in terms of response to concentration changes, lag and rise time, and/or separation efficiencies.

The Lunte group reported the first coupling of microdialysis sampling to microchip electrophoresis with laser-induced fluorescence detection to monitor the *in vitro* hydrolysis of fluorescein mono-β-d-galactopyranoside into fluorescein and galactose by β-d-galactosidase

[38]. Because both fluorescein and fluorescein mono-β-d-galactopyranoside are fluorescent, it was possible to monitor the disappearance of the substrate and appearance of the product simultaneously and in near real-time with their flow-gated device. The production of hydrogen peroxide from the enzymatic reaction of glucose peroxidase with glucose was also monitored, using an on-line all-glass flow-gated device with integrated platinum electrodes [108].

Another application of microdialysis–microchip electrophoresis results from its ability to monitor cellular events. Martin's group monitored preloaded PC-12 cells and used on-line microdialysis–microchip electrophoresis with electrochemical detection with a pneumatic valve injection scheme to monitor the release of dopamine after stimulation by a high K^+ solution in cells grown within a petri dish [109].

4.6.2 *in vivo* monitoring

Perhaps the most exciting applications of microdialysis–microchip electrophoresis concern the continuous on-line monitoring of biological events *in vivo*. More specifically, many researchers have used the devices that they developed for *in vivo* monitoring of amino acids from brain microdialysates.

Nandi et al. used their flow-gated injection device to monitor endogenous levels of amino acids after an on-line derivatization [89]. In addition to the derivatized amino acids, they also investigated blood–brain barrier permeability by injecting fluorescein peripherally and monitoring its concentration in the brain via MD–ME-LIF (Figure 4.8). They saw the appearance of fluorescein in the brain dialysate 5 min after the injection, and watched its clearance from the brain over a period of 90 min.

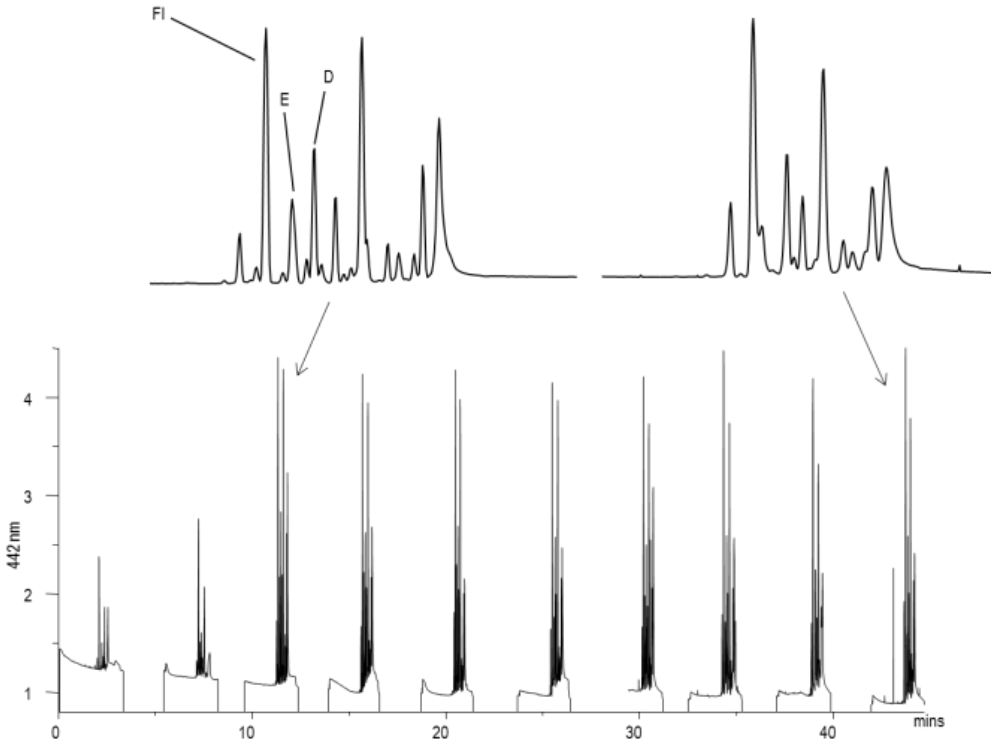

Figure 4.8 *in vivo* monitoring of amino acid neurotransmitters and fluorescein. Fl represents fluorescein, which was used as a marker of blood-brain barrier permeability. E represents glutamate and D represents aspartate. Reprinted from Nandi et al. [89].

The Kennedy group employed their flow-gated [135] and segmented flow devices [70] to monitor select amino acids in the brain following delivery of a glutamate uptake inhibitor, l-trans-pyrrolidine-2,4,-dicarboxylic acid, through the microdialysis probe. Upon administration of the inhibitor, they witnessed an increase in glutamate, and glutamate and aspartate with the flow-gated and segmented flow devices, respectively. Microchip electrophoresis with fluorescence detection was also used for off-line analysis of droplets generated by segmented flow for excitatory amino acids following microinjections of either l-trans-pyrrolidine-2,4,-dicarboxylic acid or K^+. Concentrations of amino acids (glutamate, aspartate, taurine, glycine,

and GABA) were monitored using this device with both stimulation procedures [141]. Lastly, microdialysis samples were segmented and derivativized shortly after their collection and stored for up to four days before being analyzed for amino acids by microchip electrophoresis with LIF detection [142].

Recently, our group has employed microdialysis–microchip electrophoresis with integrated electrochemical detection at platinum electrodes for on-animal monitoring [82]. To achieve on-animal sensing, all associated equipment was miniaturized and placed in a backpack on a sheep (Figure 4.9). In this study, the production of nitrite after a nitroglycerin perfusion was monitored on animal using subcutaneous microdialysis sampling coupled to the device detailed in reference [108]. Additionally, Chapters 5 and 6 in this thesis will describe progress toward the development of an on-line microdialysis–microchip electrophoresis flow-gated device with easy integration of carbon electrodes for monitoring catecholamines *in vitro* and *in vivo*. This device will ultimately be used in the future on freely roaming, untethered sheep to measure correlations between neurotransmitters and behavior.

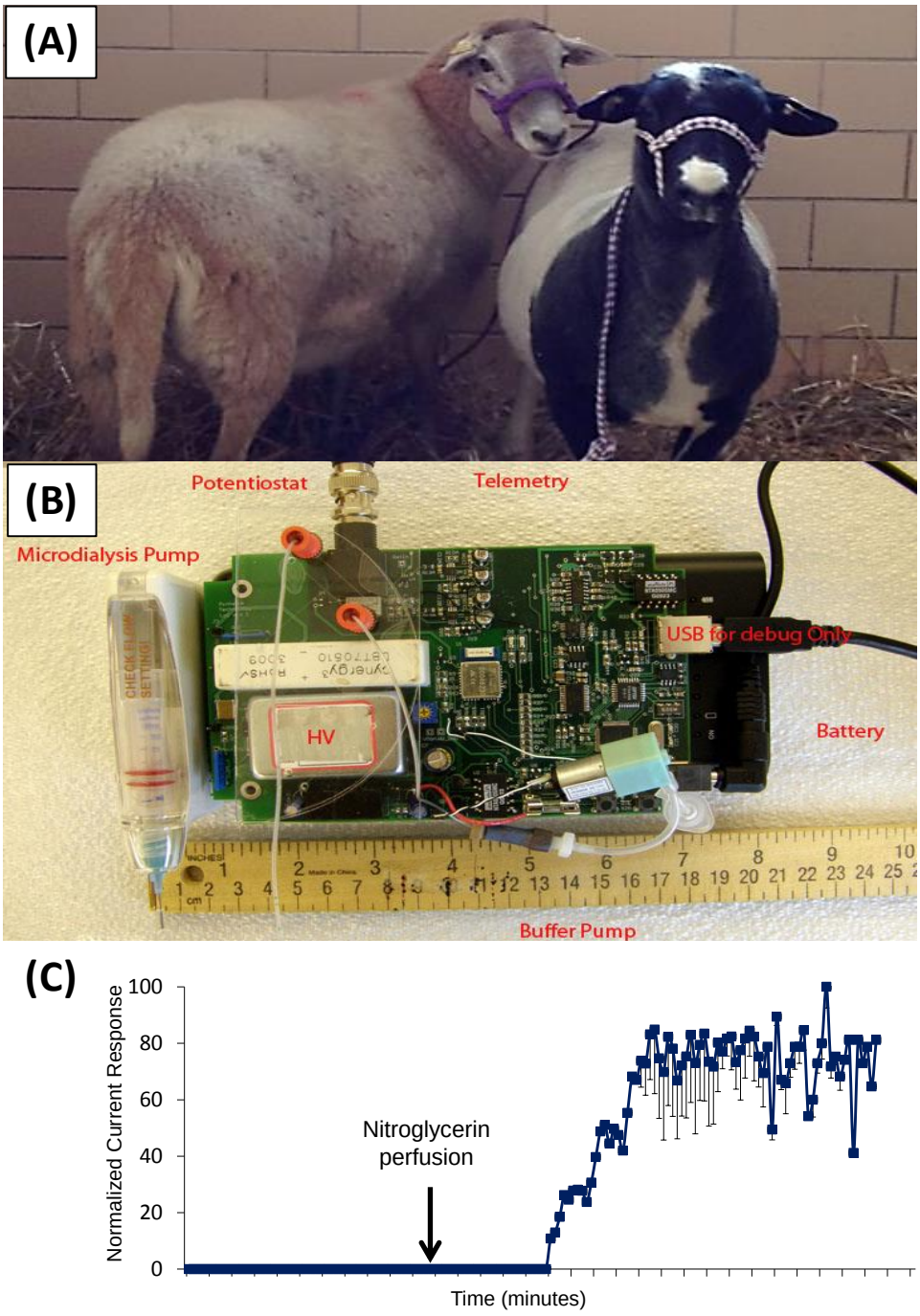

Figure 4.9 On-animal sensing. (A) Freely roaming sheep for behavioral studies. (B) Prototype of miniaturized high voltage power supply, microdialysis pump, and potentiostat for on-animal monitoring. (C) On-line monitoring of nitrite following nitroglycerin perfusion. Images adapted from [82,143].

4.7 Conclusions

Microdialysis sampling coupled to microchip electrophoresis offers a powerful method for monitoring biological events, both *in vivo* and *in vitro*. The combination of these two methods yields a separation-based sensor that can be customized for specific applications. The next two chapters of this thesis will extend existing MD-ME-EC work to include a new fabrication procedure for easily integrating carbon-based electrodes into the device. Chapter 6 will detail *in vitro* work with PC-12 cells, and Chapter 7 will extend the separation and detection of analytes in the dopamine metabolic pathway described in Chapter 3 to on-line monitoring of these compounds *in vivo*.

4.8 References

[1] D.A. Jones, M.C. Parkin, H. Langemann, H. Landolt, S.E. Hopwood, A.J. Strong, M.G. Boutelle, On-line monitoring in neurointensive care Enzyme-based electrochemical assay for simultaneous, continuous monitoring of glucose and lactate from critical care patients, J. Electroanal. Chem. 538-539 (2002) 243-252.

[2] M.L. Rogers, P.A. Brennan, C.L. Leong, S.A.N. Gowers, T. Aldridge, T.K. Mellor, M.G. Boutelle, Online rapid sampling microdialysis (rsMD) using enzyme-based electroanalysis for dynamic detection of ischaemia during free flap reconstructive surgery, Anal. Bioanal. Chem. 405 (2013) 3881-3888.

[3] M.L. Rogers, D. Feuerstein, C.L. Leong, M. Takagaki, X. Niu, R. Graf, M.G. Boutelle, Continuous Online Microdialysis Using Microfluidic Sensors: Dynamic Neurometabolic Changes during Spreading Depolarization, ACS Chem. Neurosci. 4 (2013) 799-807.

[4] G.S. Wilson, M.A. Johnson, In-vivo electrochemistry: what can we learn about living systems?, Chem Rev 108 (2008) 2462-2481.

[5] U. Ungerstedt, Introduction to intracerebral microdialysis, Tech. Behav. Neural Sci. 7 (1991) 3-22.

[6] U. Ungerstedt, Microdialysis--principles and applications for studies in animals and man, J Intern Med 230 (1991) 365-373.

[7] U. Ungerstedt, A. Hallstrom, In vivo microdialysis--a new approach to the analysis of neurotransmitters in the brain, Life Sci 41 (1987) 861-864.

[8] U. Ungerstedt, C. Pycock, Functional correlates of dopamine neurotransmission, Bull Schweiz Akad Med Wiss 30 (1974) 44-55.

[9] T. Sharp, T. Zetterstrom, in: B.H.C. Westerink, T.I.F.H. Cremers (Eds.), Handbook of Microdialysis: Methods, Applications and Clinical Aspects, Elsevier, New York, 2007, p. 5-16.

[10] M.L. Rogers, M.G. Boutelle, Real-time clinical monitoring of biomolecules, Annu. Rev. Anal. Chem. 6 (2013) 427-453.

[11] K.N. Schultz, R.T. Kennedy, Time-resolved microdialysis for in vivo neurochemical measurements and other applications, Annu. Rev. Anal. Chem. 1 (2008) 627-661.

[12] R.T. Kennedy, Emerging trends in in vivo neurochemical monitoring by microdialysis, Curr. Opin. Chem. Biol. 17 (2013) 860-867.

[13] C.D.K. Sloan, P. Nandi, T.H. Linz, J.V. Aldrich, K.L. Audus, S.M. Lunte, Analytical and biological methods for probing the blood-brain barrier, Annu. Rev. Anal. Chem. 5 (2012) 505-531.

[14] B.H.C. Westerink, T.I.F.H. Cremers, Handbook of Microdialysis: Methods, Applications and Clincal Aspects, Elsevier, New York, 2007.

[15] T.-H. Tsai, Applications of Microdialysis in Pharmaceutical Science, John Wiley & Sons, Inc., Hoboken, NJ, 2011.

[16] R.J. Shannon, K.L.H. Carpenter, M.R. Guilfoyle, A. Helmy, P.J. Hutchinson, Cerebral microdialysis in clinical studies of drugs: pharmacokinetic applications, J. Pharmacokinet. Pharmacodyn. 40 (2013) 343-358.

[17] F.J. Azeredo, T. Dalla Costa, H. Derendorf, Role of Microdialysis in Pharmacokinetics and Pharmacodynamics: Current Status and Future Directions, Clin. Pharmacokinet. 53 (2014) 205-212.

[18] P. Nandi, S.M. Lunte, Recent trends in microdialysis sampling integrated with conventional and microanalytical systems for monitoring biological events: A review, Anal. Chim. Acta 651 (2009) 1-14.

[19] E. Guihen, W.T. O'Connor, Capillary and microchip electrophoresis in microdialysis: Recent applications, Electrophoresis 31 (2010) 55-64.

[20] E. Guihen, W.T. O'Connor, Current separation and detection methods in microdialysis the drive towards sensitivity and speed, Electrophoresis 30 (2009) 2062-2075.

[21] J.C. Cooley, C.E. Lunte, Detection of malondialdehyde in vivo using microdialysis sampling with CE-fluorescence, Electrophoresis 32 (2011) 2994-2999.

[22] E.W. Crick, I. Osorio, M. Frei, A.P. Mayer, C.E. Lunte, Correlation of 3-mercaptopropionic acid induced seizures and changes in striatal neurotransmitters monitored by microdialysis, Eur. J. Pharm. Sci. 57 (2014) 25-33.

[23] S. Kaul, M.D. Faiman, C.E. Lunte, Determination of GABA, glutamate and carbamathione in brain microdialysis samples by capillary electrophoresis with fluorescence detection, Electrophoresis 32 (2011) 284-291.

[24] K.M. Steele, C.E. Lunte, Microdialysis sampling coupled to online microbore liquid chromatography for pharmacokinetic studies, J. Pharm. Biomed. Anal. 13 (1995) 149-154.

[25] C.S. Chaurasia, C.-E. Chen, C.R. Ashby, Jr., In vivo online HPLC-microdialysis: simultaneous detection of monoamines and their metabolites in awake freely-moving rats, J. Pharm. Biomed. Anal. 19 (1999) 413-422.

[26] F.-X. Mathy, B. Vroman, D. Ntivunwa, A.J. De Winne, R.K. Verbeeck, V. Preat, On-line determination of fluconazole in blood and dermal rat microdialysates by microbore high-performance liquid chromatography, J. Chromatogr. B: Anal. Technol. Biomed. Life Sci. 787 (2003) 323-331.

[27] J. Zhang, A. Jaquins-Gerstl, K.M. Nesbitt, S.C. Rutan, A.C. Michael, S.G. Weber, In Vivo Monitoring of Serotonin in the Striatum of Freely Moving Rats with One Minute Temporal Resolution by Online Microdialysis-Capillary High-Performance Liquid Chromatography at Elevated Temperature and Pressure, Anal. Chem. 85 (2013) 9889-9897.

[28] H.M. Shackman, M. Shou, N.A. Cellar, C.J. Watson, R.T. Kennedy, Microdialysis coupled on-line to capillary liquid chromatography with tandem mass spectrometry for monitoring acetylcholine in vivo, J. Neurosci. Methods 159 (2006) 86-92.

[29] B.L. Hogan, S.M. Lunte, J.F. Stobaugh, C.E. Lunte, Online Coupling of in vivo Microdialysis Sampling with Capillary Electrophoresis, Anal. Chem. 66 (1994) 596-602.

[30] S.Y. Zhou, H. Zuo, J.F. Stobaugh, C.E. Lunte, S.M. Lunte, Continuous in Vivo Monitoring of Amino Acid Neurotransmitters by Microdialysis Sampling with Online Derivatization and Capillary Electrophoresis Separation, Anal. Chem. 67 (1995) 594-599.

[31] A. Manz, N. Graber, H.M. Widmer, Miniaturized total chemical analysis systems: a novel concept for chemical sensing, Sens. Actuators, B 1 (1990) 244-248.

[32] D.J. Harrison, K. Fluri, K. Seiler, Z. Fan, C.S. Effenhauser, A. Manz, Micromachining a miniaturized capillary electrophoresis-based chemical analysis system on a chip, Science 261 (1993) 895-897.

[33] D.J. Harrison, A. Manz, Z. Fan, H. Luedi, H.M. Widmer, Capillary electrophoresis and sample injection systems integrated on a planar glass chip, Anal. Chem. 64 (1992) 1926-1932.

[34] A. Manz, D.J. Harrison, E.M.J. Verpoorte, J.C. Fettinger, A. Paulus, H. Luedi, H.M. Widmer, Planar chips technology for miniaturization and integration of separation techniques into monitoring systems. Capillary electrophoresis on a chip, J. Chromatogr. 593 (1992) 253-258.

[35] K. Seiler, D.J. Harrison, A. Manz, Planar glass chips for capillary electrophoresis: repetitive sample injection, quantitation, and separation efficiency, Anal. Chem. 65 (1993) 1481-1488.

[36] S.C. Jacobson, R. Hergenroder, L.B. Koutny, J.M. Ramsey, High-Speed Separations on a Microchip, Anal. Chem. 66 (1994) 1114-1118.

[37] S.C. Jacobson, R. Hergenroder, L.B. Koutny, R.J. Warmack, J.M. Ramsey, Effects of Injection Schemes and Column Geometry on the Performance of Microchip Electrophoresis Devices, Anal. Chem. 66 (1994) 1107-1113.

[38] B.H. Huynh, B.A. Fogarty, R.S. Martin, S.M. Lunte, On-Line Coupling of Microdialysis Sampling with Microchip-Based Capillary Electrophoresis, Anal. Chem. 76 (2004) 6440-6447.

[39] L. Sun, J.A. Stenken, Improving microdialysis extraction efficiency of lipophilic eicosanoids, J. Pharm. Biomed. Anal. 33 (2003) 1059-1071.

[40] J. Kehr, A survey on quantitative microdialysis: theoretical models and practical implications, J. Neurosci. Methods 48 (1993) 251-261.

[41] M.I. Davies, J.D. Cooper, S.S. Desmond, C.E. Lunte, S.M. Lunte, Analytical considerations for microdialysis sampling, Adv. Drug Delivery Rev. 45 (2000) 169-188.

[42] J.M. Ault, C.M. Riley, N.M. Meltzer, C.E. Lunte, Dermal microdialysis sampling in vivo, Pharm. Res. 11 (1994) 1631-1639.

[43] H. Zuo, M. Ye, M.I. Davies, Monitoring transdermal delivery of nicotine using in vivo microdialysis sampling, Curr. Sep. 15 (1996) 63-66.

[44] E.M. Siaghy, Y. Devaux, H. Schroeder, N. Sfaksi, D. Ungureanu-Longrois, F. Zannad, J.P. Villemot, P. Nabet, P.M. Mertes, High-performance liquid chromatographic analysis of muscular interstitial arginine and norepinephrine kinetics. A microdialysis study in rats, J Chromatogr B Biomed Sci Appl 745 (2000) 279-286.

[45] M.I. Davies, C.E. Lunte, Simultaneous microdialysis sampling from multiple sites in the liver for the study of phenol metabolism, Life Sci. 59 (1996) 1001-1013.

[46] N. Torto, L. Gorton, T. Laurell, G. Marko-Varga, Technical issues of in vitro microdialysis sampling in bioprocess monitoring, TrAC, Trends Anal. Chem. 18 (1999) 252-260.

[47] N. Torto, T. Laurell, L. Gorton, G. Marko-Varga, Recent trends in the application of microdialysis in bioprocesses, Anal. Chim. Acta 374 (1998) 111-135.

[48] D.O. Scott, C.E. Lunte, In vivo microdialysis sampling in the bile, blood, and liver of rats to study the disposition of phenol, Pharm. Res. 10 (1993) 335-342.

[49] Q. Wu, C. Liu, R.D. Smith, Online microdialysis desalting for electrospray ionization-mass spectrometry of proteins and peptides, Rapid Commun. Mass Spectrom. 10 (1996) 835-838.

[50] T.I.F.H. Cremers, M.G. de Vries, K.D. Huinink, J.P. van Loon, M. v. d. Hart, B. Ebert, B.H.C. Westerink, E.C.M. de Lange, Quantitative microdialysis using modified ultraslow microdialysis: direct rapid and reliable determination of free brain concentrations with the MetaQuant technique, J Neurosci Methods 178 (2009) 249-254.

[51] M. Telting-Diaz, D.O. Scott, C.E. Lunte, Intravenous microdialysis sampling in awake, freely-moving rats, Anal. Chem. 64 (1992) 806-810.

[52] J.A. Stenken, Methods and issues in microdialysis calibration, Anal. Chim. Acta 379 (1999) 337-357.

[53] P.M. Bungay, P.F. Morrison, R.L. Dedrick, Steady-state theory for quantitative microdialysis of solutes and water in vivo and in vitro, Life Sci. 46 (1990) 105-119.

[54] S. Menacherry, W. Hubert, J.B. Justice, Jr., In vivo calibration of microdialysis probes for exogenous compounds, Anal. Chem. 64 (1992) 577-583.

[55] D. Scheller, J. Kolb, The internal reference technique in microdialysis: a practical approach to monitoring dialysis efficiency and to calculating tissue concentration from dialyzate samples, J. Neurosci. Methods 40 (1991) 31-38.

[56] L. Stahle, Drug distribution studies with microdialysis: I. Tissue dependent difference in recovery between caffeine and theophylline, Life Sci 49 (1991) 1835-1842.

[57] Y. Wang, S.L. Wong, R.J. Sawchuk, Microdialysis calibration using retrodialysis and zero-net flux: Application to a study of the distribution of zidovudine to rabbit cerebrospinal fluid and thalamus, Pharm. Res. 10 (1993) 1411-1419.

[58] P. Lonnroth, P.A. Jansson, U. Smith, A microdialysis method allowing characterization of intercellular water space in humans, Am J Physiol 253 (1987) E228-231.

[59] R.J. Olson, J.B. Justice, Jr., Quantitative microdialysis under transient conditions, Anal. Chem. 65 (1993) 1017-1022.

[60] Y. Song, C.E. Lunte, Calibration methods for microdialysis sampling in vivo: muscle and adipose tissue, Anal. Chim. Acta 400 (1999) 143-152.

[61] Y. Song, C.E. Lunte, Comparison of calibration by delivery versus no net flux for quantitative in vivo microdialysis sampling, Anal. Chim. Acta 379 (1999) 251-262.

[62] P. Sood, S. Cole, D. Fraier, A.M.J. Young, Evaluation of metaquant microdialysis for measurement of absolute concentrations of amphetamine and dopamine in brain: A viable method for assessing pharmacokinetic profile of drugs in the brain, J. Neurosci. Methods 185 (2009) 39-44.

[63] P. Nandi, C.D. Kuhnline, S.M. Lunte, in: T.-H. Tsai (Ed.), Applications of Microdialysis in Pharmaceutical Science, John Wiley & Sons, Inc., Hoboken, NJ, 2011, p. 39-92.

[64] W.H. Lee, T.R. Slaney, R.W. Hower, R.T. Kennedy, Microfabricated Sampling Probes for in Vivo Monitoring of Neurotransmitters, Anal. Chem. 85 (2013) 3828-3831.

[65] E.E. Patterson, II, J.S. Pritchett, S.A. Shippy, High temporal resolution coupling of low-flow push-pull perfusion to capillary electrophoresis for ascorbate analysis at the rat vitreoretinal interface, Analyst 134 (2009) 401-406.

[66] J.S. Pritchett, J.S. Pulido, S.A. Shippy, Measurement of Region-Specific Nitrate Levels of the Posterior Chamber of the Rat Eye Using Low-Flow Push-Pull Perfusion, Anal. Chem. 80 (2008) 5342-5349.

[67] W.H. Lee, T.R. Slaney, P. Song, R.T. Kennedy, Monitoring Molecules in Neuroscience, 2014, p. 5.

[68] M.I. Davies, C.E. Lunte, Microdialysis sampling coupled online to microseparation techniques, Chem. Soc. Rev. 26 (1997) 215-222.

[69] M.W. Lada, T.W. Vickroy, R.T. Kennedy, High Temporal Resolution Monitoring of Glutamate and Aspartate in Vivo Using Microdialysis Online with Capillary Electrophoresis with Laser-Induced Fluorescence Detection, Anal. Chem. 69 (1997) 4560-4565.

[70] M. Wang, G.T. Roman, M.L. Perry, R.T. Kennedy, Microfluidic Chip for High Efficiency Electrophoretic Analysis of Segmented Flow from a Microdialysis Probe and in Vivo Chemical Monitoring, Anal. Chem. 81 (2009) 9072-9078.

[71] Q. Li, J.-K. Zubieta, R.T. Kennedy, Practical aspects of in vivo detection of neuropeptides by microdialysis coupled off-line to capillary LC with multistage MS, Anal Chem 81 (2009) 2242-2250.

[72] G. Taylor, Dispersion of soluble matter in solvent flowing slowly through a tube, Proc. R. Soc. London, Ser. A 219 (1953) 186-203.

[73] D. Chen, W. Du, Y. Liu, W. Liu, A. Kuznetsov, F.E. Mendez, L.H. Philipson, R.F. Ismagilov, The chemistrode: a droplet-based microfluidic device for stimulation and recording with high temporal, spatial, and chemical resolution, Proc. Natl. Acad. Sci. U. S. A. 105 (2008) 16843-16848.

[74] D. Wu, J. Qin, B. Lin, Electrophoretic separations on microfluidic chips, J. Chromatogr. A 1184 (2008) 542-559.

[75] B.A. Fogarty, P. Nandi, S.M. Lunte, in: J.P. Landers (Ed.), Capillary and Microchip Electrophoresis and Associated Microtechniques, CRC Press LLC, New York, 2008, p. 1327-1340.

[76] C.T. Culbertson, T.G. Mickleburgh, S.A. Stewart-James, K.A. Sellens, M. Pressnall, Micro Total Analysis Systems: Fundamental Advances and Biological Applications, Anal. Chem. 86 (2014) 95-118.

[77] J.W. Jorgenson, Electrophoresis, Anal. Chem. 58 (1986) 743A-744A, 746A, 748A, 750A, 752A, 754A, 756A-758A, 760A.

[78] G.T. Roman, K. McDaniel, C.T. Culbertson, High efficiency micellar electrokinetic chromatography of hydrophobic analytes on poly(dimethylsiloxane) microchips, Analyst 131 (2006) 194-201.

[79] Y. Wang, Q. Lin, T. Mukherjee, A model for Joule heating-induced dispersion in microchip electrophoresis, Lab Chip 4 (2004) 625-631.

[80] L.A. Legendre, J.P. Ferrance, J.P. Landers, in: J.P. Landers (Ed.), Handbook of Capillary and Microchip Electrophoresis and Associated Microtechniques, CRC Press, New York, 2008, p. 335-358.

[81] R. Weinberger, Practical Capillary Electrophoresis, Academic Press, New York, 2000.

[82] D.E. Scott, S.D. Willis, S. Gabbert, D. Johnson, E. Naylor, E.M. Janle, J.E. Krichevsky, C.E. Lunte, S.M. Lunte, Development of an on-animal separation-based sensor for monitoring drug metabolism in freely roaming sheep, Analyst 140 (2015) 3820-3829.

[83] K. Ren, J. Zhou, H. Wu, Materials for Microfluidic Chip Fabrication, Acc. Chem. Res. 46 (2013) 2396-2406.

[84] P.N. Nge, C.I. Rogers, A.T. Woolley, Advances in Microfluidic Materials, Functions, Integration, and Applications, Chem. Rev. 113 (2013) 2550-2583.

[85] V. Dolnik, Wall coating for capillary electrophoresis on microchips, Electrophoresis 25 (2004) 3589-3601.

[86] D.C. Duffy, J.C. McDonald, O.J.A. Schueller, G.M. Whitesides, Rapid Prototyping of Microfluidic Systems in Poly(dimethylsiloxane), Anal. Chem. 70 (1998) 4974-4984.

[87] B.H. Huynh, B.A. Fogarty, P. Nandi, S.M. Lunte, A microchip electrophoresis device with on-line microdialysis sampling and on-chip sample derivatization by naphthalene 2,3-dicarboxaldehyde/2-mercaptoethanol for amino acid and peptide analysis, J. Pharm. Biomed. Anal. 42 (2006) 529-534.

[88] M.W. Li, B.H. Huynh, M.K. Hulvey, S.M. Lunte, R.S. Martin, Design and Characterization of Poly(dimethylsiloxane)-Based Valves for Interfacing Continuous-Flow Sampling to Microchip Electrophoresis, Anal. Chem. 78 (2006) 1042-1051.

[89] P. Nandi, D.P. Desai, S.M. Lunte, Development of a PDMS-based microchip electrophoresis device for continuous online in vivo monitoring of microdialysis samples, Electrophoresis 31 (2010) 1414-1422.

[90] P. Nandi, D.E. Scott, D. Desai, S.M. Lunte, Development and optimization of an integrated PDMS based-microdialysis microchip electrophoresis device with on-chip derivatization for continuous monitoring of primary amines, Electrophoresis 34 (2013) 895-902.

[91] W.K.T. Coltro, S.M. Lunte, E. Carrilho, Comparison of the analytical performance of electrophoresis microchannels fabricated in PDMS, glass, and polyester-toner, Electrophoresis 29 (2008) 4928-4937.

[92] H. Makamba, J.H. Kim, K. Lim, N. Park, J.H. Hahn, Surface modification of poly(dimethylsiloxane) microchannels, Electrophoresis 24 (2003) 3607-3619.

[93] G. Ocvirk, M. Munroe, T. Tang, R. Oleschuk, K. Westra, D.J. Harrison, Electrokinetic control of fluid flow in native poly(dimethylsiloxane) capillary electrophoresis devices, Electrophoresis 21 (2000) 107-115.

[94] M.K. Hulvey, C.N. Frankenfeld, S.M. Lunte, Separation and Detection of Peroxynitrite Using Microchip Electrophoresis with Amperometric Detection, Analytical Chemistry 82 (2010) 1608-1611.

[95] J.A. Vickers, M.M. Caulum, C.S. Henry, Generation of Hydrophilic Poly(dimethylsiloxane) for High-Performance Microchip Electrophoresis, Anal. Chem. 78 (2006) 7446-7452.

[96] S. Thorslund, F. Nikolajeff, Instant oxidation of closed microchannels, J. Micromech. Microeng. 17 (2007) N16-N21.

[97] L.A. Filla, D.C. Kirkpatrick, R.S. Martin, Use of a Corona Discharge to Selectively Pattern a Hydrophilic/Hydrophobic Interface for Integrating Segmented Flow with Microchip Electrophoresis and Electrochemical Detection, Anal. Chem. 83 (2011) 5996-6003.

[98] R.P.S. Campos, I.V.P. Yoshida, J.A.F. Silva, Surface modification of PDMS microchips with poly(ethylene glycol) derivatives for μTAS applications, Electrophoresis 35 (2014) 2346-2352.

[99] R.P. Baldwin, T.J. Roussel, Jr., M.M. Crain, V. Bathlagunda, D.J. Jackson, J. Gullapalli, J.A. Conklin, R. Pai, J.F. Naber, K.M. Walsh, R.S. Keynton, Fully integrated on-chip electrochemical detection for capillary electrophoresis in a microfabricated device, Anal. Chem. 74 (2002) 3690-3697.

[100] R.S. Keynton, T.J. Roussel, M.M. Crain, D.J. Jackson, D.B. Franco, J.F. Naber, K.M. Walsh, R.P. Baldwin, Design and development of microfabricated capillary electrophoresis devices with electrochemical detection, Anal. Chim. Acta 507 (2004) 95-105.

[101] R.S. Pai, K.M. Walsh, M.M. Crain, T.J. Roussel, Jr., D.J. Jackson, R.P. Baldwin, R.S. Keynton, J.F. Naber, Fully Integrated Three-Dimensional Electrodes for Electrochemical Detection in Microchips: Fabrication, Characterization, and Applications, Anal. Chem. 81 (2009) 4762-4769.

[102] Z.H. Fan, D.J. Harrison, Micromachining of capillary electrophoresis injectors and separators on glass chips and evaluation of flow at capillary intersections, Anal. Chem. 66 (1994) 177-184.

[103] S. Carroll, M.M. Crain, J.F. Naber, R.S. Keynton, K.M. Walsh, R.P. Baldwin, Room temperature UV adhesive bonding of capillary electrophoresis devices, Lab Chip 8 (2008) 1564-1569.

[104] A. Iles, A. Oki, N. Pamme, Bonding of soda-lime glass microchips at low temperature, Microfluid. Nanofluid. 3 (2007) 119-122.

[105] Y. Akiyama, K. Morishima, A. Kogi, Y. Kikutani, M. Tokeshi, T. Kitamori, Rapid bonding of Pyrex glass microchips, Electrophoresis 28 (2007) 994-1001.

[106] R.S. Lima, P.A.G. Carneiro Leao, A.M. Monteiro, M.H. Oliveira Piazzetta, A.L. Gobbi, L.H. Mazo, E. Carrilho, Glass/SU-8 microchip for electrokinetic applications, Electrophoresis 34 (2013) 2996-3002.

[107] P.B. Allen, D.T. Chiu, Calcium-Assisted Glass-to-Glass Bonding for Fabrication of Glass Microfluidic Devices, Anal. Chem. 80 (2008) 7153-7157.

[108] D.E. Scott, R.J. Grigsby, S.M. Lunte, Microdialysis Sampling Coupled to Microchip Electrophoresis with Integrated Amperometric Detection on an All-Glass Substrate, ChemPhysChem 14 (2013) 2288-2294.

[109] L.C. Mecker, R.S. Martin, Integration of Microdialysis Sampling and Microchip Electrophoresis with Electrochemical Detection, Anal. Chem. 80 (2008) 9257-9264.

[110] The Molecular Probes handbook: A guide to fluorescent probes and labeling technologies, Life Technologies, 2011.

[111] C.T. Culbertson, Y. Tugnawat, A.R. Meyer, G.T. Roman, J.M. Ramsey, S.R. Gonda, Microchip Separations in Reduced-Gravity and Hypergravity Environments, Anal. Chem. 77 (2005) 7933-7940.

[112] M.F. Mora, F. Greer, A.M. Stockton, S. Bryant, P.A. Willis, Toward Total Automation of Microfluidics for Extraterrestial In Situ Analysis, Anal. Chem. 83 (2011) 8636-8641.

[113] M.F. Mora, A.M. Stockton, P.A. Willis, Analysis of thiols by microchip capillary electrophoresis for in situ planetary investigations, Electrophoresis 34 (2013) 309-316.

[114] M.F. Mora, A.M. Stockton, P.A. Willis, Microchip capillary electrophoresis instrumentation for in situ analysis in the search for extraterrestrial life, Electrophoresis 33 (2012) 2624-2638.

[115] J.S. Creamer, Department of Pharmaceutical Chemistry, Univeristy of Kansas, 2014.

[116] A.J. Bard, L.R. Faulkner, Electrochemical Methods: Fundamentals and Applications, John Wiley & Sons, Inc., Hoboken, NJ, 2002.

[117] P.S. Cahill, Q.D. Walker, J.M. Finnegan, G.E. Mickelson, E.R. Travis, R.M. Wightman, Microelectrodes for the Measurement of Catecholamines in Biological Systems, Anal. Chem. 68 (1996) 3180-3186.

[118] R.M. Wightman, Probing Cellular Chemistry in Biological Systems with Microelectrodes, Science 311 (2006) 1570-1574.

[119] J.J.P. Mark, R. Scholz, F.-M. Matysik, Electrochemical methods in conjunction with capillary and microchip electrophoresis, J. Chromatogr. A 1267 (2012) 45-64.

[120] N.A. Lacher, K.E. Garrison, R.S. Martin, S.M. Lunte, Microchip capillary electrophoresis/electrochemistry, Electrophoresis 22 (2001) 2526-2536.

[121] W.R.I.V. Vandaveer, S.A. Pasas-Farmer, D.J. Fischer, C.N. Frankenfeld, S.M. Lunte, Recent developments in electrochemical detection for microchip capillary electrophoresis, Electrophoresis 25 (2004) 3528-3549.

[122] P. Kuban, P.C. Hauser, Fundamentals of electrochemical detection techniques for CE and MCE, Electrophoresis 30 (2009) 3305-3314.

[123] C.-P. Chen, W. Teng, J.-H. Hahn, Nanoband electrode for high-performance in-channel amperometric detection in dual-channel microchip capillary electrophoresis, Electrophoresis 32 (2011) 838-843.

[124] A.S. Johnson, A. Selimovic, R.S. Martin, Integration of microchip electrophoresis with electrochemical detection using an epoxy-based molding method to embed multiple electrode materials, Electrophoresis 32 (2011) 3121-3128.

[125] M. Vazquez, C. Frankenfeld, W.K.T. Coltro, E. Carrilho, D. Diamond, S.M. Lunte, Dual contactless conductivity and amperometric detection on hybrid PDMS/glass electrophoresis microchips, Analyst 135 (2010) 96-103.

[126] L.C. Mecker, L.A. Filla, R.S. Martin, Use of a Carbon-Ink Microelectrode Array for Signal Enhancement in Microchip Electrophoresis with Electrochemical Detection, Electroanalysis 22 (2010) 2141-2146.

[127] D.J. Fischer, M.K. Hulvey, A.R. Regel, S.M. Lunte, Amperometric detection in microchip electrophoresis devices: Effect of electrode material and alignment on analytical performance, Electrophoresis 30 (2009) 3324-3333.

[128] C.-C. Wu, R.-G. Wu, J.-G. Huang, Y.-C. Lin, H.-C. Chang, Three-Electrode Electrochemical Detector and Platinum Film Decoupler Integrated with a Capillary Electrophoresis Microchip for Amperometric Detection, Anal. Chem. 75 (2003) 947-952.

[129] N.A. Lacher, S.M. Lunte, R.S. Martin, Development of a microfabricated palladium decoupler/electrochemical detector for microchip capillary electrophoresis using a hybrid glass/poly(dimethylsiloxane) device, Anal. Chem. 76 (2004) 2482-2491.

[130] D.B. Gunasekara, M.K. Hulvey, S.M. Lunte, In-channel amperometric detection for microchip electrophoresis using a wireless isolated potentiostat, Electrophoresis 32 (2011) 832-837.

[131] R.M. Saito, W.K.T. Coltro, D.P. de Jesus, Instrumentation design for hydrodynamic sample injection in microchip electrophoresis: A review, Electrophoresis 33 (2012) 2614-2623.

[132] J.M. Karlinsey, Sample introduction techniques for microchip electrophoresis: A review, Anal. Chim. Acta 725 (2012) 1-13.

[133] S. Attiya, A.B. Jemere, T. Tang, G. Fitzpatrick, K. Seiler, N. Chiem, D.J. Harrison, Design of an interface to allow microfluidic electrophoresis chips to drink from the fire hose of the external environment, Electrophoresis 22 (2001) 318-327.

[134] Y.-H. Lin, G.-B. Lee, C.-W. Li, G.-R. Huang, S.-H. Chen, Flow-through sampling for electrophoresis-based microfluidic chips using hydrodynamic pumping, J. Chromatogr. A 937 (2001) 115-125.

[135] Z.D. Sandlin, M. Shou, J.G. Shackman, R.T. Kennedy, Microfluidic electrophoresis chip coupled to microdialysis for in vivo monitoring of amino acid neurotransmitters, Anal. Chem. 77 (2005) 7702-7708.

[136] S.R. Quake, A. Scherer, From micro- to nanofabrication with soft materials, Science 290 (2000) 1536-1540.

[137] M.A. Unger, H.-P. Chou, T. Thorsen, A. Scherer, S.R. Quake, Monolithic microfabricated valves and pumps by multilayer soft lithography, Science 288 (2000) 113-116.

[138] H. Song, J.D. Tice, R.F. Ismagilov, A microfluidic system for controlling reaction networks in time, Angew. Chem., Int. Ed. 42 (2003) 768-772.

[139] M. Wang, G.T. Roman, K. Schultz, C. Jennings, R.T. Kennedy, Improved Temporal Resolution for in Vivo Microdialysis by Using Segmented Flow, Anal. Chem. 80 (2008) 5607-5615.

[140] G.T. Roman, M. Wang, K.N. Shultz, C. Jennings, R.T. Kennedy, Sampling and Electrophoretic Analysis of Segmented Flow Streams Using Virtual Walls in a Microfluidic Device, Anal. Chem. 80 (2008) 8231-8238.

[141] M. Wang, T. Slaney, O. Mabrouk, R.T. Kennedy, Collection of nanoliter microdialysate fractions in plugs for off-line in vivo chemical monitoring with up to 2 s temporal resolution, J. Neurosci. Methods 190 (2010) 39-48.

[142] M. Wang, N.D. Hershey, O.S. Mabrouk, R.T. Kennedy, Collection, storage, and electrophoretic analysis of nanoliter microdialysis samples collected from awake animals in vivo, Anal. Bioanal. Chem. 400 (2011) 2013-2023.

[143] D.E. Scott, Department of Chemistry, University of Kansas, 2014.

Chapter 5: Employing on-line microdialysis-microchip electrophoresis with electrochemical detection to monitor catecholamine release from PC-12 cells

5.1 Introduction

Microdialysis is a powerful sampling technique capable of continuously monitoring biological events *in vivo* and *in vitro*. By collecting sample via diffusion across a semipermeable membrane, microdialysis produces a continuous flow of sample that is free from proteins and macromolecules, containing only molecules small enough pass through the membrane.

While there are many potential advantages to sampling with microdialysis, in order for the technique to fulfill its greatest potential, analytical systems must be developed to take advantage of its powerful attributes. In particular, these analytical systems must exhibit fast analysis times to obtain the high temporal resolution that is possible with microdialysis, require low sample volumes (pL-to-nL), and, ideally, be capable of on-line analysis. Capillary electrophoresis and microchip electrophoresis fulfill these requirements, and have previously been coupled, on-line, to microdialysis sampling [1,2].

The first report of on-line microdialysis-capillary electrophoresis (MD-CE) was from the Lunte groups in 1994, and was used to monitor the pharmacokinetics of an anti-cancer drug *in vivo* [3]. Initial MD-CE studies employed LIF and UV detection, due to the ease of integrating optically-based techniques with electrophoresis. In 1999 the Lunte groups developed an on-line MD-CE-EC system using a cellulose acetate decoupler and demonstrated its potential by monitoring the transdermal delivery of nicotine [4].

In the 1990's, lab-on-a-chip devices emerged as a powerful analysis tool, capable of integrating multiple processing steps (*e.g*. sampling, separation, and detection) all on a single platform [5]. These devices were soon utilized for microchip-based electrophoresis separations [6-11]. Microchip electrophoresis, like capillary electrophoresis, is well suited to the analysis of microdialysis samples, as separations are fast (subminute), and the method requires low sample

volumes (pL-to-nL). Additionally, microchip electrophoresis allows for fluid manipulation on-chip, enabling the integration of microdialysis sampling on-line. Our group was the first report on-line MD-ME using a flow-gated interface [12] and this interface design has since been used for both *in vitro* [13,14] and *in vivo* [15,16] monitoring of various analytes. Additional methods for integrating microdialysis with microchip electrophoresis were discussed in Chapter 4 [2].

The above applications of microdialysis coupled to microchip electrophoresis employed LIF detection, due to the ease of focusing the laser directly into the channel, low detection limits characteristic of fluorescence, and the inherent separation of the optical detection electronics from the microchip and separation field. Electrochemical detection has also been used as a detection method for microchip electrophoresis since the late 1990's (reviewed in Chapter 2) [17]. An advantage of electrochemistry is that it is possible to miniaturize the detection electronics, making the entire device portable. Martin's group was the first to report on-line MD-ME-EC using a PDMS microchip with epoxy imbedded electrodes and a pneumatic valve interface [18]. More recently, we reported an all-glass device using a flow-gated interface and integrated platinum electrodes for on-line MD-ME-EC [19,20].

The goal of this work is to develop an on-line MD-ME-EC device capable of monitoring catecholamines in near-real time. As this device is ultimately intended for on-animal monitoring, the pneumatic valve injection scheme, which involves bulky gas tanks, is not optimal. In addition, catecholamines generate much better responses at carbon electrodes than metal-based electrodes; however, carbon electrodes are not currently compatible with all-glass devices. Therefore, a new method for integrating microdialysis sampling to microchip electrophoresis with electrochemical detection must be developed. In this chapter, the development of a procedure for fabricating PDMS/glass hybrid microchips with integrated

microdialysis sampling, electrophoretic separation, and electrochemical detection using a carbon electrode is described. Progress towards monitoring the *in vitro* release of dopamine and norepinephrine from adherent PC-12 cells is also presented.

5.2 Materials and methods

5.2.1 Reagents

The following chemicals were used as received: AZ 1518 positive photoresist and AZ 300 MIF developer (AZ Electronic Materials, Sommerville, NJ, USA); SU-8 10 and SU-8 developer (Micro-Chem, Newton, MA, USA), dopamine hydrochloride (DA), ascorbic acid (AA), (+/-) norepinephrine bitartrate salt (NE), sodium phosphate monobasic, and sodium phosphate dibasic (Sigma-Adrich, St. Louis, MO, USA); NaOH and isopropyl alcohol (IPA) (Fisher Scientific, Fairlawn, NJ, USA); sodium dodecyl sulfate (SDS) (Thermo Scientific, Waltham, MA, USA); and PDMS and curing agent (Sylgard 184 silicon elastomer base and curing agent, Dow Corning Corp., Midland, MI, USA). PC-12 cells (PC-12 Adh CRL-1721.1), F-12K medium, fetal bovine serum, horse serum, and penicillin-streptomycin (10,000 I.U./mL penicillin, 10,000 (μg/mL) streptomycin) were purchased from ATTC (Manassas, VA, USA). The following were also employed: high temperature fused silica glass plates (4 in x 2.5 in x 0.085 in, Glass Fab, Rochester, NY, USA); copper wire (22 gauge, Westlake Hardware, Lawrence, KS, USA); hot glue and hot glue gun (ACE Hardware); colloidal silver liquid (Ted Pella, Inc., Redding, CA, USA); PEEK tubing (0.127 mm ID, Index Health & Science); Instech microdialysis connectors (Instech Laboratories, Inc., Plymouth Meeting, PA, USA); 1.0 cm loop microdialysis probes (30 KDa MWCO PAN membrane, 15 cm of FEP tubing to the 1.0 cm membrane and 15 cm of FEP tubing to the chip, BASi, West Lafayette, IN, USA) or 3.0 cm cannula microdialysis probes (20KDa MWCO PAES membrane, CMA, Kista, Sweden) with 15

cm of both inlet and outlet tubing (BASi FEP Teflon tubing, 0.12 mm i.d.); 25 cm^2 cell culture flasks (CellBIND surface) and 100 mm treated polystyrene petri dishes (Corning, NY, USA); and 18.2 MΩ water (Millipore, Kansas City, MO, USA).

The cell-compatibility buffer was comprised of 72.5 mM NaCl, 1.4 mM KCl, 0.5 mM $MgCl_2$, 0.6 mM $CaCl_2$, and 0.25 mM NaH_2PO_4, and was adjusted to pH 7.4 [18,21]. The K^+/Ca^{2+} cell stimulation buffer was comprised of 150 mM NaCl, 80 mM KCl, 0.7 mM $MgCl_2$, 2.0 mM $CaCl_2$, 1.0 mM NaH_2PO_4, and 10 mM HEPES and was adjusted to pH 7.4 [18]. Stock solutions of 10 mM of each analyte were prepared in 18.2 MΩ water. Analysis solutions were made from these standard solutions and diluted in 15 mM sodium phosphate (pH 7.4) or indicated buffer at the time of analysis.

5.2.2 Fabrication of substrates

PDMS microchip fabrication has been described elsewhere [22] and in Chapter 3 (section 3.3.2). Briefly, a silicon master was created with raised features through classic photolithography. These features were 15 µm and determined the channel depth in the final PDMS substrate. For this flow-gated, double-t design, the separation channel length was 5 cm, each side arm was 0.75 cm and the top-t was 2 cm. The width of all the channels was 40 µm, except the top sampling channel which was 1.0 mm. This chip design can be seen in Figure 5.1. To create the PDMS microchip from the silicon master, PDMS/curing agent was mixed at a 10:1 ratio and poured onto the master to form a thickness of at least 2 mm. This channel layer is thicker than that described in Chapter 3, to provide stability and support for the microdialysis inlet stainless steel connector and tubing. The PDMS was cured overnight at 70°C, after which the PDMS channels were peeled from the silicon master. Buffer and sample waste reservoirs were punched into the PDMS using a 4 mm biopsy punch (Harris Uni-core, Ted Pella).

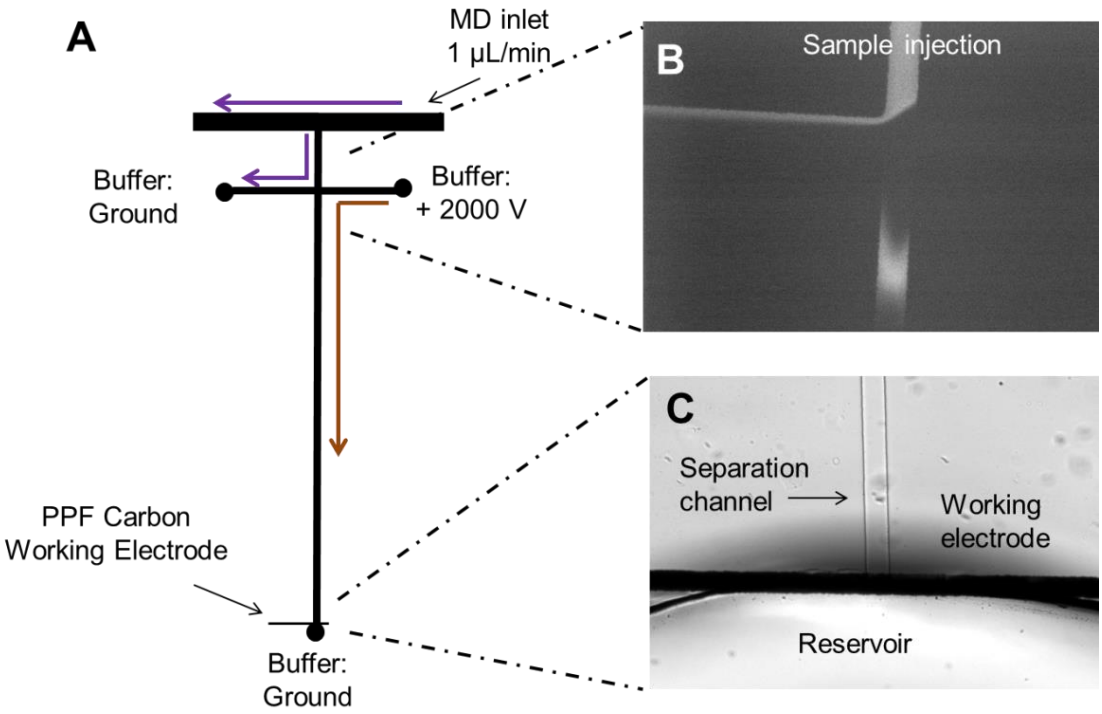

Figure 5.1 Flow-gated interface using double-t microchip design for on-line microdialysis-microchip electrophoresis with electrochemical detection. (A) Device design, applied voltages, and flow rate. (B) Example sample injection with an injection time of 1.0 s and visualized with fluorescein. (C) Alignment at the end of the separation channel with a 35 µm PPF carbon electrode.

Pyrolyzed photoresist electrode fabrication has been described previously [23-25], in Chapter 3 (section 3.2.3.2), and the fabrication process is shown in Figure 2.10. Classic photolithography techniques were used to pattern positive photoresist onto quartz glass substrates in the design of the desired electrodes. Substrates with photoresist were then placed in a Linden-BlueM Tube furnace, with a constant flow of nitrogen gas throughout the pyrolysis procedure. The temperature program was ramped from room temperature to 925°C at 5.5°C/min

and held for 1 hour. The furnace was then allowed to cool back down to room temperature. Final electrode dimensions after pyrolysis, as measured using a surface profiler, were 35 µm wide and 0.5 µm in height.

5.2.3 Microchip construction

For on-line experiments using the double-t design, a partial irreversible bond between the PDMS channels and glass electrode substrate was created. The microchip was constructed immediately after the PDMS was cured and removed from the oven. Parafilm M ®, which is normally used to store PDMS microchips prior to use, leaves a thin residue on the PDMS. This residue interferes with the PDMS/glass bonding described here, so PDMS microchips were used immediately and not stored. PDMS channels and the electrode substrate were simultaneously plasma oxidized (Harrick Plasma Cleaner/Sterilizer PDC-32G, Ithaca, NY, USA) by placing substrates under vacuum for 2 minutes, followed by oxidation at medium radio frequency (RF) for 60 seconds (also accomplished under vacuum). During this procedure, a piece of sacrificial PDMS (about 6 cm wide and 3 cm in length) was placed over the carbon working electrode and surrounding area. Immediately following oxidation, the sacrificial PDMS was removed and the PDMS channels were placed in conformal contact with the electrode substrate. This procedure created an irreversible bond in the top portion of the microchip to withstand the pressure driven microdialysis flow, and a reversible bond in the bottom portion where the electrode resides to allow the electrode to be reused. This bonding procedure can be seen in Figure 5.2. To create the electrical connection, a copper wire was attached to the electrode with silver colloid. This wire was affixed to the glass substrate using hot glue, which allowed for stability during experiments as well as easy removal after experiment completion.

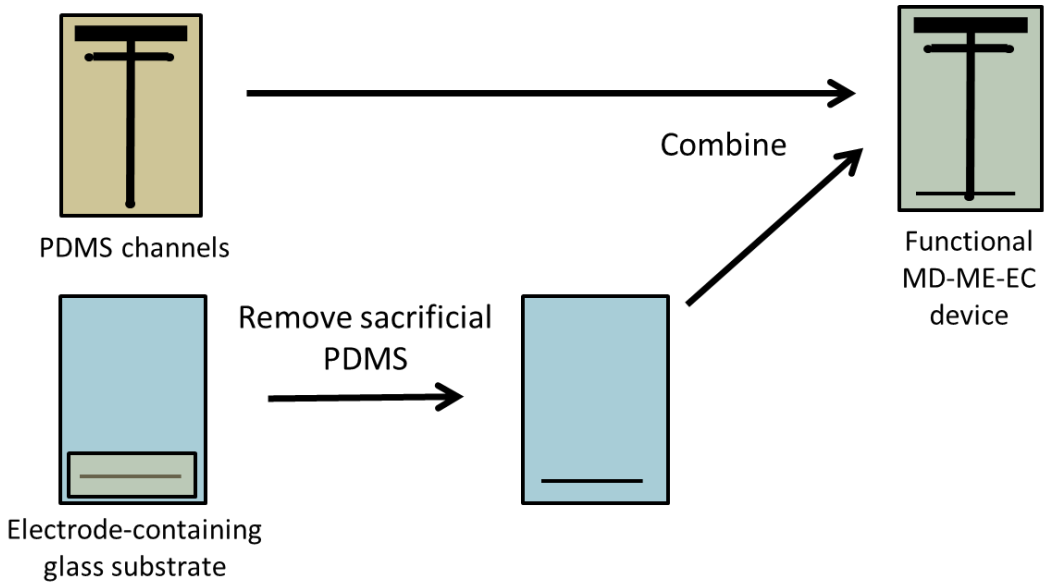

Figure 5.2 PDMS/glass bonding procedure. This procedure creates a fully functional MD-ME-ME device that is irreversibly bonded in the top, MD portion of the microchip and reversibly bonded in the bottom, electrode-containing portion of the microchip.

To couple the microchip to the microdialysis pump, a stainless steel 20 gauge blunt needle was used to make a hole in the PDMS for the sample inlet. A 20 gauge 2.0 cm stainless steel connector was used to connect the microchip to either the microdialysis probe or directly to 15 cm of PEEK tubing through Instech microdialysis connectors. Microdialysis probes employed in these studies included both 1.0 cm loop microdialysis probes and 3.0 cm cannula microdialysis probes.

5.2.4 Experimental procedure

Prior to electrophoresis experiments, the channels were flushed via negative pressure using isopropyl alcohol, 0.1 M NaOH, and the run buffer. The top-t was also conditioned and filled, first with isopropyl alcohol then 15 mM phosphate (pH 7.4) using positive pressure

through the syringe connected directly to the chip with PEEK tubing. During experiments, pressure was applied to the 1.0 mL glass syringe using a CMA 102 syringe pump (CMA, Holliston, MA, USA). Electrophoresis procedures were accomplished using a single Spellman CZE 1000R (Hauppauge, NY, USA) high voltage power supply controlled using a LabView program (National Instruments, Austin, TX, USA) written in house. A flow-gated injection scheme was employed, through the application of 2000 V at the buffer reservoir and holding the sample waste and buffer waste reservoirs at ground, paired with a microdialysis flow rate of 1.0 μL/min (Figure 5.1). Injections were accomplished by floating the buffer voltage for a specified amount of time, then reestablishing the voltage for the separation.

Electrochemical detection was accomplished using a two electrode system (pyrolyzed photoresist film working, Ag/AgCl reference (BASi, West Lafayette, IN, USA)) with an electrically isolated potentiostat (Pinnacle Technology Inc., Lawrence KS). The sampling rate for this device was 10 Hz, and data acquisition was performed through wireless transmission and visualized with Pinnacle Acquisition Laboratory (PAL 8400) software. This potentiostat has been used previously in our group for in-channel detection [26]. For all experiments described in this chapter, the working electrode was held at 1.0 V (versus Ag/AgCl) and placed at the very end of the channel outlet (as shown in Figure 5.1C). This alignment allows for higher separation efficiencies than traditional end channel alignment, as band broadening due to diffusion after the separation is limited, while still allowing the detection electrodes to be mostly decoupled from the separation field [25,27]. Data was analyzed using Origin 8.6 software (OriginLab, Northhampton, MA, USA) after baseline subtraction. In calculating peak migration time (and therefore resolution and efficiency), the end of the injection was considered the start time.

5.2.5 Cell procedure

PC-12 cells were cultured and subcultured in F-12 medium supplemented with 15% horse serum, 2.5% fetal bovine serum and 0.5% penicillin-streptomycin solution in an incubator at 37°C and approximately 5% CO_2. After the cells reached 90-100% confluency, they were suspended in fresh media, plated into cell micropallets, and left in the incubator at least overnight to adhere to the base of the micropallets. The cell micropallets were made by punching holes in PDMS and placing the PDMS on a cell culture petri dish (treated polysterene). Prior to analysis, PC-12 cells were preloaded with a solution of up to 10 mM dopamine and 10 mM norepinephrine in media for at least one hour in the incubator. After the cells were preloaded, they were rinsed three times with a cell-compatibility buffer to remove any dopamine and norepinephrine not taken up into the cells and placed in this buffer for analysis. After a baseline of cells in this solution was acquired, release was stimulated by changing the solution surrounding the cells to a high K^+/Ca^{2+} buffer. Microdialysis perfusate consisted of 50 µM ascorbic acid in 15 mM phosphate (pH 7.4) buffer at a flow rate of 1.0 µL/min. A schematic of the device and cell sampling procedure can be seen in Figure 5.3.

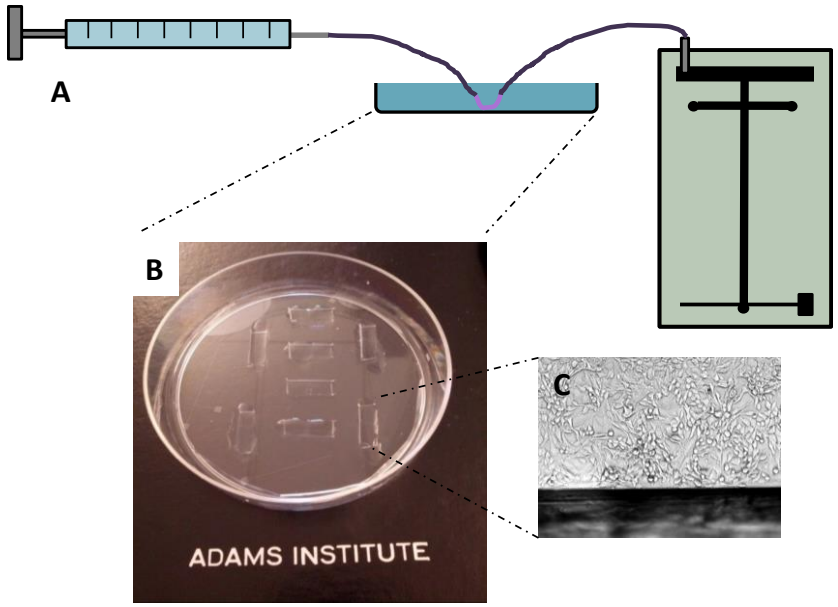

Figure 5.3 On-line sampling procedure. (A) Microdialysis sampling of cell micropallets analyzed on-line by microchip electrophoresis with electrochemical detection. (B) Example rectangular cell micropallets in a polysterene-coated cell culture petri dish. (C) Image of PC-12 cells in cell micropallet. The edge in the image is the beginning of the PDMS reservoir.

5.3 Results and discussion

5.3.1 Bonding procedure

When coupling microdialysis sampling on-line to microchip electrophoresis, great care must be taken at the interface to allow for the integration of hydrodynamic pressure from microdialysis sampling. This is accomplished by creating an irreversible bond between the two substrates (channels and base) so that when hydrodynamic pressure is introduced, the two substrates remain in contact. A bond that does not withstand this pressure will delaminate and lead to the inability to inject or separate sample. For all-glass devices, many bonding procedures

exist to irreversibly bond two pieces of glass both with [19,28-30] and without [31-36] the incorporation of metal electrodes. However, the incorporation of carbon-based electrodes, which generate better responses to many biologically important analytes, into an all glass device has not yet been reported. Prior to the work described in this thesis, bonding procedures for MD-ME PDMS microchips involved a full, irreversible seal between the PDMS channels and the substrate (glass or PDMS) and detection with LIF [14,16]. These researchers employed either plasma oxidation or semicuring methods to irreversibly bond these devices. A single report exists of an on-line MD-ME-EC system with carbon electrodes from Scott Martin's lab using epoxy- or polystyrene-embedded electrodes as the electrode substrate and the pneumatic valve injection scheme [18]. The main drawback in irreversibly bonding PDMS channels to a substrate containing a carbon electrode is that the resultant chip will have PDMS that is bonded to the electrode, destroying the electrode for any future use. As the lifetime of PDMS microchips used in ME is relatively short (usually one experiment), after which a new microchip is constructed, a bonding method that enables electrode substrates to be used multiple times is highly desirable.

The bonding procedure developed here and outlined in Figure 5.2 enables the reuse of an electrode substrate for many experiments since the PDMS channels are not bonded to the electrode-containing portion of the substrate. To bond the PDMS channels and glass substrate together, plasma oxidation was employed, which alters the surface of the PDMS from –$OSi(CH_3)_2O$– to –$O_nSi(OH)_{4-n}$– and cleans any organic residues off of the glass substrate [37,38]. When in conformal contact with one another, it is thought that covalent O-Si-O bonds form between the PDMS and glass, creating an irreversible bond [22]. In the procedure employed here, a sacrificial piece of PDMS is placed on the glass electrode substrate, over the

electrode-containing portion of the microchip. This sacrificial PDMS prevents a small area of the glass substrate from being cleaned through plasma oxidation, making the subsequent bond between PDMS and glass reversible. The upper portion of the glass (and therefore microchip) is irreversibly bonded and withstands the hydrodynamic pressure of the microdialysis flow necessary for on-line MD-ME. For subsequent experiments, the PDMS portion of the microchip can be removed (using a razor blade where irreversibly bonded) and reused; the same batch of electrodes can be reused for months or years.

In order to run MD-ME experiments using this flow-gated interface design, the microdialysis flow rate, separation voltage, and ground placement needed to be optimized, since these parameters are all important and interdependent for establishing a good, stable gate and injection. In these studies, a microdialysis flow rate of 1.0 μL/min was employed, as it is widely used in the literature and in our lab. Additionally, lower flow rates (below 0.8 μL/min), while leading to increased microdialysis recoveries, have previously been shown to result in lower signals at the detector when using the flow-gated injection design [12]. Flow-gated interfaces rely on both the microdialysis pressure and the electroosmotic flow to establish a good gate; at low flow rates not enough sample is pushed into the separation channel. A separation voltage of 2000 V, which corresponds to field strength of ~130 V/cm as calculated using Kirchhoff's laws, was used in conjunction with a microdialysis flow rate of 1.0 μL/min [39]. Higher voltages, such as 3000 V and above, establish a gate and lead to better separation efficiencies, but also result in a much smaller amount of sample being introduced into the separation channel [12]. Additionally, the microchip design used in these studies requires the use of two grounds to adequately establish a gate. While a single ground in the detection reservoir was attempted in this configuration, sample leaked into the separation channel during the separation. To inject the

sample into the separation channel, the buffer voltage is floated for a specified amount of time. The voltage is then reestablished for the separation. The optimized voltages and flow rate can be visualized, along with an example of sample injection and electrode alignment, in Figure 5.1.

5.3.2 Separation optimization

In order to detect both dopamine (DA) and norepinephrine (NE) release from PC-12 cells simultaneously, these analytes first had to be separated from one another using microchip electrophoresis. Ascorbic acid (AA) was also included in this separation as an internal standard for the migration time. Additionally, ascorbic acid was added to the perfusate in the cell studies to ensure that the device was working optimally and was free of clogs.

5.3.2.1 Background electrolyte

As in Chapter 3, phosphate was chosen as the background electrolyte to maintain biological and injection compatibility. A background electrolyte of 15 mM phosphate at pH 7.4 was employed in these studies; higher phosphate concentrations lead to excessive Joule heating and a more limited microchip lifetime. It was noted, however, that a 15 mM phosphate concentration and application of voltages employed in the double-t device did lead to a lower overall separation current than was seen in the previous chapter with the 5 cm simple-t device, due to a slightly lower field strength in the MD-ME-EC device than the ME-EC device.

5.3.2.2 Addition of SDS

SDS was added to the run buffer to help wet the channels, create a negative charge at the wall of the PDMS, and create micelles for an MEKC separation [40]. At low concentrations of SDS, dopamine comigrated with norepinephrine. As the SDS concentration is increased, the positively charged dopamine and, to a lesser extent norepinephrine, interact electrostatically with the anionic SDS micelles, causing later migration times. The affinity of SDS micelles with

norepinephrine is less than that between dopamine and the micelles, possibly due to steric hindrance caused by the alcohol functional group located on norepinephrine. Dopamine was initially resolved from all other peaks at SDS concentrations between 2.0 and 5.0 mM; however, it comigrated at SDS concentrations between 5.0 and 7.5 mM SDS. Dopamine was resolved again at SDS concentrations above 7.5 mM (Figure 5.4). While these higher concentrations of SDS (above 7.5 mM) did initially achieve complete resolution of all analytes, it was noticed in previous studies (Chapter 3) that high concentrations of SDS leads to greater migration time variability of analytes that are affected by the micelles. Therefore, the optimal concentration of SDS was determined to be 2.0 mM. Under these optimal conditions, a limit of detection for dopamine of as low as 10 µM (S/N =3) was achieved.

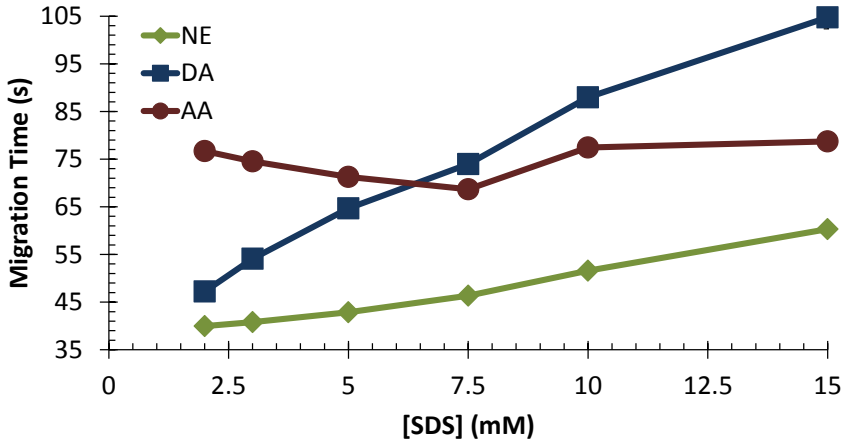

Figure 5.4 Effect of SDS concentration on analyte migration times. Separation buffer is the indicated SDS concentration and 15 mM phosphate (pH 7.4), and each point corresponds to an average of three sequential injections.

5.3.2.3 Perfusate/sample matrix

The effect of the sample matrix and ionic strength on sample injection was determined prior to performing cell studies. While it was possible to employ 15 mM phosphate as the

perfusate in these cell studies, the cells themselves must be maintained in a cell-compatible solution or a high K^+/Ca^{2+} solution (during cell stimulation). The components of these buffers are found in the experimental section 5.2.1. Both of these cell buffers are very high in salt and therefore ionic strength, and some of these salt ions will diffuse into the microdialysis probe and be injected into the system. Samples that are higher in ionic strength than the run buffer will result in destacking, a process which can decrease separation efficiency and worsen resolution. Therefore, prior to the cell studies, analytes of interest were prepared in both the cell-compatibility and high K^+/Ca^{2+} buffers to determine the effect of high ionic strength samples on the separation quality; these results can be seen in Figure 5.5. As can be seen in this figure, there was no visible reduction in separation quality as the ionic strength of the sample was increased from a 15 mM phosphate buffer to the cell-compatibility buffer and again to the high K^+/Ca^{2+} buffer.

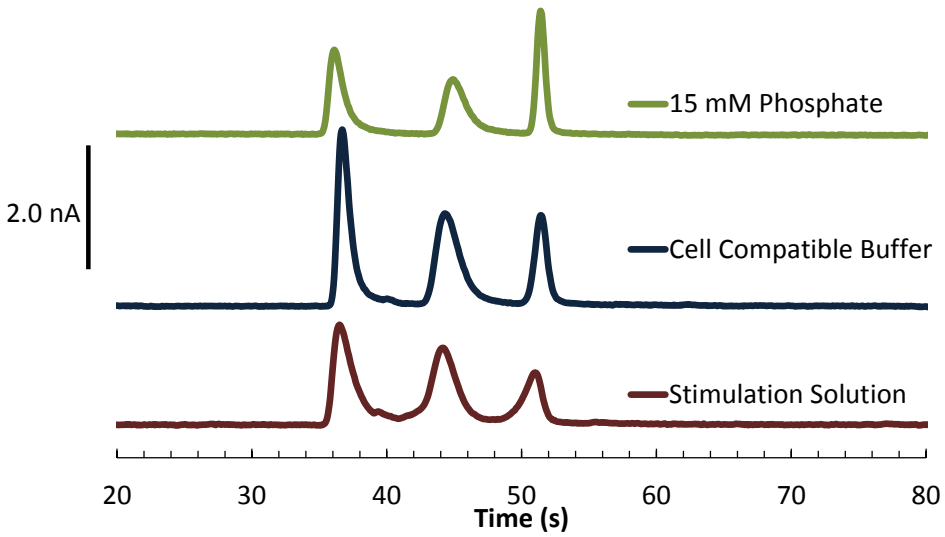

Figure 5.5 Effect of sample matrix on separation conditions. The separation buffer is 15 mM phosphate (pH 7.4) with 2.0 mM SDS, and 200 µM of each analyte was dissolved in the indicated matrix.

5.3.3 Cell micropallet and microdialysis probe optimization

For the cell sampling studies, tit was very important to maintain cell viability while limiting the amount of surrounding solution (to avoid dilution). In these studies, the extracellular supernatant was continuously sampled through a microdialysis probe placed in the solution above the cells. PC-12 cells are adherent cells that require support (*e.g.*, collagen, polystyrene, CellBIND® flasks). Therefore, it was necessary for the *in vitro* sampling vial to have a support-lined bottom. Initially, the microdialysis sampling was attempted in 25 cm^2 cell-culture flasks (CellBIND®) in which the cells are normally grown and sub-cultured. However, the single small side opening in these flasks made it difficult to place the microdialysis sampling probe in the flask and change solutions without disturbing the cells. Additionally, a large volume (~ 4 mL) was required to completely cover all the cells and the microdialysis probe, making dilution of the contents released by the cells problematic for detection. An improved approach, using a cell micropallet, with a base capable of supporting cells, was used for further experiments. While methods do exist for coating glass, plastic, or PDMS with a layer of collagen [18], here it was simpler to use a polystyrene-coated petri dish and PDMS reservoirs to create cell-sampling micropallets. PC-12 cells do not grow on native PDMS, so when cultured, the PC-12 cells only adhered to the bottom, polystyrene-coated area in the wells.

Initially, rectangular micropallets were created. These 1.5 cm x 0.5 cm micropallets were created by hand in PDMS with a razor blade and placed on the polystyrene-coated petri dish to create a complete micropallet capable of holding 200 µL of solution. After cells were incubated overnight and had adhered to the bottom of the wells, they were preloaded with dopamine and norepinephrine and a 1.0 cm linear microdialysis probe was placed into the micropallet for sampling. When this procedure was employed to sample extracellular release from K^+/Ca^{2+}

stimulated cells, the amount dopamine or norepinephrine that was released was below the limits of detection of this device. Additionally, after analysis, a visual inspection of the cells in the micropallet revealed that the placement of the microdialysis probe into the micropallet had inadvertently scraped the cells off the bottom polystyrene support.

Next, a 4 mm biopsy punch was used to create cylindrical micropallets in PDMS that were 4 mm in height (the width of the PDMS slab) and 4 mm in diameter, capable of containing 50 µL of solution. However, the 1.0 cm linear probe had to be bent to fit within the confines of the micropallet which caused it to scrape the edges and bottom, again removing cells. Therefore, for the cylindrical micropallets, a cannula microdialysis probe was employed. This probe could be easily placed into the cylindrical micropallet without the tip of the probe scraping the cells off their support. Prior to analysis, cells were incubated in the reservoirs overnight, then preloaded with dopamine and norepinephrine, washed with cell compatibility buffer, and placed in 50 µL of the cell compatibility buffer for analysis. The microdialysis probe was placed into the reservoir and cells were analyzed with the system shown in Figure 5.3. The cells were then stimulated by the high K^+/Ca^{2+} solution. While under these conditions, a dopamine and norepinephrine response was observed, although it was barely detectible. Therefore it was determined that further efforts need to be made to improve the limits of detection.

5.3.4 Increasing injection times to increase signal

One parameter that is simple to vary in ME devices is the injection time. This parameter can affect both the separation efficiency and the limits of detection. From a separation optimization standpoint, the goal is to minimize the injection plug to an infinitesimally small width to allow for reduced band broadening and enhanced separations [41]. From a detection standpoint, an increase in the volume of sample introduced into the separation channel will

generate a higher signal. When employing gated or flow-gated injection schemes, a common injection time is 1.0 s, which allows for some sample introduction into the separation channel. Most researchers do not use longer injection times to avoid a loss of resolution and separation efficiency. When visualizing gated injection with this device, it was noticed that a 1.0 s injection did not seem to inject enough sample into the separation channel; therefore, initial studies with this device employed a 1.5 s injection. Wendell Coltro's group in Brazil recently reported increasing injection times in microchip electrophoresis lowered the detection limits (increased the signal), without a loss in resolution [personal correspondence, data not published].

Figure 5.6 demonstrates the effect of increasing the injection time from 1.0 s to 50.0 s on each analyte's peak height. In Figure 5.6A, a direct comparison between the peak heights obtained for a 1.0 s and 50.0 s injection demonstrates a dramatic increase in signal with the increase in injection time. In these electropherograms, dopamine's peak area increases from 0.6 nA·s with a 1.0 s injection to over 60 nA·s with a 50 s injection. Figure 5.6B shows the linear increase in peak area with increasing injection times. The truly remarkable aspect of this modification is the lack of effect on the resolution. The resolution between dopamine and norepinephrine remained relatively constant over the entire range of injection times investigated, with the resolution only decreasing slightly (from 1.6 to 0.9). This slight loss of resolution could also be due to deterioration of the PDMS channels in the microchip over the time of the experiment.

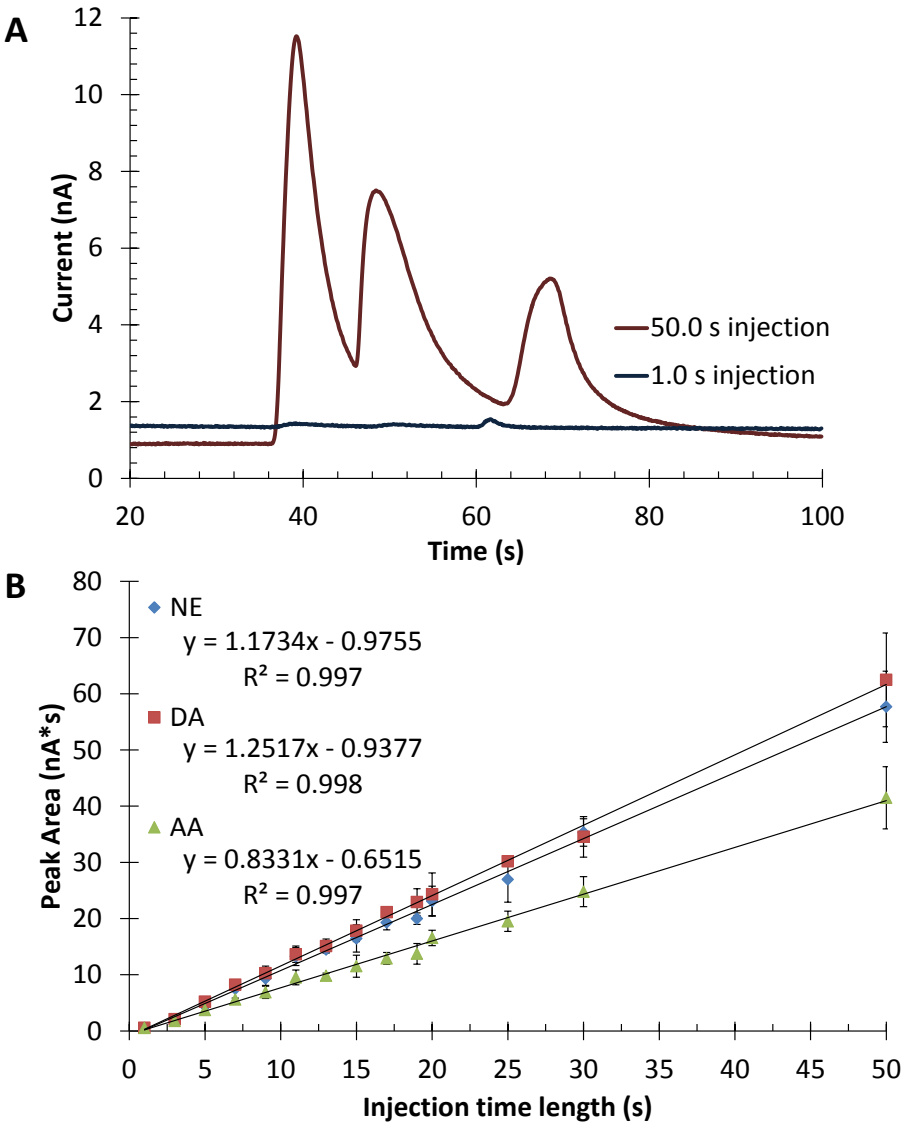

Figure 5.6 Effect of injection time length on peak area. (A) Sample electropherograms of 1.0 s injection and 50.0 s injection. (B) Linear relationship between increasing the injection time and the resultant peak area for the three analytes in this separation. The separation buffer was 15 mM phosphate (pH 7.4) with 2.0 mM SDS, and 100 μM of each analyte was dissolved in 15 mM phosphate buffer (pH 7.4). Each point corresponds to the average of three subsequent injections.

This tactic worked very well to increase the signal of standards dissolved in 15 mM phosphate and the cell compatibility buffer (data not shown). However, when dopamine and norepinephrine were prepared in the high K^+/Ca^{2+} solution, destacking became problematic and the separation suffered greatly, as seen in Figure 5.7. In these studies, the stimulation procedure requires that the solution surrounding the cells be changed from the compatibility buffer to the high K^+/Ca^{2+} solution, and then sampled though microdialysis. Unfortunately, this destacking made it impossible to detect dopamine and norepinephrine release from stimulated cells using long injection times. In the future, a stimulation procedure that does not involve such high salt concentrations, such as electrical stimulation, hypoxia, or hyperglycemia [42], will be necessary to monitor the release of dopamine and norepinephrine from PC-12 cells using the on-line device.

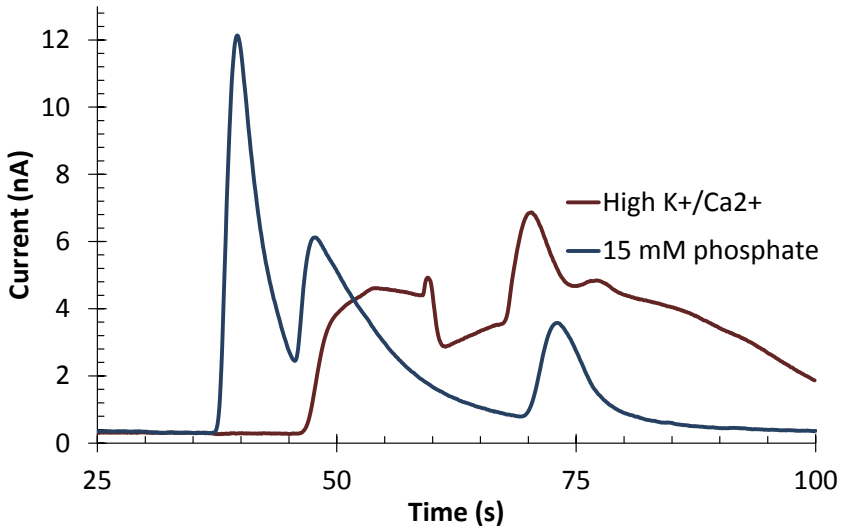

Figure 5.7 Effect of sample matrix and long injection times on separation. The separation buffer was 15 mM phosphate (pH 7.4) with 2.0 mM SDS, and 100 μM of each analyte was dissolved in the indicated sample matrix. The injection time was 50.0 s.

5.4 Concluding remarks

In conclusion, a novel fabrication method was developed for on-line microdialysis sampling coupled to microchip electrophoresis with electrochemical detection at a carbon electrode. This fabrication method featured an irreversible bond in the upper portion that allowed for pressure driven microdialysis flow to be incorporated into the microchip. This method also allowed for electrode reuse and alignment, due to a reversible bond in the lower portion of the microchip. With the goal of detecting stimulated release of catecholamines from PC-12 cells, a separation between dopamine, norepinephrine, and ascorbic acid was optimized. Cell micropallet and microdialysis sampling procedures were also optimized. Interestingly, it was found that increasing the injection time from 1.0 s to 50.0 s increased the signal by over 100-fold but had little effect on the quality of the separation when standards were dissolved in 15 mM phosphate. However, when employing a high ionic strength sample matrix, longer injection times resulted in analyte destacking and a destruction of the separation. In the future, a cell stimulation procedure that does not require high ionic strength solutions should be investigated.

5.5 References

[1] P. Nandi, S.M. Lunte, Recent trends in microdialysis sampling integrated with conventional and microanalytical systems for monitoring biological events: A review, Anal. Chim. Acta 651 (2009) 1-14.

[2] R.A. Saylor, S.M. Lunte, A review of microdialysis coupled to microchip electrophoresis for monitoring biological events, Journal of Chromatography A 1382 (2015) 48-64.

[3] B.L. Hogan, S.M. Lunte, J.F. Stobaugh, C.E. Lunte, Online Coupling of in vivo Microdialysis Sampling with Capillary Electrophoresis, Anal. Chem. 66 (1994) 596-602.

[4] J. Zhou, D.M. Heckert, H. Zuo, C.E. Lunte, S.M. Lunte, Online coupling of in vivo microdialysis with capillary electrophoresis/electrochemistry, Anal. Chim. Acta 379 (1999) 307-317.

[5] A. Manz, N. Graber, H.M. Widmer, Miniaturized total chemical analysis systems: a novel concept for chemical sensing, Sens. Actuators, B 1 (1990) 244-248.

[6] D.J. Harrison, K. Fluri, K. Seiler, Z. Fan, C.S. Effenhauser, A. Manz, Micromachining a miniaturized capillary electrophoresis-based chemical analysis system on a chip, Science 261 (1993) 895-897.

[7] D.J. Harrison, A. Manz, Z. Fan, H. Luedi, H.M. Widmer, Capillary electrophoresis and sample injection systems integrated on a planar glass chip, Anal. Chem. 64 (1992) 1926-1932.

[8] A. Manz, D.J. Harrison, E.M.J. Verpoorte, J.C. Fettinger, A. Paulus, H. Luedi, H.M. Widmer, Planar chips technology for miniaturization and integration of separation techniques into monitoring systems. Capillary electrophoresis on a chip, J. Chromatogr. 593 (1992) 253-258.

[9] K. Seiler, D.J. Harrison, A. Manz, Planar glass chips for capillary electrophoresis: repetitive sample injection, quantitation, and separation efficiency, Anal. Chem. 65 (1993) 1481-1488.

[10] S.C. Jacobson, R. Hergenroder, L.B. Koutny, J.M. Ramsey, High-Speed Separations on a Microchip, Anal. Chem. 66 (1994) 1114-1118.

[11] S.C. Jacobson, R. Hergenroder, L.B. Koutny, R.J. Warmack, J.M. Ramsey, Effects of Injection Schemes and Column Geometry on the Performance of Microchip Electrophoresis Devices, Anal. Chem. 66 (1994) 1107-1113.

[12] B.H. Huynh, B.A. Fogarty, R.S. Martin, S.M. Lunte, On-Line Coupling of Microdialysis Sampling with Microchip-Based Capillary Electrophoresis, Anal. Chem. 76 (2004) 6440-6447.

[13] B.H. Huynh, B.A. Fogarty, P. Nandi, S.M. Lunte, A microchip electrophoresis device with on-line microdialysis sampling and on-chip sample derivatization by naphthalene 2,3-dicarboxaldehyde/2-mercaptoethanol for amino acid and peptide analysis, J. Pharm. Biomed. Anal. 42 (2006) 529-534.

[14] P. Nandi, D.E. Scott, D. Desai, S.M. Lunte, Development and optimization of an integrated PDMS based-microdialysis microchip electrophoresis device with on-chip derivatization for continuous monitoring of primary amines, Electrophoresis 34 (2013) 895-902.

[15] Z.D. Sandlin, M. Shou, J.G. Shackman, R.T. Kennedy, Microfluidic electrophoresis chip coupled to microdialysis for in vivo monitoring of amino acid neurotransmitters, Anal. Chem. 77 (2005) 7702-7708.

[16] P. Nandi, D.P. Desai, S.M. Lunte, Development of a PDMS-based microchip electrophoresis device for continuous online in vivo monitoring of microdialysis samples, Electrophoresis 31 (2010) 1414-1422.

[17] A.T. Woolley, K. Lao, A.N. Glazer, R.A. Mathies, Capillary Electrophoresis Chips with Integrated Electrochemical Detection, Anal. Chem. 70 (1998) 684-688.

[18] L.C. Mecker, R.S. Martin, Integration of Microdialysis Sampling and Microchip Electrophoresis with Electrochemical Detection, Anal. Chem. 80 (2008) 9257-9264.

[19] D.E. Scott, R.J. Grigsby, S.M. Lunte, Microdialysis Sampling Coupled to Microchip Electrophoresis with Integrated Amperometric Detection on an All-Glass Substrate, ChemPhysChem 14 (2013) 2288-2294.

[20] D.E. Scott, S.D. Willis, S. Gabbert, D. Johnson, E. Naylor, E.M. Janle, J.E. Krichevsky, C.E. Lunte, S.M. Lunte, Development of an on-animal separation-based sensor for monitoring drug metabolism in freely roaming sheep, Analyst 140 (2015) 3820-3829.

[21] K.D. Kozminski, D.A. Gutman, V. Davila, D. Sulzer, A.G. Ewing, Voltammetric and pharmacological characterization of dopamine release from single exocytotic events at rat pheochromocytoma (PC12) cells, Anal. Chem. 70 (1998) 3123-3130.

[22] D.C. Duffy, J.C. McDonald, O.J.A. Schueller, G.M. Whitesides, Rapid Prototyping of Microfluidic Systems in Poly(dimethylsiloxane), Anal. Chem. 70 (1998) 4974-4984.

[23] D.J. Fischer, M.K. Hulvey, A.R. Regel, S.M. Lunte, Amperometric detection in microchip electrophoresis devices: Effect of electrode material and alignment on analytical performance, Electrophoresis 30 (2009) 3324-3333.

[24] D.J. Fischer, W.R.I.V. Vandaveer, R.J. Grigsby, S.M. Lunte, Pyrolyzed photoresist carbon electrodes for microchip electrophoresis with dual-electrode amperometric detection, Electroanalysis 17 (2005) 1153-1159.

[25] R.A. Saylor, E.A. Reid, S.M. Lunte, Microchip electrophoresis with electrochemical detection for the determination of analytes in the dopamine metabolic pathway, Electrophoresis 36 (2015) 1913-1919.

[26] D.B. Gunasekara, M.K. Hulvey, S.M. Lunte, In-channel amperometric detection for microchip electrophoresis using a wireless isolated potentiostat, Electrophoresis 32 (2011) 832-837.

[27] D.B. Gunasekara, J.M. Siegel, G. Caruso, M.K. Hulvey, S.M. Lunte, Microchip electrophoresis with amperometric detection method for profiling cellular nitrosative stress markers, Analyst 139 (2014) 3265-3273.

[28] R.P. Baldwin, T.J. Roussel, Jr., M.M. Crain, V. Bathlagunda, D.J. Jackson, J. Gullapalli, J.A. Conklin, R. Pai, J.F. Naber, K.M. Walsh, R.S. Keynton, Fully integrated on-chip electrochemical detection for capillary electrophoresis in a microfabricated device, Anal. Chem. 74 (2002) 3690-3697.

[29] R.S. Keynton, T.J. Roussel, M.M. Crain, D.J. Jackson, D.B. Franco, J.F. Naber, K.M. Walsh, R.P. Baldwin, Design and development of microfabricated capillary electrophoresis devices with electrochemical detection, Anal. Chim. Acta 507 (2004) 95-105.

[30] R.S. Pai, K.M. Walsh, M.M. Crain, T.J. Roussel, Jr., D.J. Jackson, R.P. Baldwin, R.S. Keynton, J.F. Naber, Fully Integrated Three-Dimensional Electrodes for Electrochemical Detection in Microchips: Fabrication, Characterization, and Applications, Anal. Chem. 81 (2009) 4762-4769.

[31] Z.H. Fan, D.J. Harrison, Micromachining of capillary electrophoresis injectors and separators on glass chips and evaluation of flow at capillary intersections, Anal. Chem. 66 (1994) 177-184.

[32] S. Carroll, M.M. Crain, J.F. Naber, R.S. Keynton, K.M. Walsh, R.P. Baldwin, Room temperature UV adhesive bonding of capillary electrophoresis devices, Lab Chip 8 (2008) 1564-1569.

[33] A. Iles, A. Oki, N. Pamme, Bonding of soda-lime glass microchips at low temperature, Microfluid. Nanofluid. 3 (2007) 119-122.

[34] Y. Akiyama, K. Morishima, A. Kogi, Y. Kikutani, M. Tokeshi, T. Kitamori, Rapid bonding of Pyrex glass microchips, Electrophoresis 28 (2007) 994-1001.

[35] R.S. Lima, P.A.G. Carneiro Leao, A.M. Monteiro, M.H. Oliveira Piazzetta, A.L. Gobbi, L.H. Mazo, E. Carrilho, Glass/SU-8 microchip for electrokinetic applications, Electrophoresis 34 (2013) 2996-3002.

[36] P.B. Allen, D.T. Chiu, Calcium-Assisted Glass-to-Glass Bonding for Fabrication of Glass Microfluidic Devices, Anal. Chem. 80 (2008) 7153-7157.

[37] M. Morra, E. Occhiello, R. Marola, F. Garbassi, P. Humphrey, D. Johnson, On the aging of oxygen plasma-treated polydimethylsiloxane surfaces, J. Colloid Interface Sci. 137 (1990) 11-24.

[38] M.K. Chaudhury, G.M. Whitesides, Direct measurement of interfacial interactions between semispherical lenses and flat sheets of poly(dimethylsiloxane) and their chemical derivatives, Langmuir 7 (1991) 1013-1025.

[39] K. Seiler, Z.H.H. Fan, K. Fluri, D.J. Harrison, Electroosmotic pumping and valveless control of fluid flow within a manifold of capillaries on a glass chip, Analytical Chemistry 66 (1994) 3485-3491.

[40] G.T. Roman, K. McDaniel, C.T. Culbertson, High efficiency micellar electrokinetic chromatography of hydrophobic analytes on poly(dimethylsiloxane) microchips, Analyst 131 (2006) 194-201.

[41] J.C. Giddings, Unified Separation Science, John Wiley & Sons, Inc, New York, 1961.

[42] K. Koshimura, J. Tanaka, Y. Murakami, Y. Kato, Effect of high concentration of glucose on dopamine release from pheochromocytoma-12 cells, Metabolism 52 (2003) 922-926.

Chapter 6: Development of on-line microdialysis-microchip electrophoresis with electrochemical detection to monitor catecholamines *in vivo*

6.1 Introduction

Monitoring neurotransmitters *in vivo* is an important application of on-line microdialysis coupled to microchip electrophoresis (MD-ME). Previous researchers have monitored amino acid neurotransmitters *in vivo* using MD-ME with prechannel derivatization and fluorescence detection both on-line [1-3], and off-line [4,5]. However, there have only been two devices employing MD-ME with electrochemical detection (EC) for analysis, due to difficulties integrate an electrode into the device. The first of these MD-ME-EC devices has been developed out of Scott Martin's lab and uses pneumatic valves to introduce sample into the separation channel [6-8]. The same basic device design has been employed to monitor dopamine release from PC-12 cells [6] and sample standards in solution [7,8], both *in vitro*. The only existing report of *in vivo* analysis by MD-ME-EC is from our lab [9] and employs an all-glass device with integrated platinum electrodes and a flow-gated interface developed in a previous report [10]. This device was used to monitor nitrite metabolism following subcutaneous nitroglycerin perfusion [9].

Because the analytical system and associated instrumentation for MD-ME-EC devices can be miniaturized, many exciting applications of this technology exist, including on-animal monitoring. The ability to monitor neurotransmitters or drug metabolism in an awake, freely roaming animal in its natural environment would allow for the extracellular brain concentrations of these analytes to be correlated to the animal's natural behavior, something that has not yet been accomplished. This technology would prove valuable for individuals interested in the neurochemical basis of behavior or developing drugs for neurological disorders. A single previous report did achieve on-animal monitoring [9]; however, this report did not sample from the brain and only monitored one analyte (nitrite).

Many neurotransmitters, including those in the dopamine metabolic pathway (Figure 6.1A) are natively electrochemically active. Electrochemistry is logical for on-animal analysis, as the potentiostat necessary for electrochemical detection can be easily miniaturized. Additionally, catecholamines generate better responses at carbon-based electrodes than metal-based electrodes; therefore a device that is capable of integrating carbon electrodes into a MD-ME-EC device is necessary.

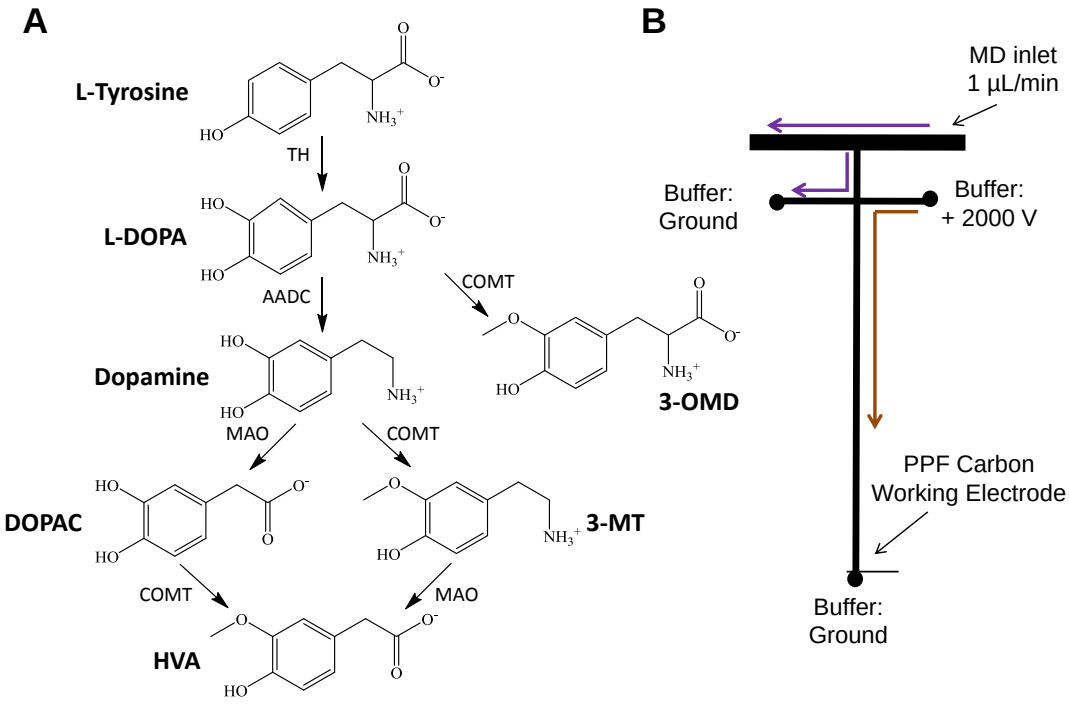

Figure 6.1 Dopamine metabolic pathway and MD-ME-EC device design used for analysis. (A) Dopamine metabolic pathway analytes investigated in this chapter. Enzymes: TH is tyrosine hydroxylase, AADC is aromatic l-amino acid decarboxylase, COMT is catechol-o-methyltransferase, and MAO is monoamine oxidase. (B) Flow-gated interface using double-t microchip design for on-line microdialysis-microchip electrophoresis with electrochemical detection. Device design, applied voltages, and flow rate are the same as were used in Chapter 5.

In the previous chapter, a device capable of on-line microdialysis-microchip electrophoresis with electrochemical detection at carbon electrodes was described for *in vitro* monitoring (Figure 6.1B). This chapter employs the same device design with the separation of analytes in the dopamine metabolic pathway (optimized in Chapter 3). In this chapter, *in vivo* analysis of analytes in this pathway after the administration of L-DOPA is achieved on-line and in the brain microdialysate of a rat. In the future, this device can be used for on-animal monitoring in larger animals, such as sheep.

6.2 Materials and methods

6.2.1 Reagents

The following chemicals were used as received: AZ 1518 positive photoresist and AZ 300 MIF developer (AZ Electronic Materials, Sommerville, NJ, USA); SU-8 10 and SU-8 developer (Micro-Chem, Newton, MA, USA), L-tyrosine (L-Tyr), 3-o-methyldopa (3-OMD), 3,4-dihydroxy-L-phenylalanine (L-DOPA), homovanillic acid (HVA), 3,4-dihydroxyphenylacetic acid (DOPAC), dopamine hydrochloride, 3-methoxytyramine hydrochloride (3-MT), sodium phosphate monobasic, and sodium phosphate dibasic (Sigma-Adrich, St. Louis, MO, USA); NaOH and isopropyl alcohol (IPA) (Fisher Scientific, Fairlawn, NJ, USA); sodium dodecyl sulfate (SDS) (Thermo Scientific, Waltham, MA, USA); and PDMS and curing agent (Sylgard 184 silicon elastomer base and curing agent, Dow Corning Corp., Midland, MI, USA). PC-12 cells (PC-12 Adh CRL-1721.1), F-12K medium, fetal bovine serum, horse serum, and penicillin-streptomycin (10,000 I.U./mL penicillin, 10,000 (μg/mL) streptomycin) were purchased from ATTC (Manassas, VA, USA). The following were also employed: high temperature fused silica glass plates (4 in x 2.5 in x 0.085 in, Glass Fab, Rochester, NY, USA); copper wire (22 gauge, Westlake Hardware, Lawrence, KS, USA); hot

glue and hot glue gun (ACE Hardware); colloidal silver liquid (Ted Pella, Inc., Redding, CA, USA); PEEK tubing (0.127 mm ID, Index Health & Science); Instech microdialysis connectors (Instech Laboratories, Inc., Plymouth Meeting, PA, USA); 1.0 or 4.0 mm cannula microdialysis probes (20KDa MWCO PAES membrane, CMA, Kista, Sweden) with 15 cm of both inlet and outlet tubing (BASi FEP Teflon tubing, 0.12 mm i.d.); infusion cannula connected to a 4.0 mm microdialysis probe (IBR, 30 KDa MWCO PAN membrane, BASi, West Lafayette, IN, USA) with 15 cm of both inlet and outlet tubing (BASi FEP Teflon tubing, 0.12 mm i.d.); 1.0 cm linear probe (30 KDa MWCO PAN membrane, 15 cm of FEP tubing before and after the membrane, BASi, West Lafayette, IN, USA); and 18.2 MΩ water (Millipore, Kansas City, MO, USA).

Artificial cerebrospinal fluid (aCSF) was comprised of 145 mM NaCl, 2.7 mM KCl, 1.0 mM $MgCl_2$, 1.2 mM $CaCl_2$, 2.33 mM Na_2HPO_4 and 0.45 mM NaH_2PO_4. Stock solutions of 10 mM of each analyte were prepared in 18.2 MΩ water. Analysis solutions were made from these standard solutions and diluted in 15 mM sodium phosphate (pH 7.4) or aCSF at the time of analysis.

6.2.2 Fabrication of substrates

PDMS microchip fabrication has been described elsewhere [11] and in Chapter 3 (section 3.3.2) Briefly, a silicon master was created with negative photoresist onto a 4 inch silicon wafer using classic photolithography techniques. The master contained 15 µm raised channels, which corresponds to the channel depth in the final PDMS chip. For this flow-gated, double-t design, the separation channel length was 5 cm, each side arm was 0.75 cm and the top t was 2 cm long. The width off all channels was 40 µm, except the top sampling channel which was 1.0 mm. The chip design can be seen in Figure 6.1B. To create the PDMS microchip from the silicon master,

PDMS/curing agent was mixed at a 10:1 ratio and poured onto the master to a form a polymer thickness of at least 2 mm. The PDMS was cured overnight at 70°C, after which the PDMS channels were peeled from the wafer. Reservoirs for buffer and pump waste were punched into the PDMS using a 4 mm biopsy punch (Harris Uni-core, Ted Pella).

Pyrolyzed photoresist electrode fabrication has been described previously [12-14] and in Chapter 3 (section 3.2.3.2). Briefly, the electrode design was transferred to the glass substrate with AZ 1518 positive photoresist using classic photolithography techniques. Substrates with photoresist were then placed in a Linden-BlueM Tube furnace (Cole-Parmer, Vernon Hills, IL, USA), with a constant flow of nitrogen gas throughout the pyrolysis procedure. The temperature program was ramped from room temperature to 925°C at 5.5°C/min and held for 1 hour. The furnace was then allowed to cool back down to room temperature. Final electrode dimensions after pyrolysis, as measured using a surface profiler, were 35 μm wide and 0.5 μm in height.

6.2.3 Microchip construction

For on-line experiments using the double-t design, a partial irreversible bond between the PDMS channels and glass electrode substrate was created, as described in Chapter 5 (section 5.2.3). This procedure will be described here briefly. The microchip was created immediately after the PDMS was cured and removed from the oven. PDMS channels and the electrode substrate were simultaneously plasma oxidized (Harrick Plasma Cleaner/Sterilizer PDC-32G, Ithaca, NY, USA) by placing both substrates under vacuum alone for 2 minutes, followed by oxidation at medium radio frequency (RF) for 60 seconds (while under vacuum). During this procedure, a piece of sacrificial PDMS was placed over the carbon working electrode and surrounding area. Immediately following oxidation, the sacrificial PDMS was removed and the two layers (PDMS channels and electrode substrate) placed in conformal contact. This

procedure created an irreversible bond in the top portion of the microchip to account for the pressure driven microdialysis flow, and a reversible bond in the bottom portion where the electrode resides. An electrical connection was created using a copper wire attached to the electrode with silver colloid. This wire was affixed to the glass substrate using hot glue, allowing for stability during experiments and easy removal after experiment completion.

A sample inlet to couple the microchip to the microdialysis system was created in the PDMS layer using a stainless steel 20 gauge blunt needle. A 20 gauge 2.0 cm stainless steel connector was used to connect the microchip to either 15 cm of PEEK tubing (Figure 6.2A) or the microdialysis probe (Figure 6.2B) through Instech microdialysis connectors. Instech microdialysis connecters were also used to connect the other side of the PEEK tubing or microdialysis probe to the syringe pump, as seen in Figure 6.2. Microdialysis probes employed in these studies included a 1.0 cm linear probe (BASi, PAN membrane), 1.0 mm and 4.0 mm cannula microdialysis probes (CMA, PAES membrane), and an infusion cannula connected to a 4.0 mm cannula microdialysis probe (BASi, PAN membrane).

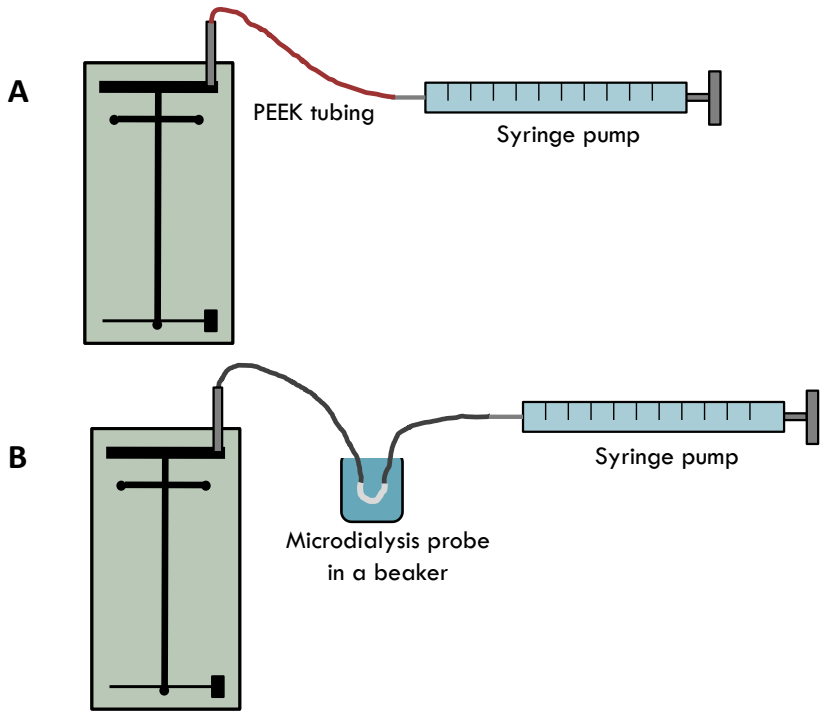

Figure 6.2 Connection schemes for on-line analysis. (A) Direct connect mode where the syringe pump containing analytes is connected directly to the microchip using PEEK tubing. (B) Microdialysis connection mode where solution is being sampled through a microdialysis probe.

6.2.4 Experimental procedure

Prior to electrophoresis experiments, the channels were flushed sequentially with isopropyl alcohol, 0.1 M NaOH, and the run buffer using negative pressure. The top-t was also conditioned and filled with 15 mM phosphate (pH 7.4) using positive pressure produced by using a syringe connected directly to the chip with PEEK tubing. During experiments, pressure was applied to the 1.0 mL glass syringe using a CMA 102 syringe pump (CMA, Kista, Sweden). Electrophoresis procedures were accomplished using a single Spellman CZE 1000R (Hauppauge, NY, USA) high voltage power supply controlled by LabView software (National

Instruments, Austin, TX, USA) written in-house. A flow-gated injection scheme was employed through the application of 2000 V at the buffer reservoir, sample waste and buffer waste reservoirs held at ground, and a microdialysis flow rate of 1.0 μL/min (Figure 6.1B). Injections were accomplished by floating the buffer voltage for 1.5 s, then reestablishing the voltage for the separation. The separation buffer for all experiments, unless stated otherwise, was comprised of 15 mM phosphate (pH 7.4), 15 mM SDS, and 2.5 mM boric acid. The separation optimization leading to this optimal run buffer is detailed in Chapter 3.

Electrochemical detection was accomplished using a two electrode (pyrolyzed photoresist film working, Ag/AgCl reference (BASi, West Lafayette, IN, USA)) system. An electrically isolated potentiostat (10 Hz sampling rate, Pinnacle Technology Inc., Lawrence KS) was used with data visualized using Pinnacle Acquisition Laboratory (PAL 8400) software. This potentiostat has been used in earlier chapters and previously in our group for in-channel detection [14,15,16]. For all experiments described in this chapter, the working electrode was held at 1.0 V (versus Ag/AgCl) and placed at the very end of the channel outlet.

6.2.4 Animal surgery

All animal experiments were performed in accordance with regulations of the Institutional Animal Care and Use Committee (IACUC) at the University of Kansas, which operates with accreditation from the Association for Assessment and Accreditation of Laboratory Animal Care (AAALAC). Sprague-Dawley or Wistar rats weighing between 250 – 400 g were anesthetized via the inhalation of isoflurane followed by an i.p. injection of 6-80 mg/kg ketamine, 3-5 mg/kg xylazine, and 1 mg/kg acepromazine diluted in saline. Supplemental doses of ketamine, diluted in saline and delivered i.p., were also administered throughout the experiment to maintain anesthesia. An alternative anesthetic protocol for some of the later

experiments used an initial dose of 100 mg/kg ketamine and 10 mg/kg xylazine dissolved in saline. This alternate method resulted in a better maintenance of a surgical level of anesthesia.

The rat was placed into a stereotaxic instrument for the placement of the microdialysis guide cannula into the striatum of the brain, following the coordinates (from Bregma) A/P +0.7, M/L -2.7 and V/D -3.4 [17]. The guide cannula and microdialysis probe were held in place using dental acrylic and metal screws. Prior to on-line experiments, the rat was allowed to recover from surgery for at least 1 hr, during which time aCSF was continually perfused through the microdialysis probe at a flow rate of 1.0 µL/min.

For on-line *in vivo* experiments, the microdialysis probe (1 mm or 4 mm PAES membrane, or 4 mm PAN membrane with infusion cannula) was connected to the syringe and microchip using 15 cm of FEP tubing through microdialysis connectors on each side of the probe. A perfusion flow rate of 1.0 µL/min was employed and the perfusate consisted of either aCSF or the indicated concentration of L-DOPA dissolved in aCSF. When using the infusion cannula, an infusion flow rate of 1.0 µL/min and perfusion flow rate (through the microdialysis probe) of 1.0 µL/min was employed.

6.3 Results and discussion

6.3.1 Method optimization

The goal of the work described in this chapter was to demonstrate the feasibility of the developed MD-ME-EC device for *in vivo*, on-animal monitoring. This initial study shows the ability of the MD-ME-EC system to monitor drug metabolism, specifically the conversion of administered L-DOPA to dopamine and its subsequent metabolism in the brain of an anesthetized rat. To achieve this goal, analytes in the dopamine metabolic pathway must be separated using microchip electrophoresis. This separation optimization in a 5 cm simple-t

device was described in detail in Chapter 3. In transitioning from the simple-t device to the double-t design, it was important to both optimize the injection procedure and verify the separation integrity prior to the addition of the microdialysis probe for *in vitro* or *in vivo* experiments.

In optimizing the flow-gated injection for this device, the flow rate was set at 1.0 µL/min through direct connection from the syringe to the microchip with PEEK tubing and the applied voltage was 2000 V which gave a field strength of ~ 130 V/cm. These parameters were found under similar conditions in Chapter 5 to give the most stable gate and injection. Higher voltages, such as 3000 V were also investigated, but it was found that less sample was injected. This trend has been previously described in Huynh et. al [18], and can be seen in the columns of Figure 6.3, where an applied voltage of 2000 V (A and C) results in the injection of a much larger sample plug than with 3000 V (B and D), which has a very strong gate.

Additionally, it quickly became apparent that the ionic strength of the sample matrix heavily influenced the integrity of the gate and amount of sample injected. When sample matrices of higher ionic strength (such as Ringer's or aCSF) than the separation buffer were employed, the flow-gate was much stronger, with little to no sample reaching the sample waste side arm. Weber's group has reported a similar effect for a gated (compared to the flow-gated employed here) injection scheme [19]. The rows in Figure 6.3 demonstrate this effect, where the sample was either dissolved in 15 mM phosphate (A and B) or 15 mM phosphate and 140 mM NaCl (C and D). A solution of 15 mM phosphate and 140 mM NaCl represented the approximate ionic strength of aCSF. Because the ultimate goal of this device is for the on-line analysis of brain microdialysis samples, where the aCSF perfusate is high in ionic strength, 2000 V was chosen as the optimal applied voltage for gating and separation with an injection time of

1.5 s. Longer injection times were also investigated, as they proved beneficial in the system described in Chapter 5; however, the separation deteriorated with longer injection times.

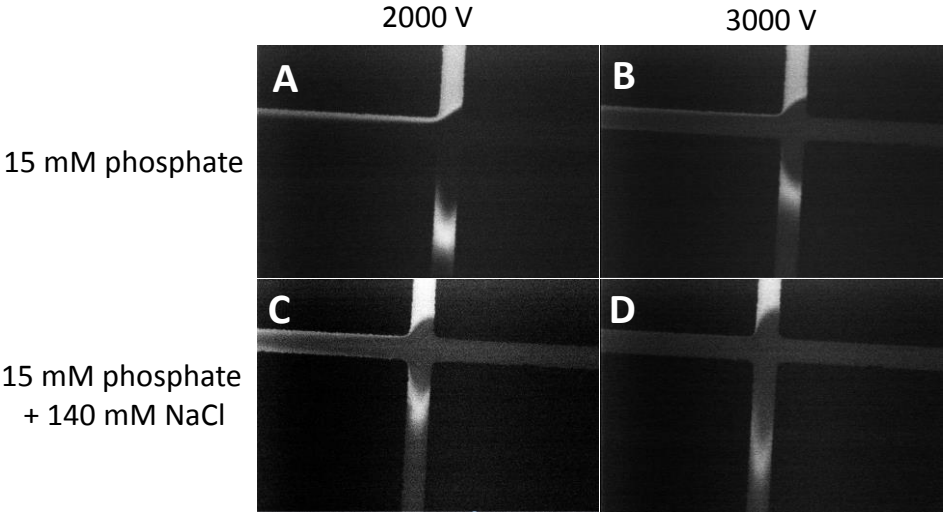

Figure 6.3 Effect of separation voltage and sample matrix on flow-gated injection. These images focus on the injection-t in the double-t microchip, and the image contrast was increased for clarity. The first column (A and C) represents flow-gated injections with an applied voltage of 2000 V, and the second column (B and D) represents an applied voltage of 3000 V. The first row (A and B) represents a sample matrix of 15 mM phosphate (pH 7.4), and the second row (C and D) represents a sample matrix of 15 mM phosphate (pH 7.4) and 140 mM NaCl. All injections were created by floating the separation voltage for 1.0 s.

Using the optimized voltage and injection scheme, the separation parameters employed in Chapter 3 were investigated with the double-t device. These experiments used a direct connection mode, where the syringe containing the sample was directly connected to the microchip using 15 cm of PEEK tubing (Figure 6.2A). The resultant separation of analytes in

the dopamine metabolic pathway can be seen in Figure 6.4. In this separation, an additional L-DOPA metabolite, 3-*O*-methyldopa (3-OMD) was added and was found to migrate at the same time as L-Tyr. This was not deemed problematic, as L-Tyr is a precursor of L-DOPA and should not increase in concentration in these studies. In addition, preliminary results suggested that the limits of detection for L-Tyr with this device were not low enough to detect endogenous levels.

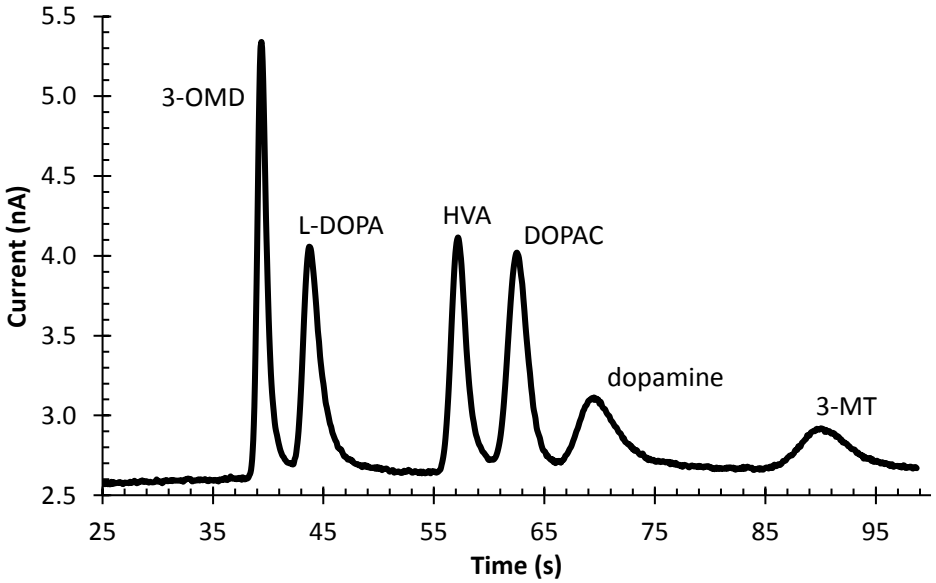

Figure 6.4 Separation of analytes in the dopamine metabolic pathway using MD-ME-EC. Analytes (100 µM each) were dissolved in 15 mM phosphate and a direct connect scheme was employed. Peak identities are indicated in the figure. A separation voltage of 2000 V, injection time of 1.5 s, perfusion flow rate of 1.0 µL/min, and separation buffer of 15 mM phosphate (pH 7.4), 15 mM SDS, and 2.5 mM boric acid were used.

6.3.2 *in vitro* analysis

Prior to *in vivo* animal studies, the device was tested *in vitro*. A completely on-line device must show the ability to monitor concentration changes over time. To demonstrate this ability, the microchip was connected to a linear microdialysis probe that was placed into a vial where the concentrations in the vial were changed through spiking. Additions were made every 5 injections so that the concentration of L-DOPA in the vial increased by 200 µM each time. The results of this experiment can be seen in Figure 6.5. Using this device, it is clear that increasing the concentration in the vial does increase the signal in a linear fashion ($R^2 = 0.986$).

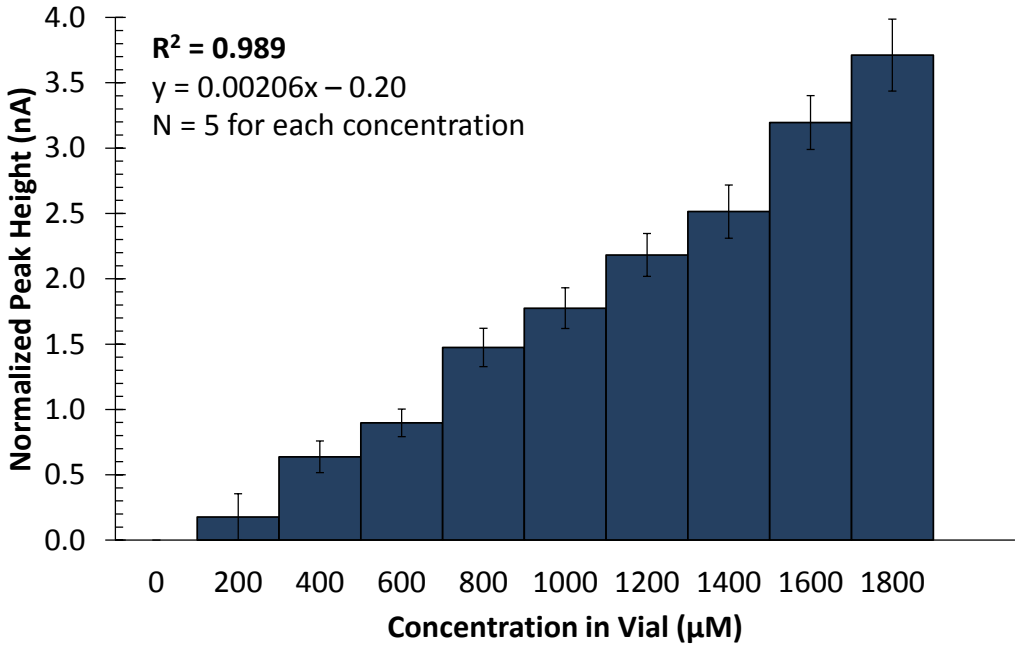

Figure 6.5 Monitoring concentration changes over time using MD-ME-EC. A linear microdialysis probe was placed into a vial where the concentration of L-DOPA was changed over time, resulting in a change in the measured peak height. N = five injections for each concentration. The separation buffer consisted of 15 mM phosphate (pH 7.4), 0.5 mM SDS, and 2.5 mM boric acid.

The lag time, or the time from the change in concentration in the vial until the change was measured by the device, was also calculated for this experiment. Lag time is dependent, in part, on the length of tubing and sampling flow rate employed [20]. With 15 cm of tubing from the probe to the device (a volume of 1.23 mm^3) and a flow rate of 1.0 µl/min, the lag time was about 500 seconds (or 5 injections). Theoretically, this time could be dramatically reduced by shortening the length of tubing, as the actual separation of analytes in the dopamine metabolic pathway using this device is completed in under 100 s.

6.3.3 *in vivo* analysis in rat striatum

While there are many brain regions where dopamine plays a role, there is a high degree of innervation of dopamine neurons in the striatum. Additionally, this brain region is relatively large, enabling the use of longer microdialysis probes that can lead to an increase in analyte recovery. Lastly, there is a wide body of research concerning the striatum; many previous researchers have employed microdialysis sampling or fast-scan cyclic voltammetry to detect dopamine in this region [21-25]. In all experiments described herein, the microdialysis probe was implanted into the rat striatum, using coordinates obtained from a stereotaxic atlas [17].

6.3.3.1 Successful retrodialysis of L-DOPA

The initial *in vivo* experiments were performed by placing a cannula microdialysis probe into the rat striatum, letting the rat recover from surgery for at least an hour while perfusing aCSF through the probe, and then connecting the microdialysis outlet tubing to the microchip. Initially, aCSF was perfused through the microdialysis probe and into the microchip to establish a baseline. While analytes in the dopamine metabolic pathway do exist endogenously in the brain, their concentrations are below the current detection limits of this method; therefore, when perfusing with only aCSF, no peaks appeared in the corresponding electropherograms. After

basal electropherograms were collected, the perfusate syringe was switched to one containing 50 µM L-DOPA in aCSF. When perfusing L-DOPA, a fraction of the perfused L-DOPA passed through the microdialysis probe and into the brain via retrodialysis. Concurrently, the samples taken up through the probe were analyzed on-line with the MD-ME-EC method for any L-DOPA metabolites. These results can be seen in Figures 6.6 and 6.7.

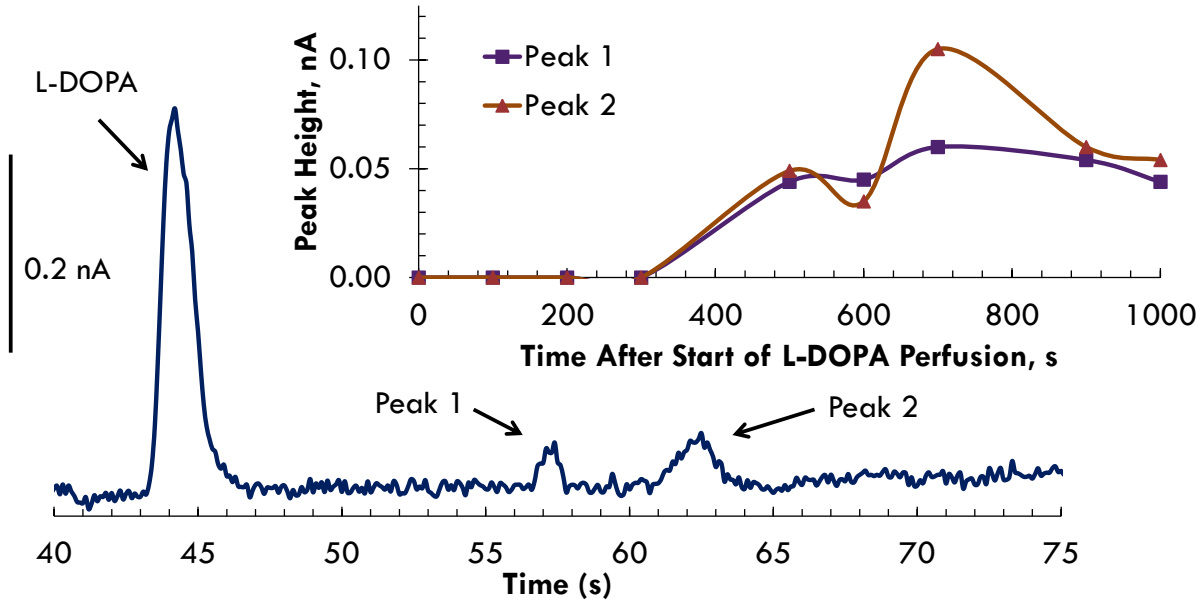

Figure 6.6 L-DOPA metabolism monitored using MD-ME-EC after retrodialysis of 50 µM L-DOPA. Blue electropherogram corresponds to ~500 s after the start of the L-DOPA perfusion, where two metabolite peaks appear. Figure inset graphs the increase of the two metabolite peaks over time.

Figure 6.6 shows a representative electropherogram obtained after the start of the L-DOPA perfusion into the brain. As can be seen in this figure, two metabolite peaks appeared after the L-DOPA perfusion. These peaks increased in size over time, as can be seen in the

figure inset. Prior to the *in vivo* experiment, an electropherogram of standards of the analytes in the dopamine metabolic pathway was obtained by directly connecting the microchip (without MD probe) to the syringe pump (Figure 6.2A). When the standards electropherogram is overlaid with one obtained during the rat experiment, some tentative peak identities can be assigned, which are shown in Figure 6.7. Based solely on migration times, Peak 1 can be tentatively identified as DOPAC and Peak 2 can be identified as dopamine.

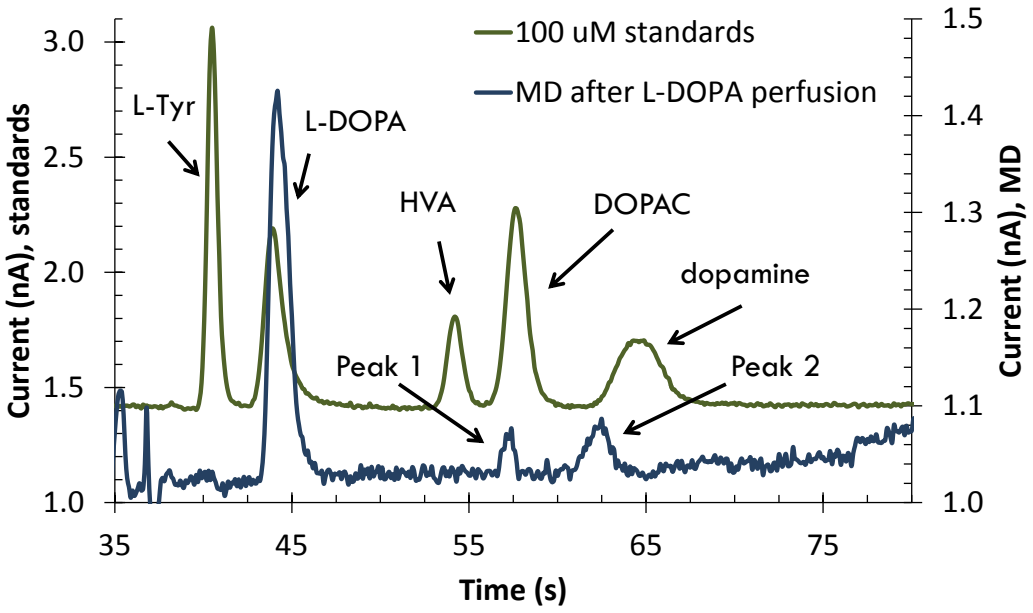

Figure 6.7 L-DOPA metabolism monitored using MD-ME-EC after retrodialysis of 50 µM L-DOPA (~ 900 s after start of L-DOPA perfusion) aligned with standards for peak identification. Metabolite Peak 1 potentially corresponds to metabolite DOPAC while metabolite Peak 2 corresponds to dopamine.

This *in vivo* data, while not definitive, does prove that the MD-ME-EC device developed in this thesis is capable of successfully integrating high ionic strength, pressure driven microdialysis flow with microchip electrophoresis and electrochemical detection at a carbon electrode for monitoring L-DOPA metabolism *in vivo*.

6.3.3.2 Moderately successful retrodialysis or infusions of L-DOPA

There are some shortcomings regarding these experiments that will need to be addressed when moving forward with this device for on-animal analysis. While a 50 µM L-DOPA perfusion does result in metabolite generation (as seen in the previous section), the signal using the MD-ME-EC device is small. Subsequent experiments attempted to improve the signal by increasing the concentration of L-DOPA in the brain, either by increasing the concentration in the perfusate or using an infusion cannula. When performing retrodialysis, only a small fraction of the L-DOPA perfused enters into the brain, whereas use of an infusion cannula results in complete infusion of L-DOPA into the brain. Results of selected experiments can be seen in Figure 6.8.

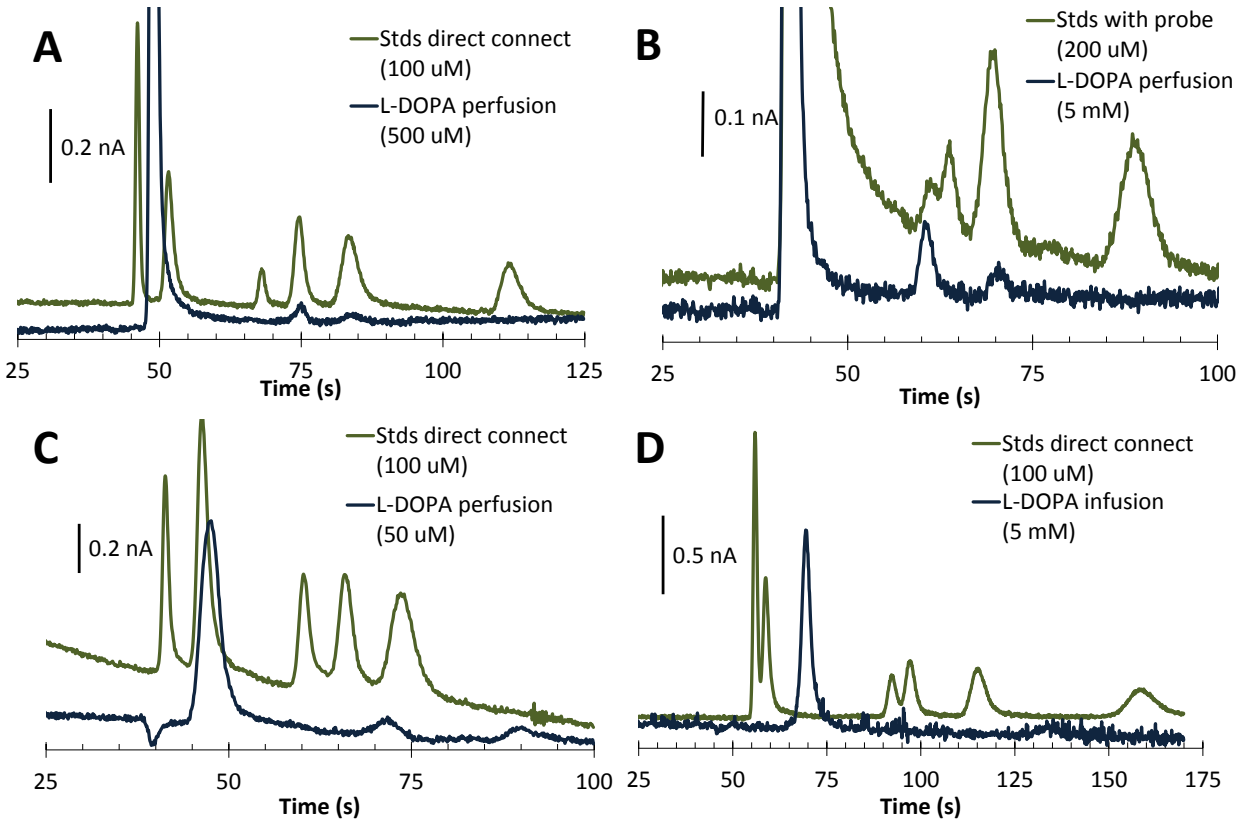

Figure 6.8 On-line analysis after L-DOPA perfusion. (A) Comparison between 100 µM standards analyzed via direct connection and on-line analysis after the retrodialysis of 500 µM L-DOPA. (B) Comparison between 200 µM standards sampled through the MD probe and on-line MD-ME-EC after the retrodialysis of 5 mM L-DOPA. (C) Comparison of 100 µM standards analyzed via the direct connect scheme and on-line analysis after the retrodialysis of 50 µM L-DOPA. (D) Comparison between 100 µM standards analyzed via the direct connect scheme and on-line analysis after an 5 mM L-DOPA infusion next to the MD probe.

These results highlight some of the limitations of the device that future researchers will need to overcome prior to continuous on-line analysis of endogenous levels of neurotransmitters. As can be seen in Figure 6.8 A and B (and also Figures 6.6 and 6.7), it is possible to obtain peaks with migration times that can be correlated with those of standards remarkably well. However, these are only single injections; in the experiments highlighted in 6.8A and 6.8B clogs developed at the flow-gated interface that halted sample injection. One such clog can be seen in Figure 6.9. While rinsing the microchip with either negative or positive pressure can remove these clogs, this mechanism has not yet been incorporated into the on-line device.

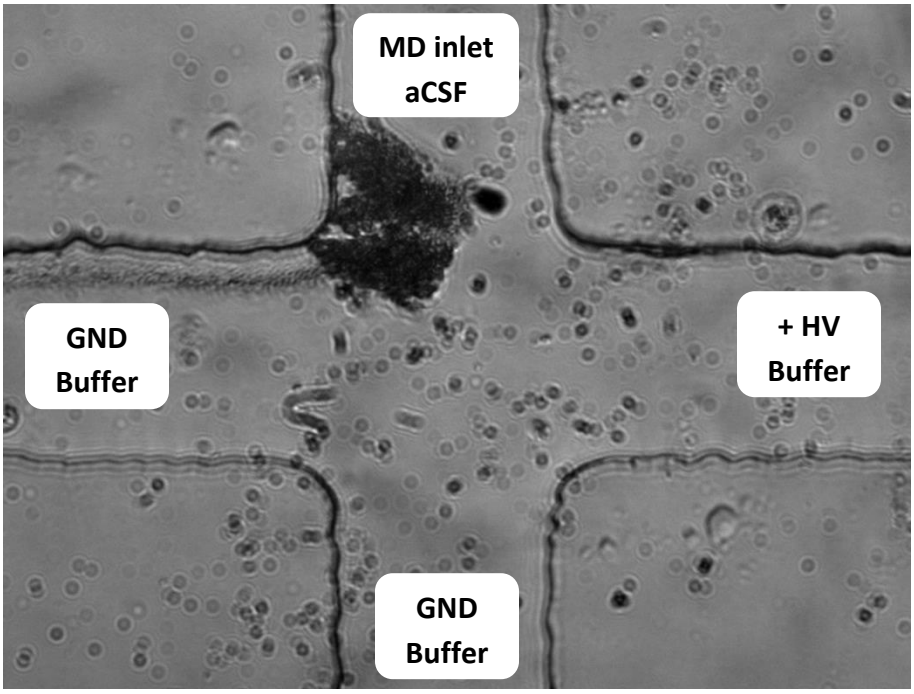

Figure 6.9 Clog developed at the injection cross in an MD-ME-EC device which limits or halts sample introduction into the separation channel.

Figure 6.8C shows an additional aspect of these microchips, namely peaks slowly changing migration time over the microchip lifetime. These on-line experiments are generally run over the course of a few (2-3) hours, and during this time the surface chemistry of the PDMS channel is slowly altered, which results in increasing migration times due to the change in electroosmotic flow. This makes analyte identification difficult, and a strategy to overcome this is discussed in section 6.3.5.3.

The largest limitation of the present MD-ME-EC device is the high limits of detection; under optimal conditions and analytes dissolved in aCSF, limits of detection of about 25 μM (S/N = 3) were achieved. The consequence of these high limits of detection can be seen in Figure 6.8D, where the L-DOPA infused into the brain is detectable; however, no metabolites are detected due to the high noise and low signal for this particular microchip. Additionally, this microchip was able to collect data continuously for over one hour without any other major difficulty (the migration time shift of L-DOPA is due to this timeframe), making it incredibly disheartening that limits of detection were not capable of detecting metabolite peaks.

6.3.4 Dual series electrodes

As stated in the previous section and highlighted in Figure 6.8C, over the long timeframes that these experiments are performed, the migration times of the analytes can vary due to a change in surface of the PDMS, making definitive identification difficult. Dual electrodes, held at different potentials, enable a current ratio to be determined. This current ratio is specific for each analyte of interest, and can be used for unambiguous peak identification in the sample. An example of dual electrodes in series can be seen in Figure 6.10A. These electrodes are 15 μm wide electrodes with 15 μm spacing between each electrode. Figure 6.10B shows the response of these two electrodes, the first at a low oxidation potential (0.4 V) and the

second at the higher oxidation potential used for the majority of this thesis (1.0 V). The 1.0 V end channel electrode generates good responses for all analytes, as it is higher than the oxidation potential for all the analytes of interest. The 0.4 V electrode, however, only generates a response for easily oxidized analytes, namely L-DOPA, ascorbic acid, DOPAC, and dopamine.

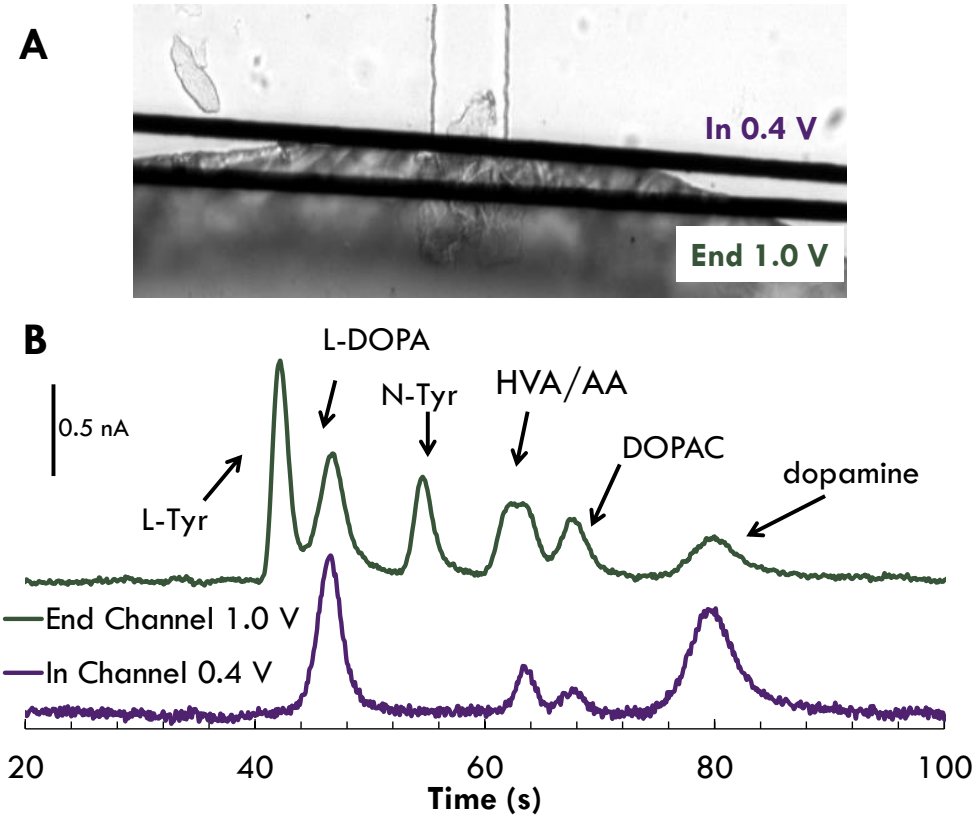

Figure 6.10 Dual series electrodes. (A) Pyrolyzed photoresist film carbon electrodes in series within a microfluidic device. (B) Data obtained after the separation described in Chapter 3 with 100 µM standards on a simple-t microchip with integrated dual electrodes in series. The in-channel electrode was held at 0.4 V and the end-channel electrode was held at 1.0 V.

With the dual electrode configuration, it is possible to determine current ratios for the analytes of interest that are oxidizable at both 1.0 V and 0.4 V. In order to generate an accurate current ratio, different factors must be taken into account, including the sensitivity difference between electrodes, the oxidation difference (how much analyte is left to oxidize at the second electrode), and the difference in response at end- vs. in-channel electrodes; these considerations have been discussed in detail previously [26]. The current ratios of the standards can then be compared to those in microdialysate samples, and, along with the migration times, more definitive peak identities can be determined.

6.4 Conclusions

On-line microdialysis-microchip electrophoresis with electrochemical detection at a carbon electrode was accomplished using a PDMS/glass hybrid device. The effect of the separation voltage and sample matrix on sample injection was investigated. This MD-ME-EC device was found to give a linear response to concentration changes *in vitro* sampled though microdialysis. Lastly, the separation method optimized in Chapter 3 was used with this on-line device to investigate the dopamine metabolic pathway. This method was used to monitor the metabolism of the pathway *in vivo* in rats following L-DOPA administration through both retrodialysis and direct infusion into the rat striatum. Although metabolites were detected, the limits of detection of the device were not sufficient for *in vivo* monitoring. Future directions, including addressing some device limitations and the use of this device for on-animal monitoring, are presented in the next chapter.

6.5 References

[1] Z.D. Sandlin, M. Shou, J.G. Shackman, R.T. Kennedy, Microfluidic electrophoresis chip coupled to microdialysis for in vivo monitoring of amino acid neurotransmitters, Anal. Chem. 77 (2005) 7702-7708.

[2] M. Wang, G.T. Roman, M.L. Perry, R.T. Kennedy, Microfluidic Chip for High Efficiency Electrophoretic Analysis of Segmented Flow from a Microdialysis Probe and in Vivo Chemical Monitoring, Anal. Chem. 81 (2009) 9072-9078.

[3] P. Nandi, D.P. Desai, S.M. Lunte, Development of a PDMS-based microchip electrophoresis device for continuous online in vivo monitoring of microdialysis samples, Electrophoresis 31 (2010) 1414-1422.

[4] M. Wang, T. Slaney, O. Mabrouk, R.T. Kennedy, Collection of nanoliter microdialysate fractions in plugs for off-line in vivo chemical monitoring with up to 2 s temporal resolution, J. Neurosci. Methods 190 (2010) 39-48.

[5] M. Wang, N.D. Hershey, O.S. Mabrouk, R.T. Kennedy, Collection, storage, and electrophoretic analysis of nanoliter microdialysis samples collected from awake animals in vivo, Anal. Bioanal. Chem. 400 (2011) 2013-2023.

[6] L.C. Mecker, R.S. Martin, Integration of Microdialysis Sampling and Microchip Electrophoresis with Electrochemical Detection, Anal. Chem. 80 (2008) 9257-9264.

[7] L.C. Mecker, L.A. Filla, R.S. Martin, Use of a Carbon-Ink Microelectrode Array for Signal Enhancement in Microchip Electrophoresis with Electrochemical Detection, Electroanalysis 22 (2010) 2141-2146.

[8] A.S. Johnson, A. Selimovic, R.S. Martin, Integration of microchip electrophoresis with electrochemical detection using an epoxy-based molding method to embed multiple electrode materials, Electrophoresis 32 (2011) 3121-3128.

[9] D.E. Scott, S.D. Willis, S. Gabbert, D. Johnson, E. Naylor, E.M. Janle, J.E. Krichevsky, C.E. Lunte, S.M. Lunte, Development of an on-animal separation-based sensor for monitoring drug metabolism in freely roaming sheep, Analyst 140 (2015) 3820-3829.

[10] D.E. Scott, R.J. Grigsby, S.M. Lunte, Microdialysis Sampling Coupled to Microchip Electrophoresis with Integrated Amperometric Detection on an All-Glass Substrate, ChemPhysChem 14 (2013) 2288-2294.

[11] D.C. Duffy, J.C. McDonald, O.J.A. Schueller, G.M. Whitesides, Rapid Prototyping of Microfluidic Systems in Poly(dimethylsiloxane), Anal. Chem. 70 (1998) 4974-4984.

[12] D.J. Fischer, M.K. Hulvey, A.R. Regel, S.M. Lunte, Amperometric detection in microchip electrophoresis devices: Effect of electrode material and alignment on analytical performance, Electrophoresis 30 (2009) 3324-3333.

[13] D.J. Fischer, W.R.I.V. Vandaveer, R.J. Grigsby, S.M. Lunte, Pyrolyzed photoresist carbon electrodes for microchip electrophoresis with dual-electrode amperometric detection, Electroanalysis 17 (2005) 1153-1159.

[14] R.A. Saylor, E.A. Reid, S.M. Lunte, Microchip electrophoresis with electrochemical detection for the determination of analytes in the dopamine metabolic pathway, Electrophoresis 36 (2015) 1913-1919.

[15] D.B. Gunasekara, M.K. Hulvey, S.M. Lunte, In-channel amperometric detection for microchip electrophoresis using a wireless isolated potentiostat, Electrophoresis 32 (2011) 832-837.

[16] D.B. Gunasekara, J.M. Siegel, G. Caruso, M.K. Hulvey, S.M. Lunte, Microchip electrophoresis with amperometric detection method for profiling cellular nitrosative stress markers, Analyst 139 (2014) 3265-3273.

[17] G. Paxinos, C. Watson, The Rat Brain in Steriotaxic Coordinates, Academic Press, Inc, 1986.

[18] B.H. Huynh, B.A. Fogarty, R.S. Martin, S.M. Lunte, On-Line Coupling of Microdialysis Sampling with Microchip-Based Capillary Electrophoresis, Anal. Chem. 76 (2004) 6440-6447.

[19] J. Wu, K. Xu, J.P. Landers, S.G. Weber, An in Situ Measurement of Extracellular Cysteamine, Homocysteine, and Cysteine Concentrations in Organotypic Hippocampal Slice Cultures by Integration of Electroosmotic Sampling and Microfluidic Analysis, Anal. Chem. 85 (2013) 3095-3103.

[20] D.A. Skoog, F.J. Holler, S.R. Crouch, Principles of Instrumental Analysis, Thomson Brooks/Cole, Belmont, CA, 2007.

[21] J.D. Cooper, K.E. Heppert, M.I. Davies, S.M. Lunte, Evaluation of an osmotic pump for microdialysis sampling in an awake and untethered rat, J. Neurosci. Methods 160 (2007) 269-275.

[22] K.M. Nesbitt, E.L. Varner, A. Jaquins-Gerstl, A.C. Michael, Microdialysis in the Rat Striatum: Effects of 24 h Dexamethasone Retrodialysis on Evoked Dopamine Release and Penetration Injury, ACS Chem. Neurosci. 6 (2015) 163-173.

[23] P.S. Cahill, Q.D. Walker, J.M. Finnegan, G.E. Mickelson, E.R. Travis, R.M. Wightman, Microelectrodes for the Measurement of Catecholamines in Biological Systems, Anal. Chem. 68 (1996) 3180-3186.

[24] H. Gu, E.L. Varner, S.R. Groskreutz, A.C. Michael, S.G. Weber, In Vivo Monitoring of Dopamine by Microdialysis with 1 min Temporal Resolution Using Online Capillary Liquid Chromatography with Electrochemical Detection, Anal. Chem. 87 (2015) 6088-6094.

[25] T. Zetterstroem, T. Sharp, A.K. Collin, U. Ungerstedt, In vivo measurement of extracellular dopamine and DOPAC in rat striatum after various dopamine-releasing drugs; implications for the origin of extracellular DOPAC, Eur. J. Pharmacol. 148 (1988) 327-334.

[26] D.B. Gunasekara, Departmet of Chemistry, University of Kansas, 2014.

Chapter 7: Summary and future directions

7.1 Dissertation summary

The overall goal of this dissertation was to develop a microdialysis-microchip electrophoresis with electrochemical detection at a carbon electrode device for near-real time on-line monitoring of catecholamines with the eventual goal of on-animal monitoring. Specifically, in this dissertation the dopamine metabolic pathway was investigated, first *in vitro* and off-line and then *in vivo* and on-line.

Initial studies focused on the separation and detection of all analytes in the dopamine metabolic pathway using a 5 cm simple-t device. These catecholamine analytes are electrochemically active, and an alignment of the electrode at the channel outlet with a working electrode potential of higher than 800 mV (vs. Ag/AgCl) was employed. Using a PDMS/PDMS microchip device with integrated carbon fiber electrode, a separation of analytes in the dopamine metabolic pathway was achieved in under 60 s with resolutions of 1.2 or better using an optimized run buffer of 15 mM phosphate (pH 7.4), 15 mM SDS, and 2.5 mM boric acid. Unfortunately, migration time variability (ranging from 14% - 21% RSD) with this device proved to be problematic due to the instability of the EOF in PDMS/PDMS devices. Therefore, a PDMS/glass hybrid device with a pyrolyzed photoresist film carbon electrode was developed. This hybrid device yielded much more consistent migration times (ranging from 7% - 9% RSD); however, the efficiency and resolution did decrease slightly, when compared to the PDMS/PDMS device, due to the differences in EOF between the two layers which caused band-broadening. The optimized separation using the PDMS/glass hybrid device with a pyrolyzed photoresist film carbon electrode was then employed to monitor L-DOPA conversion into dopamine by a rat brain slice *in vitro* and off-line.

For on-line analysis with microdialysis sampling, a flow-gated interface was employed using a double-t design. Because carbon electrodes have not been integrated into an all-glass device, and previous methods for fabricating PDMS-based on-line devices would destroy the carbon electrode after one use, a novel fabrication method was developed. This fabrication procedure allows for the integration of a carbon electrode into a PDMS/glass device that is capable of integrating the hydrodynamic, microdialysis flow with the electrophoretic flow of the separation, making on-line analysis possible. In this procedure, plasma oxidation was performed on both the channel and electrode substrates; however a sacrificial piece of PDMS was placed over the electrode substrate to prevent the plasma from oxidizing the bottom portion of the electrode substrate. The two substrates were then placed in conformal contact. This procedure creates a functional MD-ME-EC device, where the top portion was irreversibly bonded to withstand the hydrodynamic microdialysis pressure and the bottom portion was reversibly bonded to enable electrode reuse and alignment. This fabrication method and microchip design were employed both in Chapter 5 toward monitoring catecholamine release from PC-12 cells *in vitro* and in Chapter 6 to monitor the dopamine metabolic pathway after a L-DOPA administration *in vivo*.

Progress was made toward monitoring the stimulated release of dopamine and norepinephrine from PC-12 cells *in* vitro using MD-ME-EC. To perform these studies, the separation of dopamine, norepinephrine, and ascorbic acid was optimized leading to a separation buffer consisting of 15 mM phosphate and 2.0 mM SDS. Using this separation buffer and an injection time of 1.5 seconds, the effect of the sample matrix on the quality of the separation was then investigated. When using a cell compatible buffer, high K^+/Ca^{2+} stimulation solution, and 15 mM phosphate as sample matrices, minimal differences were seen in the resultant separation

under these conditions. Additionally, longer injection times were investigated as a method of improving the signal. Increasing the injection time from 1.0 s to 50.0 s increased the peak area for dopamine by over 100-fold, with minimal effect on the separation quality when the sample was dissolved in a 15 mM phosphate buffer. Unfortunately, analytes dissolved in a high ionic strength buffer, such as that in cell stimulation protocol, destack and the separation quality suffers. Future work for this project will investigate alternative stimulation procedures.

Finally, the on-line MD-ME-EC device was used to monitor the dopamine metabolic pathway after the administration of L-DOPA *in vivo*. Prior to *in vivo* work, the separation of analytes in the dopamine metabolic pathway (optimized in Chapter 3 with a simple-t device) was performed on the on-line double-t device using a direct connect scheme. Next, a microdialysis probe was connected to the device and a concentration change in a solution of standards in a vial was monitored, yielding linear results (R^2 = 0.986), proving that the developed MD-ME-EC system is capable of monitoring concentration changes over time. This device was then employed to monitor the dopamine metabolic pathway *in vivo* after an administration of L-DOPA into the rat striatum, and two metabolite peaks were detected. Lastly, some limitations of the current device were discussed.

7.2 Future directions

Microdialysis sampling coupled to microchip electrophoresis offers a powerful method for monitoring biological events, both *in vivo* and *in vitro*. The combination of these two methods yields a separation-based sensor that can be customized for specific applications. Up to this point, MD–ME has been used primarily for monitoring release of neurochemicals, specifically, amino acid neurotransmitters and catecholamines, as in the case of this dissertation. The incorporation of electrochemical detection into the devices enables a smaller overall

footprint, as associated instrumentation can also be miniaturized. In the future, this can allow for both on-animal monitoring and monitoring of biomarkers of diseases and disorders in the clinic.

7.2.1 Immediate future directions

As discussed in the last chapter, there are some limitations and areas for improvement in the original MD-ME-EC device design. Three main improvements need to be made: (1) integration of a system prior to the microchip that is capable of flushing with various buffers to eliminate clogs, (2) incorporating an internal standard, and (3) lowering the limits of detection.

When running this on-line device, one of the difficulties is the development of clogs, over time, in the injection cross. These clogs (as seen in Figure 6.8) limit or halt the introduction of sample into the separation channel. Often, these clogs can be removed by flushing the microchip with buffers, base (0.1 M NaOH), or acid (0.1 M HCl). With the current design, when a clog presents itself, the microchip is removed from the system (electrical leads and microdialysis pump disconnected, microchip removed from holder) and flushed either through negative pressure applied at a reservoir or positive pressure applied through the syringe pump which is filled with the flushing solution (and not connected via microdialysis to the animal). Unfortunately, this procedure completely halts the collection of useable data. In the future, the incorporation of an in-line t junction after the microdialysis probe but before the microchip would allow for positive pressure flushing of the microchip, potentially eliminating clogs. This on-line microchip cleaning would allow clogs to be dealt with rapidly, without a pause in data collection.

The incorporation of an internal standard would be incredibly beneficial to the function of the overall device. An internal standard that is placed in the perfusate and goes through the microdialysis probe and into the chip would allow for three things: 1) easy characterization of

the recovery of the microdialysis probe, 2) insuring that the same amount of sample is injected into the separation channel (*e.g*. detect the appearance of clogs), and 3) serve as an internal standard for the separation (migration time) and detection (any electrode fouling). After a survey of over 30 compounds, 3-nitrotyrosine (N-Tyr) was identified as a potential internal standard. This analyte was well separated from the analytes of interest (Figure 7.1) under the optimized separation conditions outlined in Chapter 3. However, this compound can be detrimental to dopamine neurons [1], so while it is possible to incorporate this internal standard into the system after the microdialysis probe, this configuration is not ideal. In the future, a different internal standard needs to be identified that is biologically compatible. This would allow both microdialysis probe recovery information to be obtained in addition to ensuring injection and separation quality over time.

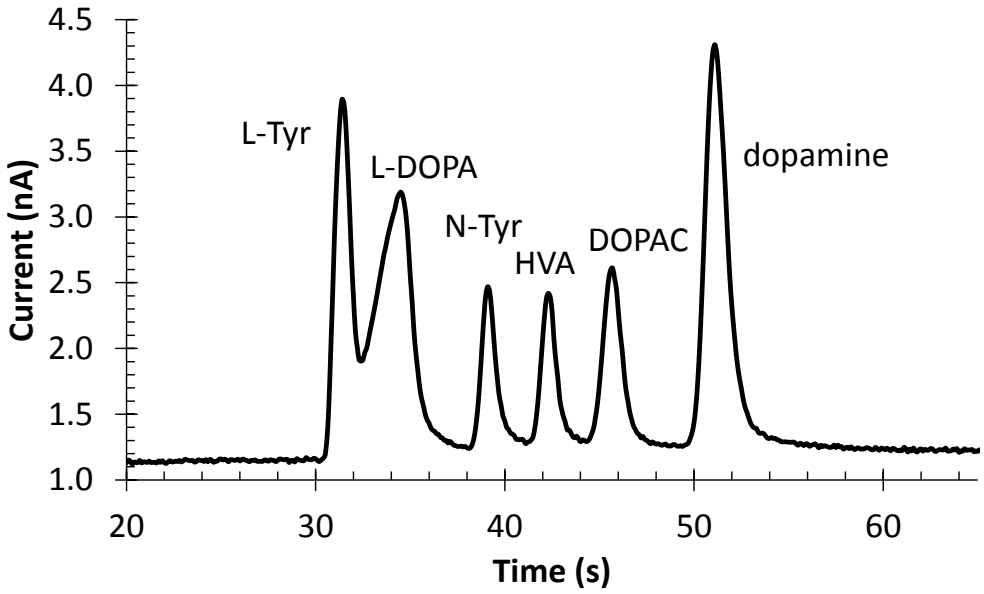

Figure 7.1 Potential internal standard. N-Tyr was identified as a potential internal standard, due to its separation from other analytes of interest. However, it was not biologically compatible.

Lastly and most importantly, the limits of detection need to be improved. In the animal experiments described herein, concentrations of the metabolites were artificially enhanced by the L-DOPA administration, and even then metabolite peaks were very small and near the detection limits. There are a few ways of decreasing the limits of detection, including sample stacking techniques, incorporating analyte affinity preconcentration, and employing different types of carbon electrodes and/or incorporating a decoupler. Previous researchers have employed the first of these, specifically transient isotachophoresis, and experienced over a million-fold enhancement in signal on the simple-t microchip format for detecting dyes [2]. This method could be modified for use in the double-t microchip design. An additional sample preconcentration technique employing boronate affinity monoliths incorporated into a microchip has been shown to decrease limits of detection for analytes with a catechol moiety, specifically epinephrine, norepinephrine, and dopamine [3,4]. Lastly, different carbon electrode materials such as carbon nanotubes or modified graphene electrodes could enhance analyte signals. In addition to modifying the electrode material, a decoupler could be added to the system, decreasing the noise at the detector and therefore the limits of detection [5]. A combination of some or all of these techniques will be necessary to enhance the limits of detection into a practical range.

7.2.2 Long-term future directions

There are many possible future applications of the separation-based sensors using on-line microdialysis-microchip electrophoresis with electrochemical detection. The small footprint of the microfluidic chips and associated instrumentation makes these sensors especially amenable to on-animal and on-site analysis.

7.2.2.1 On-animal monitoring

The simultaneous monitoring of neurochemistry or drug metabolism and behavior in awake, freely roaming animals is an important future application of this technology, as has been discussed in previous chapters of this thesis. On-line MD-ME-EC has been placed on animal previously by our group to measure subcutaneous nitrite production after a nitroglycerin perfusion [6]. The main future direction of this work is to employ the device described here for on-animal (sheep) monitoring of analytes in the dopamine metabolic pathway (Figure 7.2). After this has been accomplished and the limits of detection are lowered to measure endogenous concentrations, behavior and neurochemistry can be simultaneously monitored.

Some of the behaviors that would prove interesting to monitor in sheep are related to their happiness and sense of community. Sheep are herd animals, and enjoy being with other sheep; therefore it would be interesting to monitor their emotional state when interacting with various stimuli, such as hearing a dog bark, being with another sheep, being with the herd, a mother sheep seeing her baby sheep, etc. These emotional states can be determined using the position of the sheep's ear [7-10], recorded through video monitoring. In addition to endogenous concentrations of neurotransmitters, the effect of neuroactive drugs on both behavior and neurochemistry can be determined. This would be invaluable to developing new and better drugs for disorders such as depression. Also, as microchips and probes become smaller, it may become possible to place devices directly on smaller freely roaming animals, such as the rabbits or rats more traditionally used in laboratory research. In summary, these on-line MD-ME-EC devices could be employed in the future to study the effects of neuroactive drugs as well as to better understand the biochemical basis of natural behaviors.

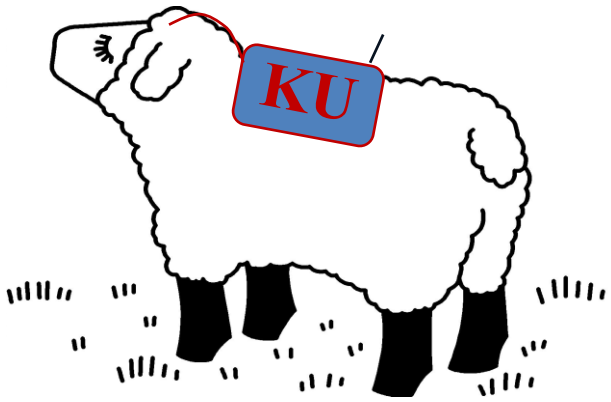

Figure 7.2 Lab-on-a-sheep. Analysis of neurotransmitters on-line in a freely roaming animal. The concentration of neurotransmitters will then be correlated with the animal's behavior in its natural environment.

7.2.2.2 Monitoring biomarkers of traumatic brain injury

An additional application of on-line MD-ME-EC devices is for monitoring biomarkers in the clinic. In particular, traumatic brain injury (TBI) is a devastating condition with many long-term effects. It is estimated that around 1.7 million individuals in the US and over 1 million individuals in the UK are affected [11]. While the initial injury is damaging in its own right, a secondary cascade of effects can lead to further brain damage. In addition to the death of brain cells, the primary injury also causes ischemia, or loss of blood flow and oxygen, to neighboring regions of the brain resulting in, among other things, oxidative stress and spreading neuronal death [11-14]. The aim of medical intervention is to develop treatments that arrest these secondary effects, a goal that requires judicious timing. Drugs given too early or too late will have little to no effect. Portable analysis systems using sensors coupled to microdialysis sampling for monitoring biomarkers of tissue injury in traumatic brain injury are currently under

development and some are commercially available [15-17]. However, these methods are limited by the biosensors that are available for specific analytes such as glucose, lactate, and pyruvate.

The separation-based sensor approach would make it possible to develop integrated systems to separate and detect biomarkers that are not currently monitored, such as catecholamines, amino acid neurotransmitters, antioxidants, neuropeptides, and markers of oxidative stress. These sensors could be coupled to the microdialysis sampling that is already taking place in the traumatic brain injury patients in the clinic. This technology could be used to better understand the disease or injury state, allowing for the development of better drugs, in addition to better informing clinicians so that the administration of drugs can be more effectively timed.

7.3 References

[1] B. Blanchard-Fillion, D. Prou, M. Polydoro, D. Spielberg, E. Tsika, Z. Wang, S.L. Hazen, M. Koval, S. Przedborski, H. Ischiropoulos, Metabolism of 3-nitrotyrosine induces apoptotic death in dopaminergic cells, J. Neurosci. 26 (2006) 6124-6130.

[2] B. Jung, R. Bharadwaj, J.G. Santiago, On-Chip Millionfold Sample Stacking Using Transient Isotachophoresis, Anal. Chem. 78 (2006) 2319-2327.

[3] C. Cakal, J.P. Ferrance, J.P. Landers, P. Caglar, Microchip extraction of catecholamines using a boronic acid functional affinity monolith, Anal. Chim. Acta 690 (2011) 94-100.

[4] C. Cakal, J.P. Ferrance, J.P. Landers, P. Caglar, Development of a micro-total analysis system (μ-TAS) for the determination of catecholamines, Anal. Bioanal. Chem. 398 (2010) 1909-1917.

[5] D.J. Fischer, M.K. Hulvey, A.R. Regel, S.M. Lunte, Amperometric detection in microchip electrophoresis devices: Effect of electrode material and alignment on analytical performance, Electrophoresis 30 (2009) 3324-3333.

[6] D.E. Scott, S.D. Willis, S. Gabbert, D. Johnson, E. Naylor, E.M. Janle, J.E. Krichevsky, C.E. Lunte, S.M. Lunte, Development of an on-animal separation-based sensor for monitoring drug metabolism in freely roaming sheep, Analyst 140 (2015) 3820-3829.

[7] N. Reefmann, F. Butikofer Kaszas, B. Wechsler, L. Gygax, Physiological expression of emotional reactions in sheep, Physiol. Behav. 98 (2009) 235-241.

[8] N. Reefmann, F. Butikofer Kaszas, B. Wechsler, L. Gygax, Ear and tail postures as indicators of emoptional valence in sheep, Applied Animal Behavior Science 118 (2009) 199-207.

[9] N. Reefmann, B. Wechsler, L. Gygax, Behavioural and physiological assessment of positive and negative emotion in sheep, Animal Behavior 78 (2009) 651-659.

[10] A. Boissy, A. Aubert, I. Desire, L. Greiveldinger, E. Delval, I. Veissier, Cognitive sciences to relate ear postures to emotions in sheep, Anim. Welfare 20 (2011) 47-56.

[11] A. Rodriguez-Rodriguez, J.J. Egea-Guerrero, F. Murillo-Cabezas, A. Carrillo-Vico, Oxidative Stress in Traumatic Brain Injury, Curr. Med. Chem. 21 (2014) 1201-1211.

[12] T. Janowitz, D.K. Menon, Exploring new routes for neuroprotective drug development in traumatic brain injury, Sci. Transl. Med. 2 (2010) No pp. given.

[13] N. Marklund, K. Salci, G. Ronquist, L. Hillered, Energy metabolic changes in the early post-injury period following traumatic brain injury in rats, Neurochem. Res. 31 (2006) 1085-1093.

[14] J.W. Bales, A.K. Wagner, A.E. Kline, C.E. Dixon, Persistent cognitive dysfunction after traumatic brain injury: A dopamine hypothesis, Neurosci. Biobehav. Rev. 33 (2009) 981-1003.

[15] D.A. Jones, M.C. Parkin, H. Langemann, H. Landolt, S.E. Hopwood, A.J. Strong, M.G. Boutelle, On-line monitoring in neurointensive care Enzyme-based electrochemical assay for simultaneous, continuous monitoring of glucose and lactate from critical care patients, J. Electroanal. Chem. 538-539 (2002) 243-252.

[16] M.L. Rogers, D. Feuerstein, C.L. Leong, M. Takagaki, X. Niu, R. Graf, M.G. Boutelle, Continuous Online Microdialysis Using Microfluidic Sensors: Dynamic Neurometabolic Changes during Spreading Depolarization, ACS Chem. Neurosci. 4 (2013) 799-807.

[17] R.J. Shannon, K.L.H. Carpenter, M.R. Guilfoyle, A. Helmy, P.J. Hutchinson, Cerebral microdialysis in clinical studies of drugs: pharmacokinetic applications, J. Pharmacokinet. Pharmacodyn. 40 (2013) 343-358.

Appendix: Trials and tribulations of carbon electrode fabrication

8.1 Carbon fiber electrode in a PDMS substrate

These electrodes are fairly simple to create, so only a few common pitfalls and suggestions are detailed here. The fabrication is also described in Chapter 2 (section 2.6.1) and Figure 2.7. When creating these electrodes, a carbon fiber is placed into a trench built into a PDMS substrate. This PDMS substrate is placed on a glass plate to lend stability and rigidity to the electrode substrate.

When making the substrate (prior to the insertion of the carbon fiber), the cured PDMS layer containing the electrode trench is placed on top of the glass plate. The PDMS layer is about 2 mm smaller (length and width) than the glass plate, which leaves a small edge. A thin layer of uncured PDMS is then placed on the glass edge, around the sides of the cured PDMS layer. A razor, run carefully over the top of the cured PDMS will remove any excess uncured PDMS, providing a flat surface for the channel layer in microchip electrophoresis experiments. When cured, the edge of uncured PDMS will seal the PDMS to the glass, making the device more rugged.

After the base of the substrate is created, the carbon fiber is placed into the PDMS trench. It is optimal if the trench is the same diameter or slightly larger than the carbon fiber; a trench that is too small will not allow for carbon fiber insertion and a trench to wide will allow for solution to leak in around the electrode, raising the background current. Placement of the carbon fiber into the trench is usually performed under a microscope. It is easiest to perform this step outside of the cleanroom and using an inverted microscope. First, place the carbon fiber as close as possible to the trench. Then, after placing the substrate on the microscope stage and visualizing the trench and fiber using the microscope, use a pair of fine tweezers to gently roll the fiber into the channel. When doing this, it is important to use a gentle, slow sweeping motion

to roll the carbon fiber into the channel. These carbon fibers are very brittle, so poking the fiber into the channel will only result in a broken fiber and sadness. After the fiber is in the channel, a gentle nudge on the top of the carbon fiber (a gentle push downward into the channel) will ensure the fiber is secure. Once a portion of the fiber is in the trench, small pieces of PDMS can be placed over the fiber to hold that section in place.

8.2 Pyrolyzed photoresist film carbon electrode on a glass substrate

Pyrolyzed photoresist film (PPF) carbon electrodes are incredibly tedious to fabricate and getting a good set of electrodes is part skill and large part luck. A brief description of their fabrication can be found in Chapter 2 (section 2.6.2) and outlined in Figure 2.10. Here, a SOP with helpful hints is presented for future researchers.

Cleaning quartz glass

- Make sure old features are scraped off with a razor blade
- Clean in acid and base piranha according to acid/base piranha SOP
    - This step is vital in creating a good, clean surface for photoresist adhesion. Make sure to properly clean the plates, 15 minutes each minimum in both the acid and base piranha. Additionally, the piranha usually only lasts for about 4 plates, so if you are doing more be sure to make up fresh solution.

Depositing photoresist

1. Deposit positive photoresist (AZ 1518) onto quartz glass using the following conditions:
    - Spin program: 100 rpm for 10 seconds (Ramp: 100 R/s), then 2000 rpm for 20 seconds (Ramp: 500 R/s).

- When using the 25 mL syringes, deposit 4 mL x 2 during the first step of the spin program. Also, make sure that there are no bubbles in the photoresist by pouring it into the syringe and allowing enough time for the bubbles to rise.

2. Perform a soft bake at 100°C for 1.5 minutes. Take glass off the hotplate and wait for it to cool.
3. Use the Mask Aligner SOP to expose your substrate with these modifications/conditions:
    - Use positive photoresist masks (features in black, what shows goes)
    - Either place a silicon wafer (shiny side up) under your substrate and mask for a 4 s exposure (at 21.5 mW/cm^2) OR expose just the substrate and mask for 7 s (at 21.5 $mW.cm^2$)
4. Develop using MIF 300 developer for about 10 seconds, rinse with water ONLY and dry with N_2
    - Check that your features are all present and accounted for. If you are not happy with your design, wash off the features with acetone and then rinse heavily with water. Place the substrate on a hot plate at 200°C for a few hours, and then start over with new photoresist. If the photoresist doesn't stick well after this treatment, you will have to acid/base piranha wash and start over.
5. Hard bake for 1 minute at 100°C
6. Carefully remove any excess photoresist (around the edges of the glass, etc) using wipes and acetone. Any remaining photoresist will be pyrolyzed and much much more difficult to remove after this step.

Burning in Tube Furnace

1. Make sure that you have two full nitrogen tanks.
2. Place your substrates into the tube furnace by carefully removing one of the end caps and putting your substrate inside.
    - To move your substrate further into the furnace, place your substrate on the end of a meter long ruler and carefully push it inside the tube.
    - Your substrate should be all the way in the tube furnace, not hanging out in the end caps. The caps do not get hot enough and your photoresist will not pyrolyze.
    - Carefully replace the end cap.
3. Flush with nitrogen for about 5 minutes. Start with a fresh tank and use a pressure of less than 5 psi (with the flow gage opened all the way). The first tank should last at least 6 hours. Using too high of a flow rate will blow off your features, and too low of a flow rate will not make the chamber inert (causing your electrodes to burn off).
4. Turn on furnace power- toggle switch on the bottom right of the unit.
5. If no one has touched the furnace and everything is preprogrammed, press and hold the down arrow keys on all three zone simultaneously until the "run" light illuminates.
    - To program the furnace, look at the tube furnace SOP and use the following for all three zones:
        - A1: 935
        - SSP: 25
        - SP1: 925, tM1: 2.45
        - SP2: 925, tm2: 1.00

- This starts the temperature at 25°C, ramps at 5.5°C/min to 925°C. It holds there for 1 hour and then cools back down to room temperature.

6. Monitor the process, periodically checking the pressure in the nitrogen tank. When the pressure in the first tank becomes low (usually about 6-8 hours into the burning step) switch tanks. When switching the nitrogen tanks, do NOT turn off the tube furnace; this needs to remain on and running throughout the entire procedure. The second N_2 tank can be turned off when all three zone temps are below 100°C.
7. After all three zones cool to room temp, turn off the oven, and remove your electrodes. Finally, test your electrode and decide if you have mastered electrode making or if you must try again.